Structural Response of Multi-Story Buildings Subjected to Differential Settlements of its foundation

Wenxue Chen

A Thesis

In the Department

of

Building, Civil and Environment Engineering

Presented in Partial Fulfillment of the Requirements
For the Degree of
Doctor of Philosophy (Civil Engineering) at
Concordia University
Montreal, Québec, Canada

December 2020

CONCORDIA UNIVERSITY

SCHOOL OF GRADUATE STUDIES

This is to certify that the thesis prepared

By: **Wenxue Chen**

Entitled: **Structural Response of Multi-Story Buildings Subjected to Foundation Differential Settlements**

and submitted in partial fulfillment of the requirements for the degree of

DOCTOR OF PHILOSOPHY (Civil Engineering)

complies with the regulations of the University and meets the accepted standards with respect to originality and quality.

Signed by the final examining committee:

_____ Chair

Dr. John Xiupu Zhang

_____ External Examiner

Dr. Hany El Naggar

_____ External to Program

Dr. Mingyuan Chen

_____ Examiner

Dr. Ashutosh Bagchi

_____ Examiner

Dr. Anjan Bhowmick

_____ Thesis supervisor

Dr. Adel Hanna

Approved by _____

Dr. Michelle Nokken, Graduate Program Director

December 22, 2020 _____

Dr. Mourad Debbabi

Gina Cody School of Engineering and Computer Science

Abstract

Structural Response of Multi-Story Buildings Subjected to Differential Settlements of its foundation

Wenxue Chen, Ph.D.

Concordia University, 2020

Differential settlement between foundation units of a multi-story structure has been responsible for serious damage to buildings, and often catastrophic failure and loss of life. The dynamic changes in the loading conditions of the structure, and the variability of the underlying ground due to environmental changes, are causing the undesirable differential settlement, which is manifested in the form of additional stresses in beams, columns and distortion of the structure elements.

The structural response to the differential settlements depends on the type of the structure (concrete or steel), type of beam-to-column connections (rigid or semi-rigid), the number of floors, height of the floor and the spans of the beams in the building.

Due to the complexity of the problem, and the enormous amount of the governing parameters, research in this field is lagging behind, which further attributed to the lack of communication between structure and geotechnical engineers. Yet, the current design codes of structures do not include these additional stresses. Engineers are dealing with this problem by using empirical formula, recommendations given in the literature, or by increasing the factor of safety of the superstructure.

This study presents experimental and numerical investigations on the problem stated. Experimentally a four-floor aluminum structure was developed in the laboratory. The model was instrumented to measure the stresses and strains induced in beams and columns as a result of the settlement of a center, edge and corner column respectively, which are the critical columns in the structure. Numerically a 3-D finite Element model was developed using the commercial software "ABAQUS"

After being validated with the present experimental results, the numerical model was used to analyze a 9-floor steel structure and to conduct a parametric study. The results are presented in the form of stress distributions in the structure, the role of beam-to-column connections and guideline for the design of these structures.

Acknowledgements

I would like to express my sincere appreciation to my supervisor Dr. Adel M. Hanna. His remarkable insight and unparallel wisdom have tremendously helped to materialize this thesis. His passion to create communications between the superstructure and the substructure has been his on-going research for many years, I am pleased to be part of it. His deep knowledge and vast experience had transferred me from a rock mechanics engineer to structure/geotechnical engineer. Exceptionally, during the pandemic, Dr. Hanna invited me few times to his residence to discuss my research. It is an honor to be his Ph.D. student.

I would like to thank my former co-supervisor Professor Lan Lin for her assistance, encouragement, and valuable discussions she provided me, which has shaped this thesis at the early stage.

Thanks are due to Mr. Riccardo Gioia, the residence engineer, and his team, namely Mr. Josef Hrib, Mr. Roberto Avila-Perez, and Mr. Andy Shin-Pong for their tremendous help during the construction of the 3-D experimental model.

Thanks also go to Dr. Ashutosh Bagchi and Dr. Khaled Galal for allowing me to use the structural laboratory to conduct my experimental work. And a very special thank to my uncle Prof. Mingju Liu to give a huge support during this study.

I am grateful for the financial support I received from the "Natural Sciences and Engineering Research Council of Canada" (NSERC) and the scholarship I received from Concordia University.

Finally, this thesis cannot be completed without the endless support I received from my parents. Last but not least, the love, support and patience, I received from my dear wife, Xiao Wang and my four children: Jiahui Chen, Allen Chen, Abby Chen and George Chen, have made it possible for me to pursue this endeavor.

Wenxue Chen

Table of Contents

List of Figures

List of Tables

Table 5.4 Summary of vertical displacement of column comparison for center, edge and corner at settlement of 32 mm, 80 mm and 196 mm

Chapter 1

Introduction

1.1 Background

Foundations are the structural elements, which transfer the building loads to the ground. Often the building loads are not uniform or due to water infiltration or nearby excavation activity and other environmental changes, differential settlement between the structural elements may occur (Boone et al., 1999; Hanna, 2003; Laefer et al., 2009; Son and Cording, 2011; Zhu et al., 2012; Anastasopulos, 2013; Bray and Dashti, 2014; and Camos et al., 2014). Differential settlement is largely responsible for developing additional stresses in most of the structural elements. Such stresses are often not considered during the design stage.

Figure 1.1 illustrates the three typical types of foundation settlement, namely: uniform, tipping or overturning and differential settlement. Uniform settlement is the process in which the entire foundation settles at the same rate. This phenomenon does not usually lead to foundation problems. In tipping settlement, part of the foundation settles unevenly without cracks or damage and causes the building to be leaning on one side. The worst settlement is the differential settlement of the foundation, in which parts of the foundation settle at different rates, which may cause serious damage to the structure and affect the structure integrity and its safety. Differential settlement of the foundation may cause damage to the building walls, doors and windows, and in some cases, it may cause catastrophic failure, see Figure 1.2.

Uniform settlement. Tipping settlement Differential settlement

Figure 1.1 Types of foundation settlement (Copyright of InterNACHI)

(a) (b) (c)

Figure 1.2 Impact of differential settlement on structure: (a) Failure of wall and façade (https://www.omnibasementsystems.com/foundation-repair/foundation-warning-signs.html); (b) Failure of wall and windows; (c) Failure of a building (Song, 2010)

Due to unpredictable soil and environment conditions, it is difficult to predict the amount of differential settlement. That settlement generates extra stress in structures, depending on the stiffness and displacement. Meyerhof (1947) investigated the relationship between stress redistribution of a building and its differential settlement, where enough unequal settlement led to considerable damage to the superstructure. Subsequently reports by K. Terzaghi (1948), Meyerhof (1953), Skempton & MacDonald (1956), Polshin & Tokar (1957), Beeby & Miles (1969), Burland & Worth (1974), Boone et al. (1996, 1999), Finno et al. (2005) and Halim & Wong (2012) have been devoted to that issue. Additionally, a number of researcher published recently have considered the relationship between economic design and allowable differential

settlements of foundation (Hanna et al., 1981 and Hanna, 2003). In practice, both structural and geotechnical engineers are involved in the design of a structure with safety and economic factors in mind. Specifically, structural engineers design the structures in such a way that all the structural components should be able to carry the design loads and remain safe under all loading conditions. Geotechnical engineers review the soil properties on the proposed site and select the type of the foundation that can efficiently transfer safely the load from the super-structure to the sub-soil. However, the communication between these two engineering groups is inadequate; they each follow their own design theories, codes and guidelines, which could lead to uneconomical design or failure. Given this, the communication gap between structural engineers and geotechnical engineers should be overcome to make the design both economical and safe.

In order to estimate soil-structure interaction most researches are based on empirical and/or theoretical methods, which cannot clearly understand the mechanism of structural responses to differential settlement. On the other hand, no study has investigated the effect of rigidity of joints on differential settlement and stress distribution. Thus, only allowable settlement or recommendations are given as guideline in some building codes. For example, in ACI (2017) the design manual proposes an allowable differential settlement (0.75 inch) for a traditional building as guidance in safety measures. ACI 318 (2014) stated differential settlement might affect safety of the building and ductile connections may be implemented to reduce severe effect of settlement. In some cases, load combinations can be modified to consider differential settlement effect. ASCE/SEI 7-16 (2017) recommends adding the load induced by the settlement into the load combination. The American Association of State Highway and Transportation Officials gives an allowable settlement with angular distortion (<0.008 for simple span and <0.004 for continuous span) (AASHTO 2010). In the current National Building Code of Canada 2015 (NBCC), the

effects of the differential settlement on the design of buildings are not considered. However, the Canadian Geotechnical Society (2006) suggested comprehensive investigation should be taken by both structural and geotechnical engineers to address soil-structure interaction.

1.2 Objectives and Scope of Work

This thesis research serves to shed light on how the superstructure respond to the settlement of its foundation, mainly:

1. To examine building performance of structure elements due to the excessive differential settlement of a center, side or corner column settlement respectively.
2. To evaluate the displacements of column and beam in vertical and horizontal directions, and the axial forces in column and the bending moment of beam as a result of a settling column within the structure.
3. To identify the critical elements of a structure during settling a column within the structure.
4. To propose a guideline for the design of a steel structure subjected to differential settlement.

1.3 Research Methodology

In order to achieve the above-mentioned objectives, experimental and numerical modelling were performed:

The experimental work is comprised of three phases. Phase I is an experimental study conducted on an aluminum frame building with semi rigid joints. The building is a four story, four-bay frame whose columns experienced differential settlement. Three columns (center, side,

and corner) separately underwent 50 mm settlement. The resulting strains, displacements, and stresses were recorded.

Phase II is a 3D finite element model was developed using ABAQUS and the data collected in Phase I. Once the model was validated, it was used to analyze multi-story steel structure with rigid and semi-rigid connections, to evaluate the response of structural elements due to settlement. The failure mode and critical elements were determined for the settlement of the critical columns namely: center, edge and corner column settlement respectively.

Phase III is a parametric study to examine the effect of span number, floor level and span length, floor height and the type of connections during the differential settlement.

1.4 Organization of Dissertation

This thesis includes the following six chapters:

Chapter 1 introduces the research background, objectives and scope of work and organization of the dissertation

Chapter 2 reviews the major findings in the literature on the structure response to differential settlement of its foundation, which has established the motives to pursue this study.

Chapter 3 describes the experimental methodology including the test setup design, model fabrication and installation, the configuration of instrument and test procedures, and data collection.

Chapter 4 describes the numerical modeling developed and the results produced. The model was validated by the present experimental results.

Chapter 5 analyzes the responses of steel structure due to the excessive settlement of center, edge and corner column respectively, for the case of rigid and semi rigid connection structures. Furthermore, parametric study on the parameters governing the structure response to include: number of spans, number of floors, length of span and height of floor to stiffness of connection was conducted.

Chapter 6 Highlights the findings obtained in this study and the contributions to knowledge for the subject matter. Limitation of the study and recommendation for future work are also given in this chapter.

Chapter 2

Literature Review

2.1 Introduction

A building is comprised of two distinct components, working together as one unit, namely: superstructure and substructure. The superstructure is a part of building above the ground and responsible for transfer of loads from different stories up to the ground level. The substructure or the foundation is the component below the ground level which, safely transfers the loads to supporting soil. Design of a foundation deals to bearing capacity of soil and settlement. The amount of settlement a building can undergo is a major concern for the stability of the building. Given that soil below the foundation is not uniform in nature and distribution of gravity or lateral loads among columns is non-uniform, differential settlement between the foundation units is expected. Excavation at neighborhood of the building, underground water movement, consolidation and liquefaction also cause differential settlement. This settlement is likely to produce additional stress for which superstructure elements have not been designed for. If alternate load paths have not been considered to redistribute the extra stresses or capacity has not been taken into consideration in the design process, extra stresses would induce to partial or comprehensive collapse (Pearson et al. 2005).

Researchers began to study structural responses of buildings to differential settlement as early as the 1930s. This chapter reviews the literature related to differential settlement to include: experimental and numerical works and field observations. Furthermore, the current codes related to allowable differential settlement of foundations are also reviewed in this chapter.

2.2 Background

(Meyerhof 1947) was the first one to provide a recommendation regarding the allowable settlement of structures. He presented a general procedure of analysis in which the structure and its foundations are treated as one complete system. Some expressions regarding displacement and slop of members were developed to estimate bending moments, direct and shearing forces. The expressions showed the stresses in the members are directly related to the elastic modulus, stiffness of that member and differential settlement of its support. A relatively small unequal settlement of footings would result significant stress in all members. These stresses are largely reduced in the members not adjacent to settling support if the frame is more than three spans. (Meyerhof 1947) showed bending moment is considerably increased in beams at external joints particularly at lower stories. The bending moment decreased in internal joints as a consequence of the increase in bending moment at mid span of beams. He also reported a decrease in rigidity of connections leads to more differential settlement and less stress in structural members.

In order to help engineering practitioners understand the amount of settlement allowed for the buildings under design, (Skempton A. W. and MacDonald 1956) conducted an analysis on data collected from 98 conventional buildings, including both concrete and steel frame buildings. Among them, 40 buildings had been damaged due to settlement. According to the survey results, limited values for angular distortion, maximum and differential settlement was proposed to mitigate major damages. In terms of uncertainty, safety factor of 1.5 and 1.25 were advised for angular distortion and differential settlement, respectively. The limitations are reported in Table 2.1.

Table 2.1 Limited settlement provided by (Skempton A. W. and MacDonald 1956).

Condition	Considering safety factors			
	Angular distortion (max.)	Angular distortion (min.)	Differential settlement (in.)	Max. settlement (in.)
Frame	1/150	1/500	\	\
Bearing wall	1/300	1/500	\	\
Without any settlement damage	1/500	1/1000	\	\
Footing on clay	\	\	1 ½	2 ½
Footing on sand	\	\	1	1 ½
Raft on clay	\	\	\	2 ½ - 4
Raft on sand	\	\	\	1 ½ - 2 ½

Polshin and Tokar (1957) monitored settlement for some buildings for several years at Soviet Union. They categorized the foundation deformation based on slope (the difference of settlement of two adjacent columns relative to the distance between them), elative deflection (the ratio of deflection to the deflected part length), and the average settlement under the building. It was found out rigid box section reinforced concrete slab foundation in multi-story building decreased the non-uniform settlement below the structure. Additionally, no crack appeared on brick cladding if the slope was limited to 0.0005.

Burland and Worth (1974) have demonstrated that the prediction of differential settlements and induced damage is a very complex problem through comparing the analyses of many studies. However, in general terms, design philosophy should be concentrated on a simple approach of assessing the global stiffness of a structure and its finishes. (Burland and Worth 1974) have proposed a new fundamental approach for building damage assessment in which the structure is

assumed to be a simple, equivalent, uniform, weightless elastic beam with only considering its tensile capacity of material. A limiting or critical tensile strain range of 0.0005 to 0.00075 for cracking to become noticeable was advised by Burland and Worth (1974). However, the equivalent rigidity of the assumed beam is difficult to determine, and it cannot be applied to multi-story structures.

Brown (1975) examined the interaction between structure, foundation and soil in plan frames with pined based columns above finite length strip foundation. He showed that soil-structure interaction is dependent on relative stiffness rather than absolute one. The relative stiffness is ratio between building, foundation and soil stiffness and defined as equations 2.1 to 2.3.

$$K_b = \frac{nEI}{l^4} \qquad \text{Eq. 2.1}$$

$$K_r = \frac{E_r I_r}{l^4} \qquad \text{Eq.2.2}$$

$$K_b = \frac{E_s}{1 - \nu_S^2} \qquad \text{Eq.2.3}$$

where n is number of stories, “E” is Young modulus of structural materials, "E_r is Young modulus of foundation materials, E_s is Young modulus of soil; “I” is the second moment of area of beams; l is length of beams; I_r is second moment of foundation area; L is length of foundation and υ_s is Piosson ratio of soil.

He proposed graphs to estimate variations in the amount of stress in columns. So, it is possible to decide if complete analysis is necessary to consider the differential displacement or effect of interaction between structure and foundation is negligible. Brown (1975) also stated that effect of differential settlement declined where number of frame bays increased. Additionally,

fixity of the end of the columns has a little effect on the interaction between structure and foundation.

Man (1977) has studied the performance of a reinforced concrete frame subjected to differential settlement and has concluded that the most prominent damage area induced by settlement was within one span away from the settling column. The effect of differential settlement was more prominent for the lower stories of the building. Additionally, beam members were more likely to be affected by differential settlement than column members.

Boscardin and Cording (1989) have evaluated the tolerance of brick-bearing wall and small frame structures due to excavation-induced settlement using analytic models and field data. They concluded that when a structure is subjected to increasing lateral strains, its tolerance to differential settlement decreases. As a consequence, measures to mitigate excavation-related building damage should include provisions to reduce the lateral strains sustained by the structure. Boscardin and Cording (1989) mentioned tolerance of a building to deformation is governed by its ability to tolerate shearing deformation and horizontal expansion while angular distortion is a practical parameter to reflect deformability of a building. So that, increasing the number of stories enhances shear stiffness of a structure and it tends to tilt more than distort. However, increase in the number of bays makes a structure to distort more to accommodate ground movement.

Boone (1996) showed assessments based on one single criterion such as angular distortion is not precise to predict damage following from differential settlement. Then, more effective parameters should be considered. He proposed a strain superposition method (SSM) that uses both equations of fundamental geometry and engineering principles to assess building damage. The results obtained using data from over 100 case histories of damaged buildings are in

reasonable agreement with those obtained by Boscardin and Cording (1989).

Lefebvre and Théroux (2000) studied the effect of different settlement on formulation of load combination according to the available codes. They used a software called Visual Design to integrate structural response with foundation. That software considers structure-soil interaction by calculation of settlement corresponded to that load combination. The calculated settlement is applied to the structure under that load combination and a new settlement is calculated. This process continued till the settlement became convergent. Lefebvre and Théroux (2000) analyzed a structure under three conditions: without settlement, settlement as transient load and as permanent load. The load combinations used by Lefebvre and Théroux (2000) are presented in Table 2.2.

Table 2.2 Load combination to analysis (Lefebvre and Théroux 2000).

Without interaction	Transient settlement	Permanent settlement
0.85D+1.5L	0.85D+0.7(1.5L+1.25T)	0.85(D+T)+1.5L
1.25D+1.5L	0.85D+1.5L	1.25(D+T)+1.5L
D+E	1.25D+0.7(1.5L+1.25T)	D+T+0.5L+E
D+0.5L+E	1.25D+1.5L	D+T+E
/	D+0.5L+E	/

Results showed that bending moments in beam or column, in case of transient settlement are close to one without considering settlement. However, noticeable difference was observed in distributed load in members when permanent settlement was considered. As soil is heterogeneous in nature, different settlement is more likely to occur below foundation. Therefore, (Lefebvre and Théroux 2000) suggested differential settlement should be classified in permanent load category

and followed as

$$(D+T_D) + (E+T_E) \quad \text{Eq. 2.4}$$

$$(D+T_D) + 0.5\,(L+T_L) + (E+T_E) \quad \text{Eq. 2.5}$$

Roy and Dutta (2001) provided a simple methodology to calculate the effect of soil-structure interaction on building frames with isolated footings. Their results showed that interaction led to the increase in forces and bending moments in corner columns. That increase in bending moments is more severe than the increase in axial forces. This effect seems independent of footing size. Tie beams and diagonal braces' limited effect of soil-structure interaction in some extend through truss action. However, increase in moment of outer columns is inevitable and should be considered for design purpose. Roy and Dutta (2001) suggested that the soil below isolated footing can be modeled as a spring to study the interaction of soil-structure. An analysis based on three-dimension space frame is also more accurate than two-dimension plan frame.

300 structural frames varied in bays and stories were studied by (Hanna 2003) to estimate the magnitude of stresses in members due to differential settlement. According to his analysis, an interior foundation settlement significantly affects beams and columns just in adjacent neighborhood. Effect of that settlement is ignorable in further elements for design purpose. However, exterior settlement produces extra bending moment even beyond adjacent bays. This is because of lateral displacement in frame following from settlement. Although a precise analysis should be done to estimate the settlement which can be tolerated by a structure, to calculated the allowable differential settlement Hanna (2003) developed an equation as

$$M_{ac} \leq \frac{EI_B}{L_B^2}\left[\beta_i\Delta_i+\beta_j\Delta_j\right] \quad \text{Eq. 2.6}$$

Where M_{ac} is the allowable cracking bending moment, β_i is the bending moment coefficient of column i, L is the span length, E is the modulus of elasticity, Δ_i and Δ_j are allowable settlement of column i and column j, and I_B is the moments of inertia of the beams.

Progressive collapse of a reinforced concrete structure due to loss of a column, resulting from too much settlement, was investigated in a four bay and three story one third scale model by (Yi et al. 2008). Their study showed force transfer and internal resisting mechanism during progressive collapse. The experimental test was carried out in a load displacement manner to simulate gradual failure till steel reinforcement ruptured. The collapsed frame was presented in Figure 2.1. Four-behavior was observed in load displacement curve of the middle column as drawn in Figure2. 2. Elastic behavior from stage O by A. Elastic-plastic from A to B where bottom steel reinforcement has yield at the end of the first floor beam adjacent to the middle column. That is a sign of plastic hinge formation. From Point B to C, the beam showed plastic behavior inducing massive concrete crushing at the top of the beam. After this point, concrete crushing relieved in somewhat and tension cracks penetrated in the compression region and stain gages installed on steel bars at the top of the beam showed tension strain. This was the result of shifting natural axis in beam section toward top and force transmission in the beam changed from Vierendeel action to centenary one so that outer column moved toward the middle one. This stage ended up to the rupture of reinforcement at the top of the beam while dissertation angle was 10.3. According to the experimental results (Yi et al. 2008) provided a simplified model to estimate the capacity of the frame at the plastic phase and centenary one as presented in Figure 2.3. However, these models are limited to plain frame and not considered slab contribution.

Figure 2.1 Failure of the frame and detail of steel rupture in beam close to connection (Yi et al. 2008).

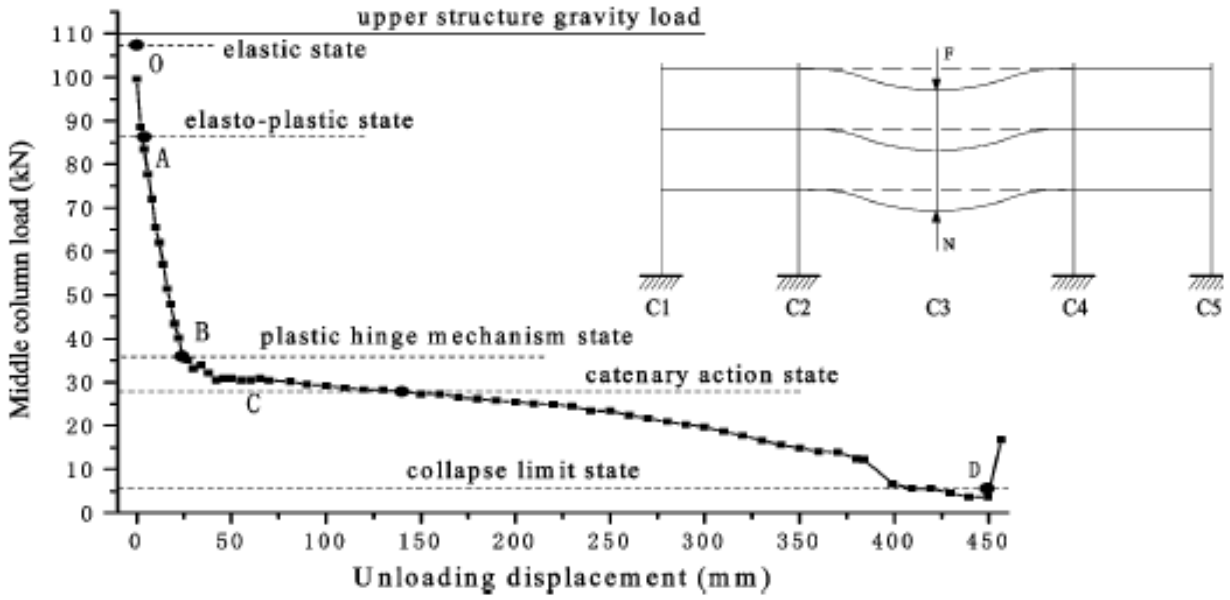

Figure 2.2 Middle column load versus unloading displacement of failed middle column *(Yi et al. 2008)*.

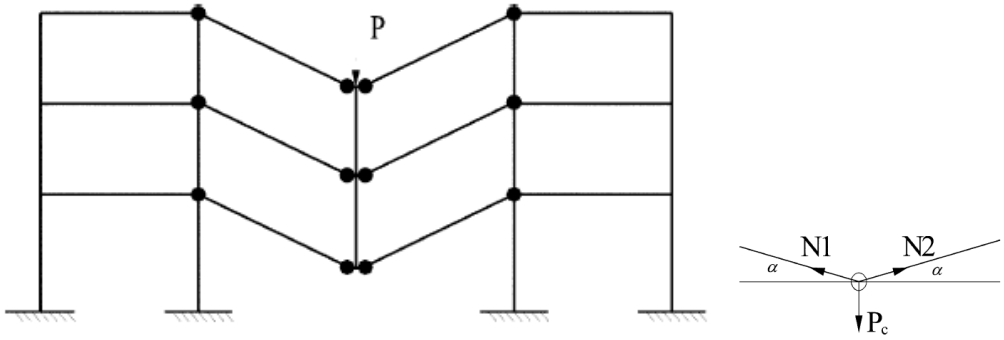

Figure 2.3 Simplified model to calculate load capacity of the middle column at the different phases: a) Plastic phase, b) centenary phase (Yi et al. 2008).

Sasani and Kropelnicki (2007) carried out a hybrid experimental test on a 3/8 scaled model of continues beam, in a reinforced concrete (RC) structure, following the removal of a supporting column. They also developed two finite element three-dimensional non-liner models. Experimental results showed end rotation of the beam before rupture of top reinforcement was about 11 degrees while catenary action had developed. It was concluded that the removal of a column caused the beams to bridge over the column as weaker top beams are supported by stronger bottom ones. Sasani and Kropelnicki (2007) also mentioned a rigid floor assumption led to more axial load in the beams in comparison to the beams in a non-rigid floor system. That would lead to less bending moment capacity and vertical displacement.

Laefer et al. (2009) conducted analytical and large-scale experimental works to examine response of a two 1/10 scaled RC plan frames to an adjacent excavation. They were set on dry sand, perpendicular to the excavation. Each frame was four stories high (30 cm each) and three bays wide (60 cm each). Figure 2.4 shows the set up and frames. Figure 2.5 and Figure 2.6 presented the cracks and vertical displacement on a frame. By examination of forces and deflections in the frames, the bays closer to the excavation withstood more loads and deflections. Additionally, the amount of deflection developed in the bays was disproportional to the level of excavation. So that, a quarter of excavation produces half of final deflection of the bays. Laefer et al. (2009) stated horizontal displacements negatively affect the structure because they generate tension stresses and rotation in the structure. This matter is more complicated where a soft story exists or the structure is flexible.

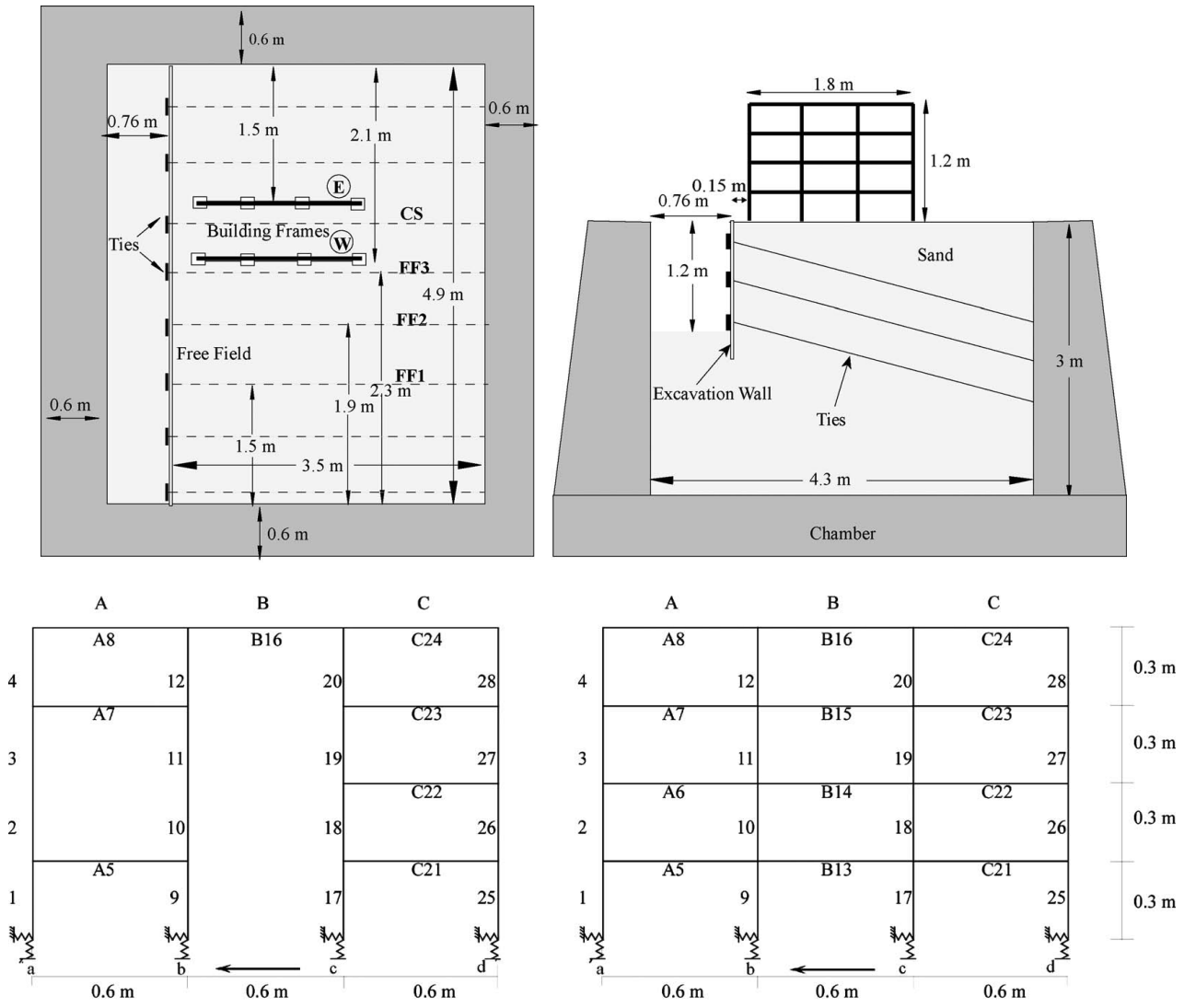

Figure 2.4 Details of the frames and test set up (Laefer et al. 2009).

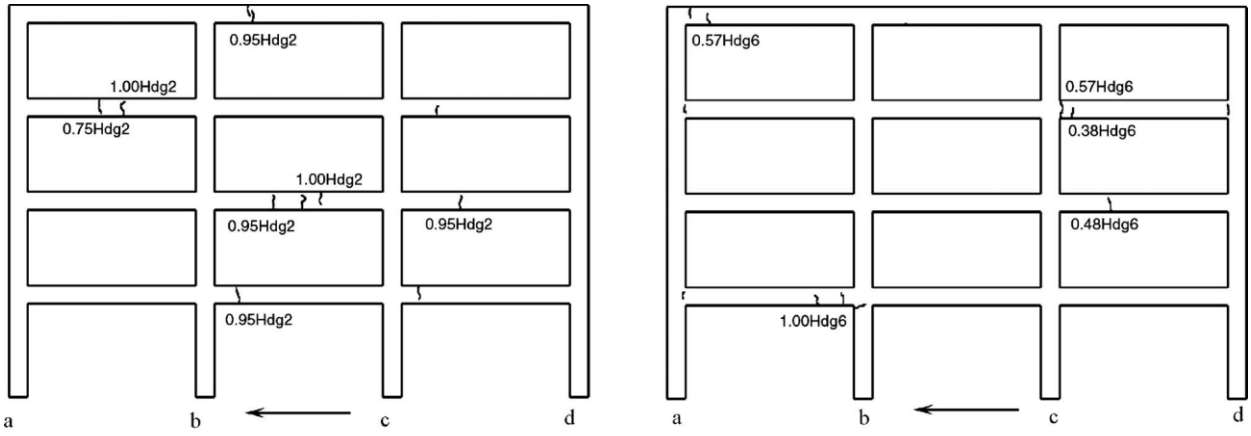

Figure 2.5 Localization of the cracks on the frame and corresponding excavation level. Arrows show the excavation position. Side notation indicated the level of excavation where that crack appeared (Laefer et al. 2009).

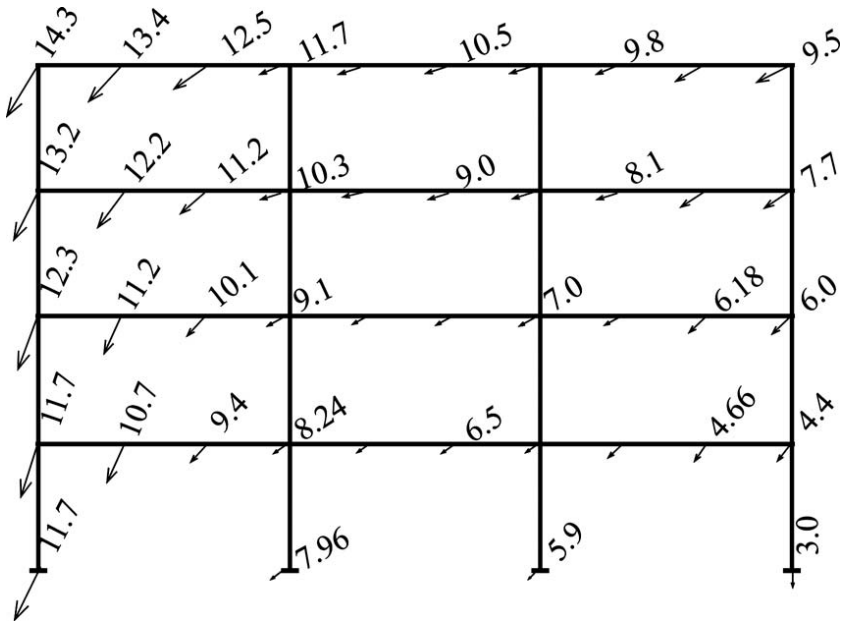

Figure 2.6 Vertical displacement of a frame subjected to actual foundation displacement at completed excavation. (Laefer et al. 2009)

Kim et al. (2011) reported a case study including settlement of 35-year-old building and its rehabilitation process. A finite element (FE) model developed on basis of one-dimension consolidation for 20 years, exhibited that differential settlement does not produce significant stress in the structure. However, that settlement caused cracking in masonry walls.

The collapse behavior of a single layer barrel vault as seen in Figure 2.7 with different slope under differential settlement was investigated by Sheidaii et al. (2013). They found out that internal forces arising from non-uniform settlement may have destructive effect on the structure. Thus, the more settlement, the less bearing capacity. In the same way, stiffness of the structure decreased while applied settlement was increased. This matter is important where sufficient deformation is necessary for serviceability condition. The analytical results revealed that the structure lose more capacity undergoing settlement in middle span support in comparison to the corner one. The studied models showed collapse initiates from those parts which are closer to the support experiencing settlement.

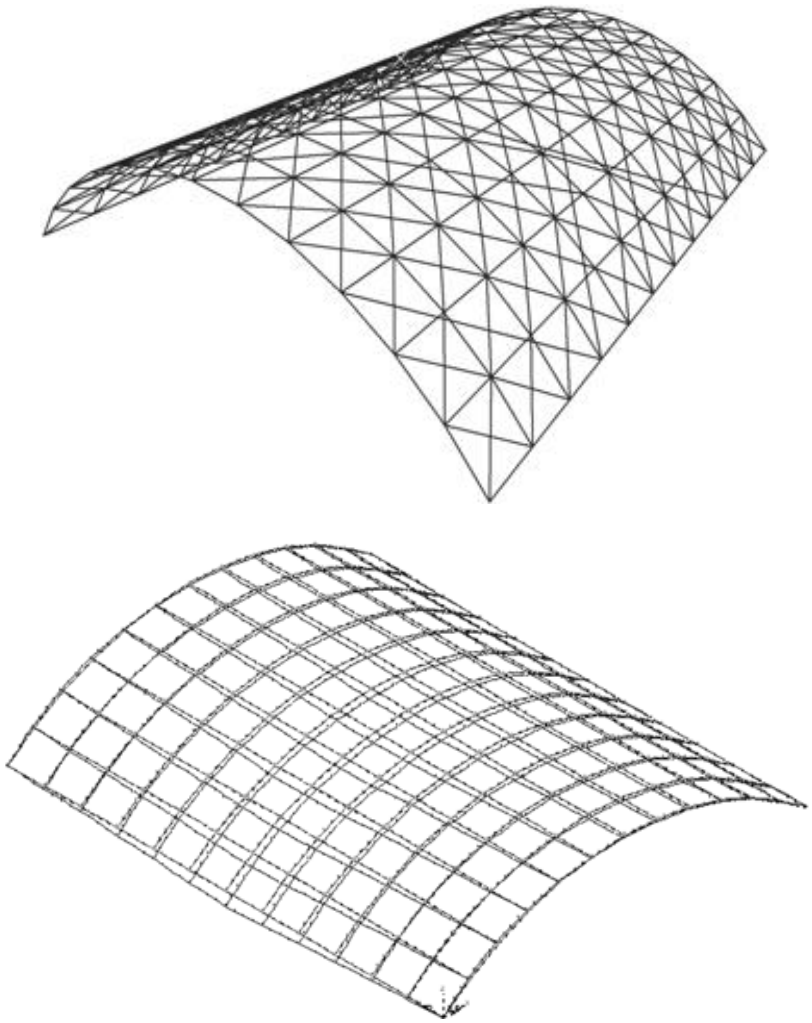

Figure 2.7 Undeformed and deformed barrel vaults under settlement of middle supporting column (Sheidaii et al. 2013)

Russo et al. (2013) studied a mat foundation of a 3-story building on clay soil. Progressive cracks appeared along the foundation as a result of both incorrect design and fluctuation of groundwater pressure (Figure 2.8). Their results showed that the situation may lead to structural collapse under service loads. In conclusion, they reported that the rigid slab was under designed for the uplift pressure, while it should have been designed as a beam on an elastic soil to withstand larger displacement.

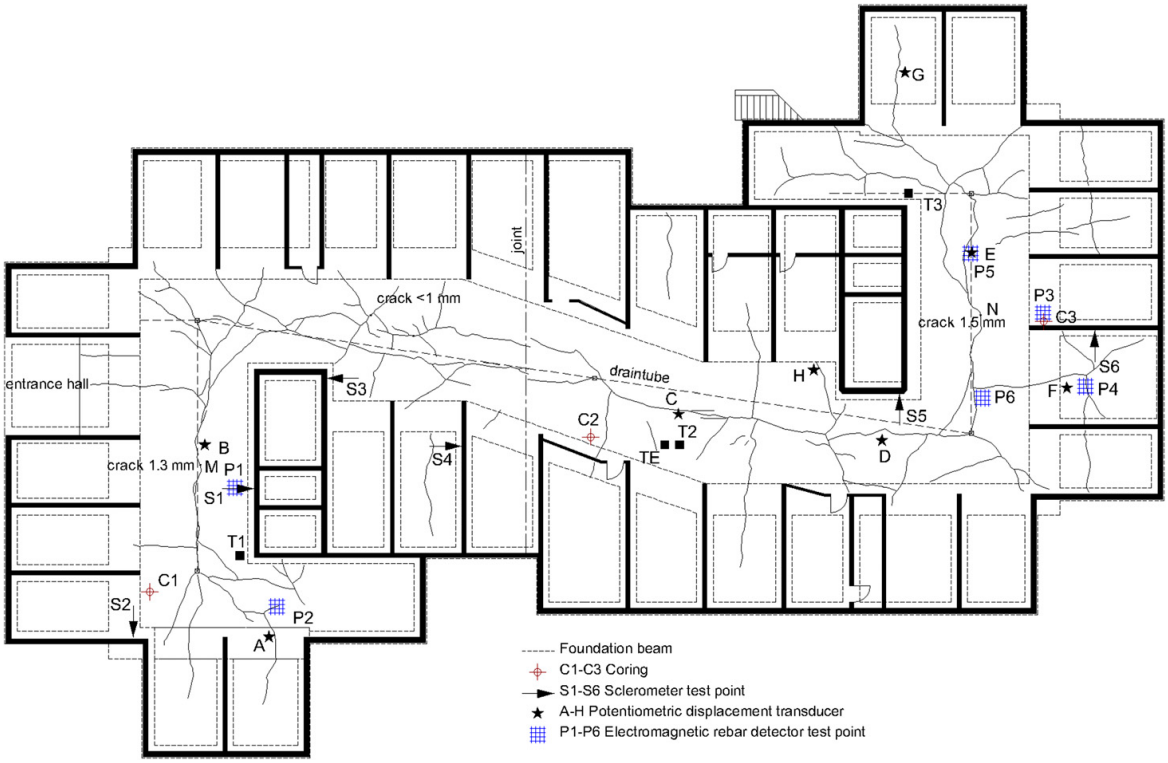

Figure 2.8 Plan of case study and cracks propagated in the mat foundation (Russo et al. 2013)

Qian et al. (2013) assessed load distribution at corner of a RC frame while it goes under progressive collapse. Their test setup is presented in Figure 2.9. The first flexural cracks were observed at the corner and shear cracks at the fixed end. It indicated Vierendeel action is the major mechanism to distribute load in the frame at that load level. Then shear cracks appeared at the corner. After joint shear cracks widened, longitudinal reinforcement stress decreased while the other side experienced rapid increase in reinforcement stress even though the vertical load capacity decreased (Figure 2.10). That is because resistance mechanism had changed to cantilever beam. Increase in vertical displacement led to increase in load bearing capacity since catenary action developed in the frame. Their experimental results showed increase in the transverse reinforcement improved the ultimate load bearing capacity as long as shear cracks and shear failure are a concern at the plastic hinges. The tie strength method (maximum tensile strength can be developed by top longitudinal reinforcement) suggested by DoD (2016) is not a safe practical design method, unless sufficient horizontal constraint is provided at the joints.

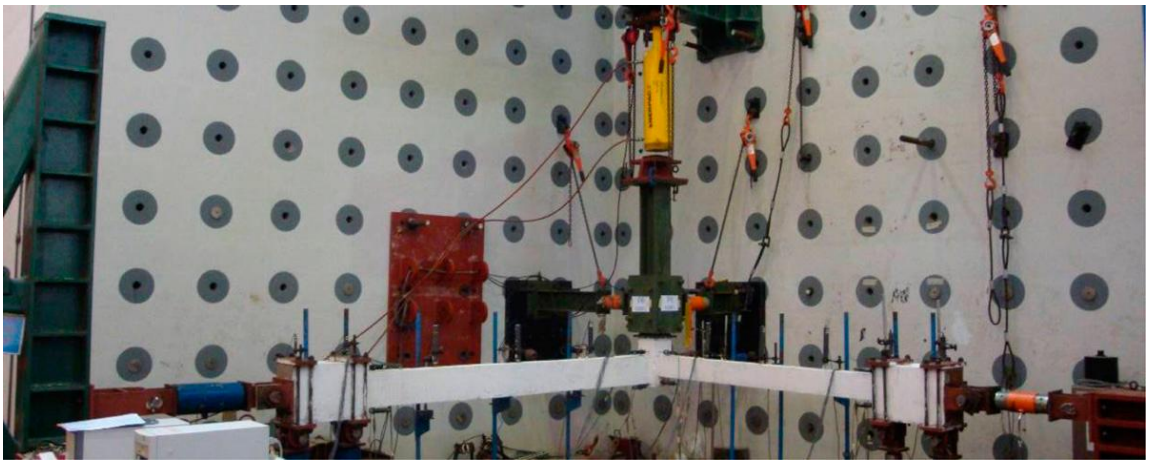

Figure 2.9 test setup and the specimen (Qian et al. 2013)

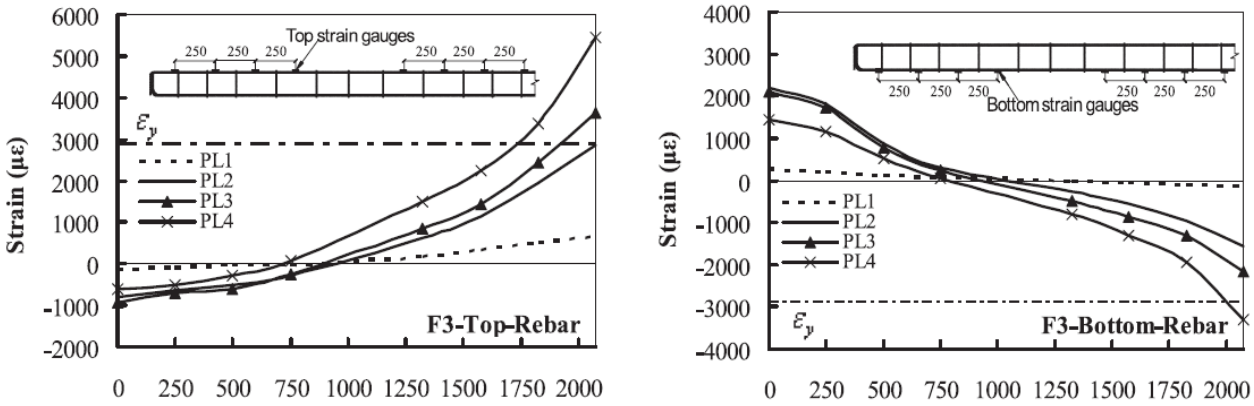

Figure 2.10 Strain profile of beam longitudinal reinforcement for a specimen (Qian et al. 2013)

The influence of excavation near a building on frame action was investigated by Hun and James (2014). They used a finite element model with various configurations to study frame response to excavation in a soft clay soil. A column stiffening factor defined to estimate bending stiffness of the frame. The structural behavior of the frame achieved by the finite element model, was close to that calculated by simple beam model, when new column stiffening factor was considered. To consider horizontal displacement, continuous and individual footing was also considered. According to the results, the effect of horizontal strains are negligible on frames with continuous footing even though that effect is considerable in case of individual footing. (Hun and James 2014) mentioned that the quantities of the strains occurred at ground floor are related to the frame properties. They finally stated that the damage of a construction, causing by ground movement, depends on load distribution, load pattern and properties of a construction which should be analyzed for each structure.

Lahri and Garg (2015) investigated the effect of a limited differential settlement on the force developed in a construction using a structural analysis software (STAAD Pro.). According to the results, height and length of columns and beams have a reverse effect on the amount of force developed in them.

So, increase in length of members leads to decrease in the stresses for the same settlement. Also decrease in moment of inertia of the elements cause the decrease in the stresses due to rigidity. In the same way, the effect of settlement in a frame comprising several bays is more severe than one bay frame since continued beams provide more rigidity in the frame. It was also found that the bays closer to the support experiencing settlement is more influenced as compared to other bays and the effect of settlement is higher at lower stories while it rapidly diminishes at higher levels.

Lin et al. (2015) analyzed a 10 story RC building subjected to an allowable differential settlement. Three columns (center, edge and corner column) separately underwent prescribed settled columns. Details of the model have been presented in Figure 2.11, which used a nonlinear finite element software (SAP2000) to conduct a non-linear pushover analysis. The length of rigid joint was defined as the half depth of the beam or column. The behavior of the plastic joint was defined according to the (FEMA 356 2000). The length of the hinge joints was 0.05 span length. Evaluation of results showed beams and column adjacent to the settling column (one span away) significantly affected by the settlement. However, effect of differential settlement on further elements is negligible. Increase in shear forces following from settlement was much less than that in bending moments. Then, (Lin et al. 2015) reported the damage of bending moment is more as compared to shear. That damage is more likely to occur in beams at the lowest floor or on the top one. The settling columns were under tension and the maximum displacement was monitored at the foundation level and it decreased at upper floors. However, displacement in other columns was reverse. So that, they were under compression and the amount of displacement increased at the upper floors. Settling column at the corner generated the most displacement in other columns, so that settling edge column was advised as the most critical situation for differential settlement of the columns.

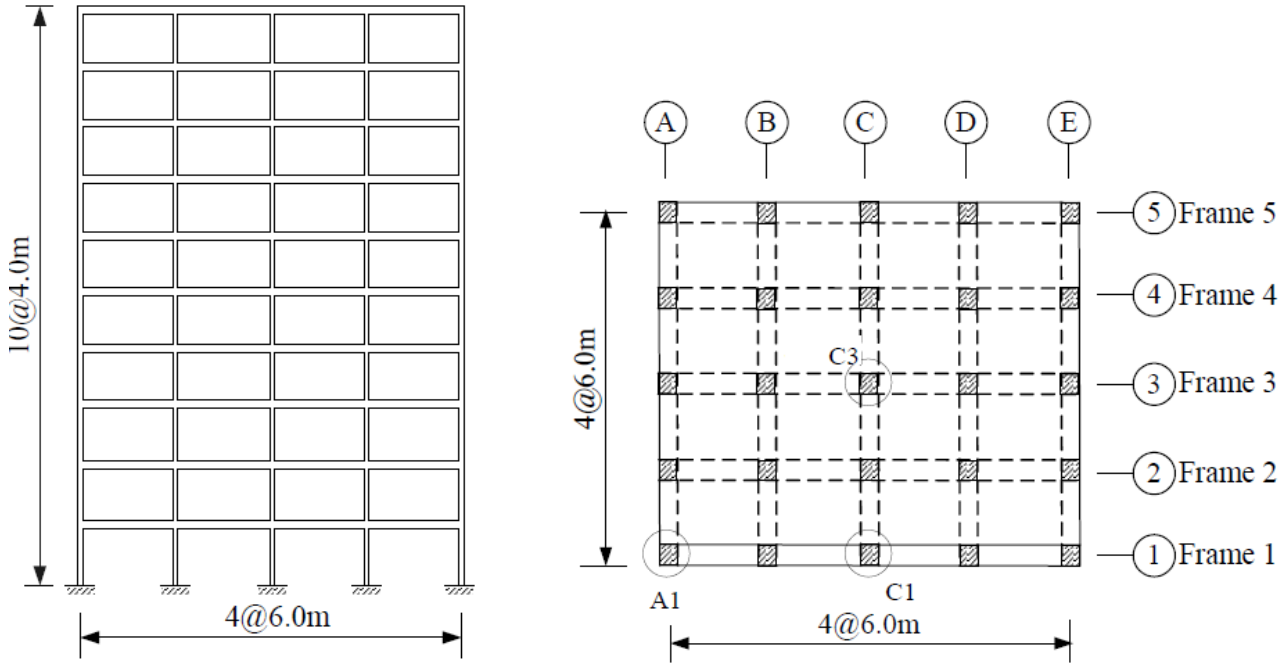

Figure 2.11 Details of model (Lin et al. 2015).

Hou et al. (2016) tested a two span, two bay, one story one third scaled RC frame undergoing center column loss to provide insight into load pattern and failure mechanism. The frame and test set up was presented in Figure 2.12. The test was carried out under displacement control at a rate of 3 mm/min. Figure 2.13 showed load versus vertical displacement of the middle column and corresponding load bearing stages. Figure 2.14 presents the moment diagram of a frame before and after removal of a frame and, it indicates after removal of a column, that the beams bridge over the damaged area can withstand the extra stresses. Based on the experimental results, catenary action in beams and tensile membrane mechanism in the slab contribute to tolerate the loads, and the frame withstood almost twice more load and vertical displacement after the formation of plastic hinge at the end of elastoplastic stage before collapse. (Hou et al. 2016) also proposed a simplified calculation method to predict the progressive collapse resistance of a RC frame.

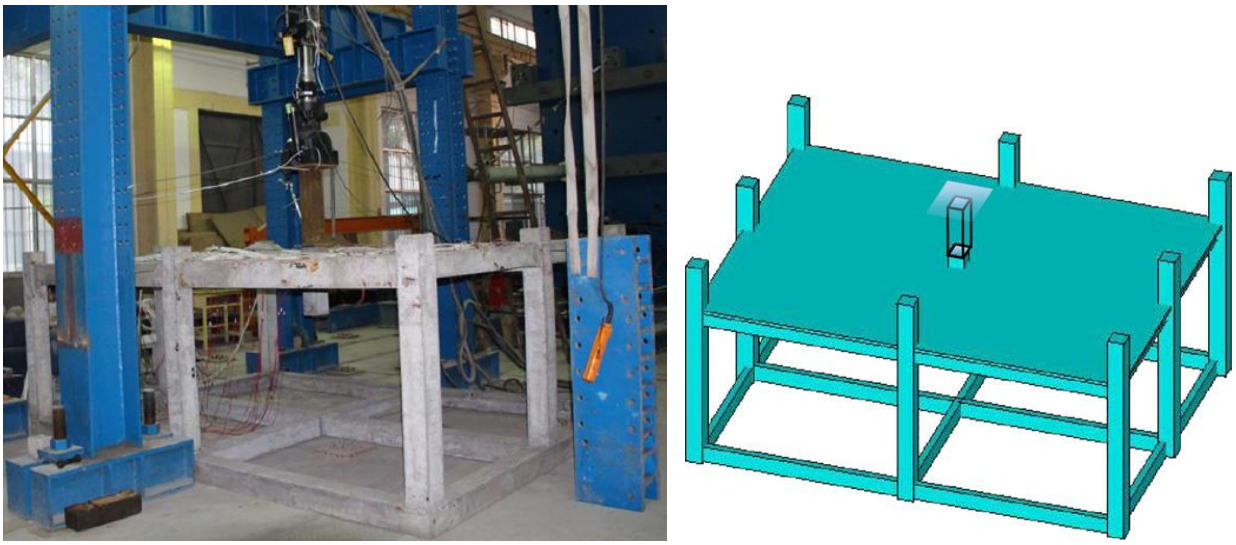

Figure 2.12 Test setup (Hou et al. 2016).

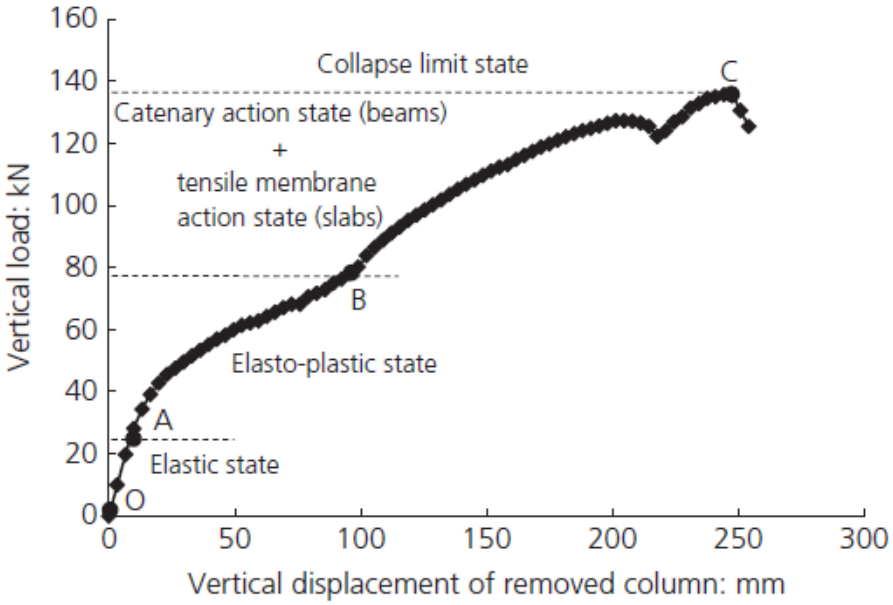

Figure 2.13 Load displacement curve for the middle column (Hou et al. 2016).

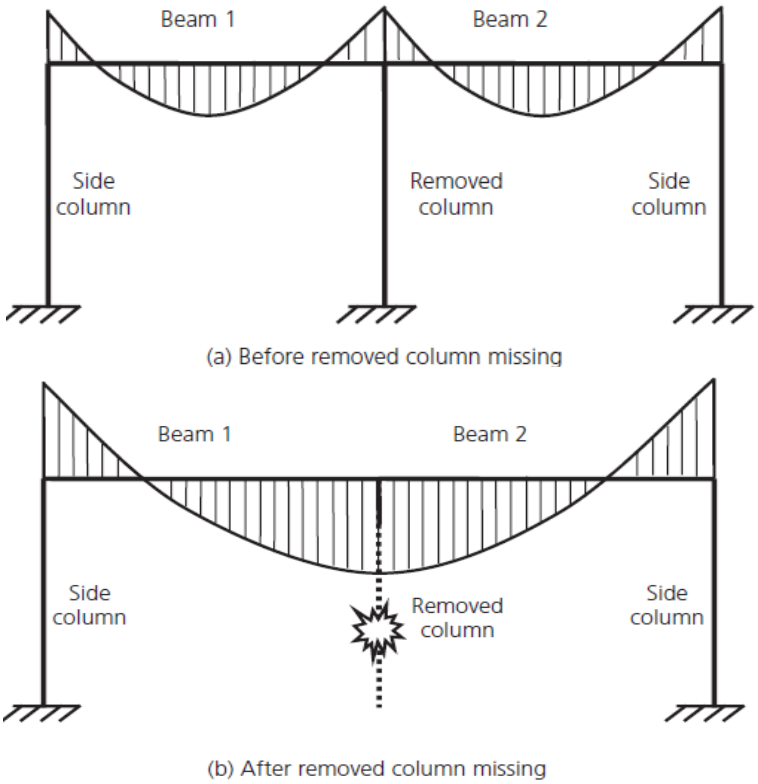

Figure 2.14 Difference in bending moment diagram before and after removal of a column in two span frame (Hou et al. 2016)

Liu and Zhu (2018) conducted a study on progressive collapse of steel frame structures with different lateral braces while vertical displacement is applied to the middle column. They established a nine story, two-dimension steel structure in SAP2000 and analyzed with static pushdown method and nonlinear dynamic method. Performance of the structures were compared with structural residual bearing capacity of the structures and defined as

$$RI = \left|\frac{P_c\delta_{max} - P_n\delta_n}{P_c\delta_{max}}\right| + \left|\frac{P_e\delta_e - P_n\delta_n}{P_e\delta_e}\right| \qquad \text{Eq. 2.7}$$

where, P_n is the nominal vertical design load and δ_n is vertical displacement of top on the removed column under static analysis, corresponding time t =1.0 s. P_c is structural collapse load under a column removed and δ_{max} is the ultimate vertical displacement when structure collapses. P_e and δ_e are the applied load and vertical displacement when the first plastic hinge occurs in some beam. Figure 2.15 shows location of plastic hinges in the frames. Analytical results showed braces enhance the residual bearing capacity of a structure due to energy dissipation of braces and X-shape braces are better than V-shaped one.

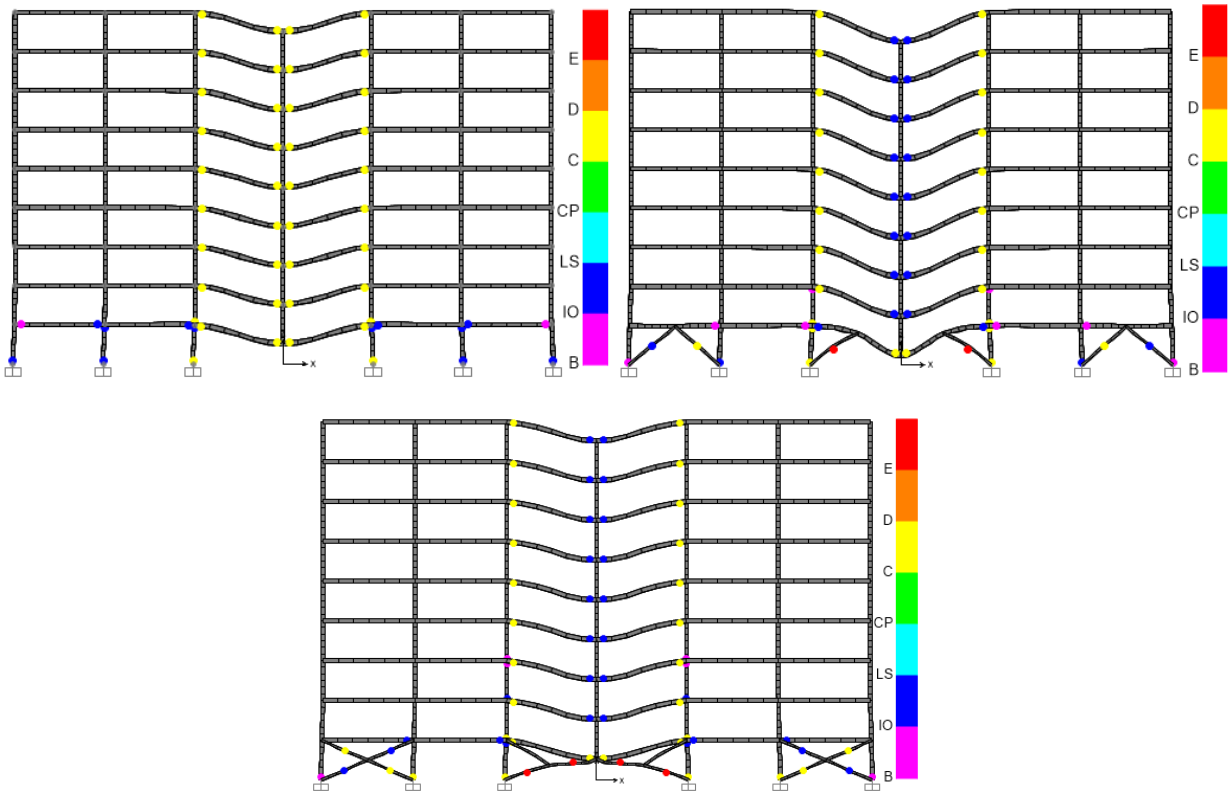

Figure 2.15 Location of plastic hinges in the structures with different braces (Liu and Zhu 2018).

Ameri et al. (2019) conducted a numerical analysis to investigate the effect of progressive collapse on redundancy of RC structure. 16 finite element models were designed in Open Sees and several damage scenarios including column removal at different locations (in plan and elevation) were considered. Finally, some predictive graphs were proposed to estimate the response of structures to progressive movement of columns. Based on analysis of results, an equation to predict rotation of beam adjacent to removal column was developed with curve fitting method as seen in Figure 2.16 and Figure 2.17. They also derived an equation correlating between beam rotation and degree of indeterminacy. These graphs make it possible to estimate the rotation of beams and developed moment at the hinges and compare with allowable one as well. It is worth noting that moving a column at the corner led to larger rotation in adjacent beams and that rotation increased while the removed column was at upper floors. Furthermore, removing middle column generated greater axial force.

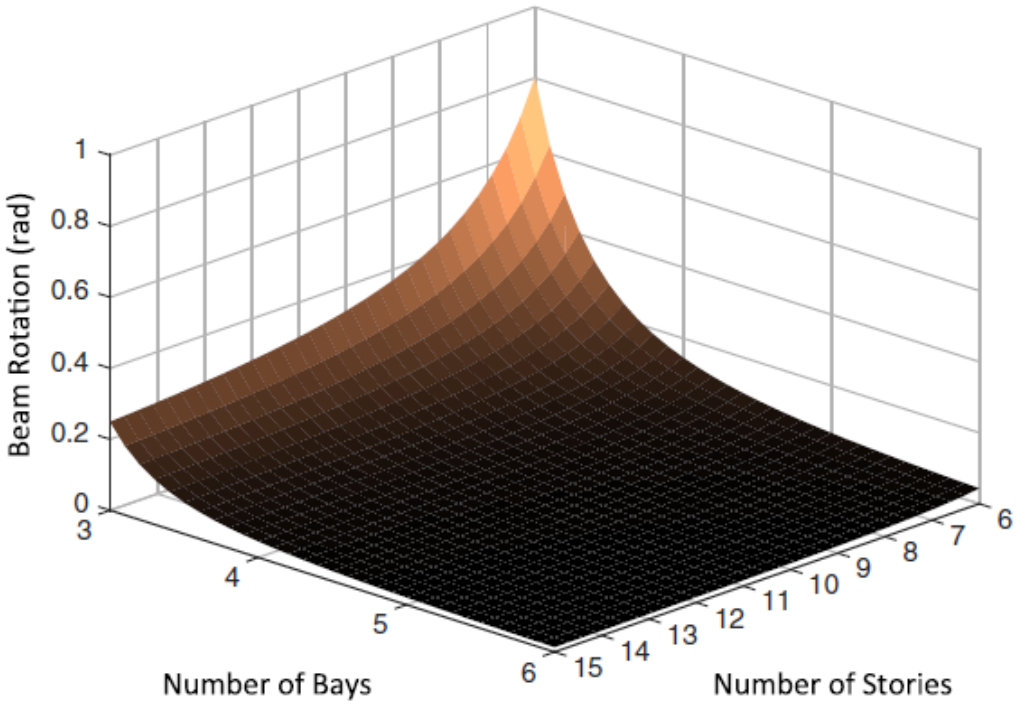

Figure 2.16 Beam rotation estimation based on number of stories and bays (Ameri et al. 2019).

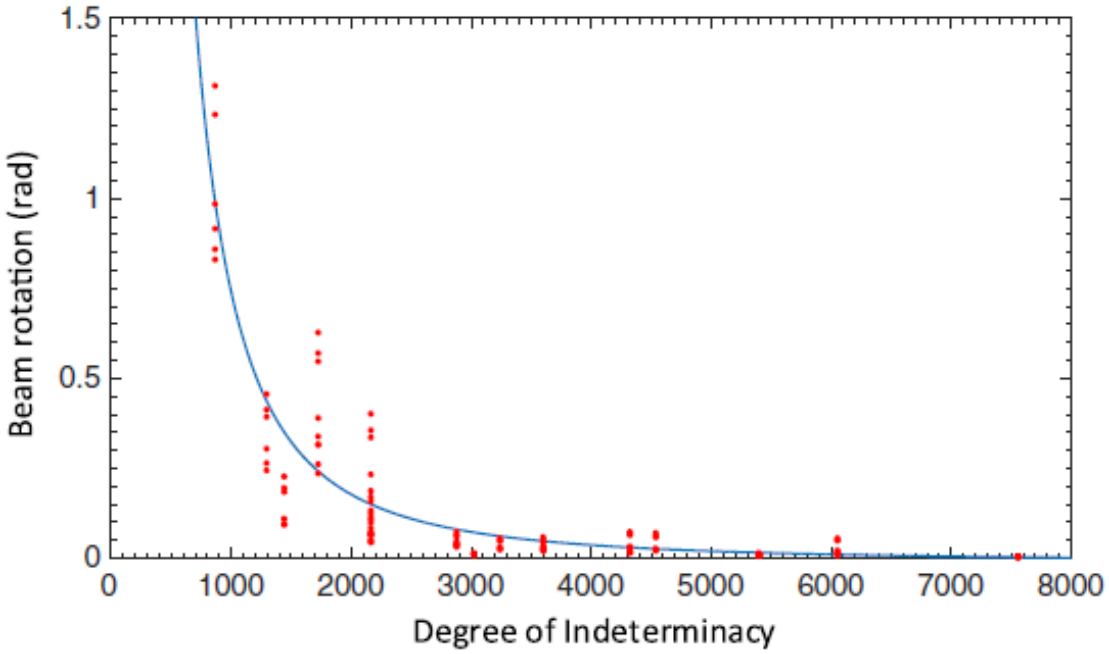

Figure 2.17 Prediction of beam rotation in correlation to degree of indeterminacy (Ameri et al. 2019).

Hanna et al. (1981) have analyzed a multi-story framed structure due to differential settlement. The program can calculate actual bending moments in members of structure induced by settlement. Additionally, Hanna et al. introduced a three-step procedure for structural engineers to facilitate the design of economical and safe structures, namely:

(1) Design the building for the external loading cases and then determine the tolerable settlements of the foundation.

(2) Superimpose the moments in the structure due to external loads and the differential settlement, then obtain the forces in the foundation.

(3) Design the foundation to tolerate the allowable settlement; accordingly, the foundation should be designed for the superimposed loads to limit the settlement to the allowable value.

In order to consider the nonlinear performance of the building, Lin et al. (2017) further investigated the structural response to a prescribed 75 mm settlement assigned to the center column with a three-dimensional (3-D) finite element model developed by the program SAP2000 (CSI 2013), where the scenario of the center column settlement represented the most critical case for a building (proofed by Lin et al.). The building performances in linear and nonlinear states due to the settlement of the center column were discussed, and some important findings are summarized below:

(a) During the nonlinear pushover analysis, the plastic hinges were formed in the beams first, followed by columns. Furthermore, the plastic hinges were first developed first in the beams on the first floor and then progressed to higher floors. In the columns, the hinges were concentrated on the first floor. Accordingly, it can be reported herein that the differential foundation settlement will cause more damage to the members in the lower floors than to those in higher floors. Therefore,

attention should be paid to the design of the elements of the lower floors if excessive settlement is expected.

(b) The threshold of the settlement in which the building performed elastically was about 25 mm, since significant inelastic deformations were observed when the settlement was larger than this value.

(c) Additionally, it can be concluded that there was a large vertical displacement in the column, and a large axial force developed in the column and the large bending moment of the beam, which are located at ground level. One should pay attention to the ground floor when designing buildings.

Although the study of the structural responses of the building due to the settlement of its foundation was analyzed in linear and nonlinear states with numerical modeling, the relationship between forces and settlement must be validated with an experimental study. Additionally, the damage of members due to the settlement of the foundation must be studied in detail and could be used to guide the design of the structure and foundation.

2.3 Requirements in Design Codes and Guidelines

According to building codes and current practice, including the National Building Code of Canada (NBCC), the differential settlement of the foundation should be assessed in the analysis or design stage of all types of buildings, and its effect on the supported structure should be checked to ensure that it is acceptable in terms of strength and serviceability. Although values of the allowable differential settlements have been recommended for certain types of structures, the current practice for the design of buildings, only as stipulated in the NBCC (2015), does not account for the effects of the differential settlement for the design of buildings.

Settlement of a building should be limited to prevent damage to services related to building

operations such as habitant comfort ability, openings and piping. However, differential settlement needs to be limited to assure structural strength. (Canadian Geotechnical Society 2006) proposed some limitation based on (Burland and Worth 1974) study. For frame structures, differential settlement is addressed regarding to angular distortion which is equal to differential settlement divided to overall distance which differential settlement occurs. For bearing walls, deflection ratio should be limited. Deflection ratio equals to relative sag or hog divided to the wall length. The above-mentioned parameters are illustrated in Figure 2.18 and allowable limits are presented in Table 2.3. The values in Table 2.3 may be used for shallow foundation and low risk building or an initial guide for high risk building. (Canadian Geiotechnical Society 2006) advised to consider recommendation provided by (Boone 1996) and deep investigation should be implemented by both structural and geotechnical engineers to adequately address limit state criteria.

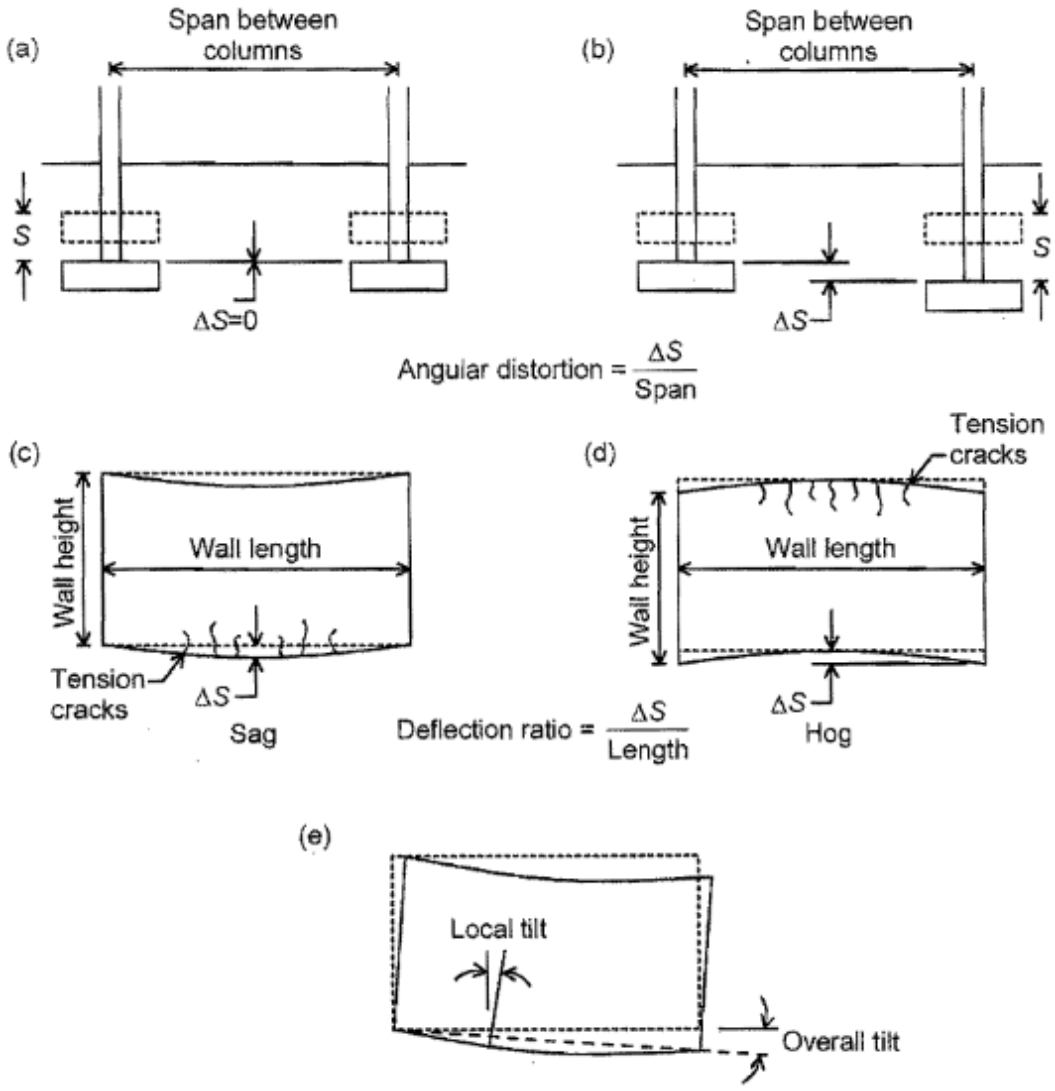

Figure 2.18 Illustration of angular distortion and deflection ratio (Canadian Geotechnical Manual, 2006).

Table 2.3 Limited values for framed structures and bearing wall to consider differential settlement (Canadian Geotechnical Society 2006).

Type of Damage	Criterion	Limiting Value
Structural damage	Angular distortion	1/500-1/250
Cracking in walls & partitions	Angular distortion	1/500-1000
Visual appearance	Tilt	1/300
Connection to services	Total settlement	50-75 mm: sands 50-135 mm: clays
Cracking by relative sag	Deflection ratio	1/2500: wall length/height=1 1/1250: wall length/height=5
Cracking by relative sag	Deflection ratio	1/5000: wall length/height=1 1/2500: wall length/height=5

ACI Committee 318 (2014) states differential settlement may severely affect structures and geotechnical recommendation should be taken into consideration. It is advised to provide ductile connection to accommodate differential settlement. Although differential settlement is not considered in load combination, it should be included in load combination if it severely affects safety and performance of structure. The load factor needs to reflect uncertainty related to magnitude of differential settlement and simultaneous occurrence with other loads. However, the load factor may not be considered less than one.

(ASCE/SEI 7-16 2016) classified the structures to 4 risk categories based on the risk to human life, health and welfare as described in Table 2.4. According to section 12.13 of (ASCE/SEI 7-16 2016), foundation should be designed to support gravity and earthquake loads and combination of them. (ASCE/SEI 7-16 2016) provides some limits to permanent horizontal displacement induced by earthquake motion as described in Table 2.4. It also mentioned, that the foundation faced differential settlement caused by liquefaction should still support the structure. For structures classified in Risk Categories II and III, the remained strength of members and connection might be at least 67% of the nominal strength of undamaged structure considering nonlinear behavior of the structure. For structures assigned to Risk Category IV, the demand strength when subjected to the differential settlement should not exceed the element's nominal strength. Table 2.5 provides limitation to differential settlement to assure of collapse resistance.

Table 2.4 Risk category of buildings (ASCE/SEI 7-16 2016).

Use or Occupancy of Building	Risk Category
Buildings representing low risk to human life in the event of failure	I
All buildings not listing in Risk categories I, II and IV	II
Building the failure of which could pose a substantial risk to human life	III
Building designated as essential facilities	IV

Table 2.5 Differential settlement threshold (ASCE/SEI 7-16 2016).

Structure Type	Risk Category		
	I or II	III	IV
Single story structures with concrete or masonry wall system	0.0075L	0.005L	0.002L
Other single-story structures	0.015L	0.010L	0.002L
Multistory structures with concrete or masonry wall system	0.005L	0.003L	0.002L
Other multistory structures	0.010L	0.006L	0.002L

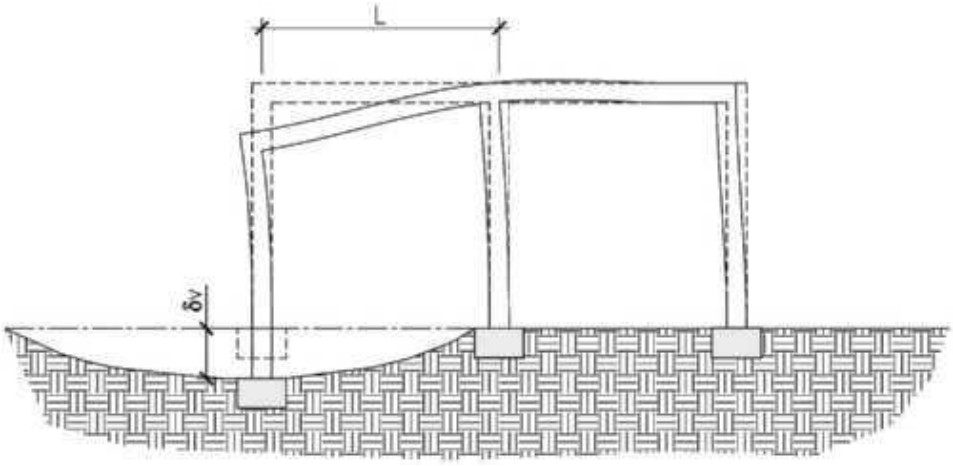

Figure 2.19 Differential settlement and parameters used in Table 2. (ASCE/SEI 7-16 2016)

In Hong Kong's Code of Practice for Foundations (2004), the following movement criteria (evaluated at the base of a shallow foundation or, for a deep foundation, the base of the pile cap) may be used as a reference for developing case-specific criteria: (a) The maximum total settlement should not exceed 30 mm; (b) The differential settlement between columns/vertical elements should be limited to 1:500; (c) The maximum angular rotation should not exceed 1:500 due to wind or other transient loads. These criteria should be assessed based on working loads. For Criteria (a) and (b), the full dead loads should be considered, and the imposed loads may be reduced.

The Korean Society of Architectural Engineers (2004) has recommended a general range of allowable maximum total settlements for frame buildings, which is from 100 mm to 150 mm and 20 mm to 60 mm for differential settlement.

Some allowable values of settlement are listed in some codes or standard. In the Soviet Code of Practice (1995), allowable values of settlements L/H and Δ/L are given according to type of building as shown in Table 2.6.

The European Committee for Standardization (1994) has provided limiting values for serviceability and the maximum accepted foundation movements, as listed in Table 2.7.

Table 2.6 Ultimate values of settlement of foundation for buildings and industrial structures.

Description of standard value	Subsoil	
	Sand and clay in hard condition	Clay in plastic condition
Slope of crane way, as well as tracks for bridge crane truck	0.03	0.03
Difference in settlement of civil and industrial building column foundations:		
(a) For steel and reinforced concrete frame structure	0.002 L	0.002 L
(b) For end rows of columns with brick cladding	0.007 L	0.001 L
(c) For structures where auxiliary strain does not arise during non-uniform settlement of foundations (L: distance between foundation centers)	0.005 L	0.005 L
Relative deflection of plain brick walls:		
(a) For multi-story dwellings and civil buildings		
at $L/H \leq 3$	0.003	0.004
at $L/H \geq 5$	0.005	0.007
(L: length of deflected part of wall; H: height of wall from foundation footing)		
(b) For one-story mills	0.001	0.001
Pitch of solid or ring-shaped foundations of high rigid structures (smoke stacks, water towers, silos, etc.) at the most unfavorable combination loads	0.04	0.04

Table 2.7 Accepted values of settlement (European Committee for Standardization, 1994).

Item	Parameter	Magnitude	Comments
Maximum acceptable foundation movement	S_T	25 mm 50 mm	Isolated shallow foundation Raft foundation
	ΔS_T	5 mm 10 mm 20 mm	Frames with rigid cladding Frames with flexible cladding Open frames
	β	1/500	—
	S_T	50	Isolated shallow foundation
	ΔS_T	20	Isolated shallow foundation
	β	≈1/500	—

The codes and guidelines provide a limitation for allowable settlement and differential settlement. It seems the structural effect of settlement and how this settlement generates extra stresses in a building, has not been fully understood. That lack of knowledge causes inefficient communication between structural and geotechnical engineers which would lead to uneconomical and unsafe design. This dissertation is trying to fill that gap and develop the basic mechanism of structural responses to differential settlement with experimental study and numerical modeling.

2.4 Summary

In the literature, researchers focused on the soil and the geographical impacts on the aboveground superstructures. Others focused purely on aboveground structures. There is very little literature that explores the impact of differential settlement on the structural elements of a building regarding load redistribution. This is due to the poor communication between the designers of superstructure and substructure for structural responses to the differential settlement of the foundation. Highly problematic experimental tests lead to less experimental study on this topic. The study of responses of structures to differential settlements relies heavily on empirical equations and is highly uncertain due to a lack of theoretical analysis and test validation. No researchers have attempted to examine the nonlinear performance of structures except for Lin et al. (2017).

This research will serve to add value to the existing literature and outline the critical structural elements and their failure modes that are important for building safety and economic design.

Chapter 3

Experimental Investigation

3.1 General

This chapter presents the description of the set-up of a 4-story, 4-bay structure made of aluminum developed in the laboratory, as well as test procedure and test results. Details of the material used, loading and measuring devises is also given. The set-up is capable to allow one column to settle while the rest of the structure remained in location. In this investigation the settlement of a corner, edge and center columns will be investigated.

The stresses and strains developed in beams and columns will be recorded by data acquisition system during loading. The present test results will be used to validate the numerical model developed in this investigation.

3.2 Experiment Setup

3.2.1 Testing Frame

In order to accommodate the testing facility in the structure lab at Concordia, a down-sized aluminum frame building was proposed. The frame has four spans in longitudinal and transverse directions, and each span is *45 cm*. The story height is *25 cm*. Figure 3.1 presents the configuration of the set-up and Figure 3.2, present the connection used between beams, columns and the base. The beams are of a rectangular section, measures *2.54×3.81 cm* (i.e., *1″×1.5″*), while columns are *5.08×5.08 cm* (i.e., *2″×2″*). The beams and columns were connected using angles (Angles type *I*: *2.5″×2.5″×1″×0.375″*) tied with bolts (Bolt type *I*: Length 1", thread size *3/8"-16*; Bolt type *II*:

Length *3"*, thread size *3/8"-16*). Bolts "*I"* were screwed to the columns and Bolts "*II"* were screwed to the beams. The columns were connected to square plates (*H3"×W4"×L4"*) with angles (Angle type II: *1.5"×1.5"×2"×0.375"*) and bolts (Bolt type III: Length *1"*, thread size *3/4"-10*). Moreover, all gaskets were fixed on a base (*82.723"×82.723"×1"*). In order to facilitate the realization of the column settlement, removable gaskets are placed under the columns. All gaskets connect the column and the foundation in a rigid connection. The real down-sized frame building shows as Figure 3.3.

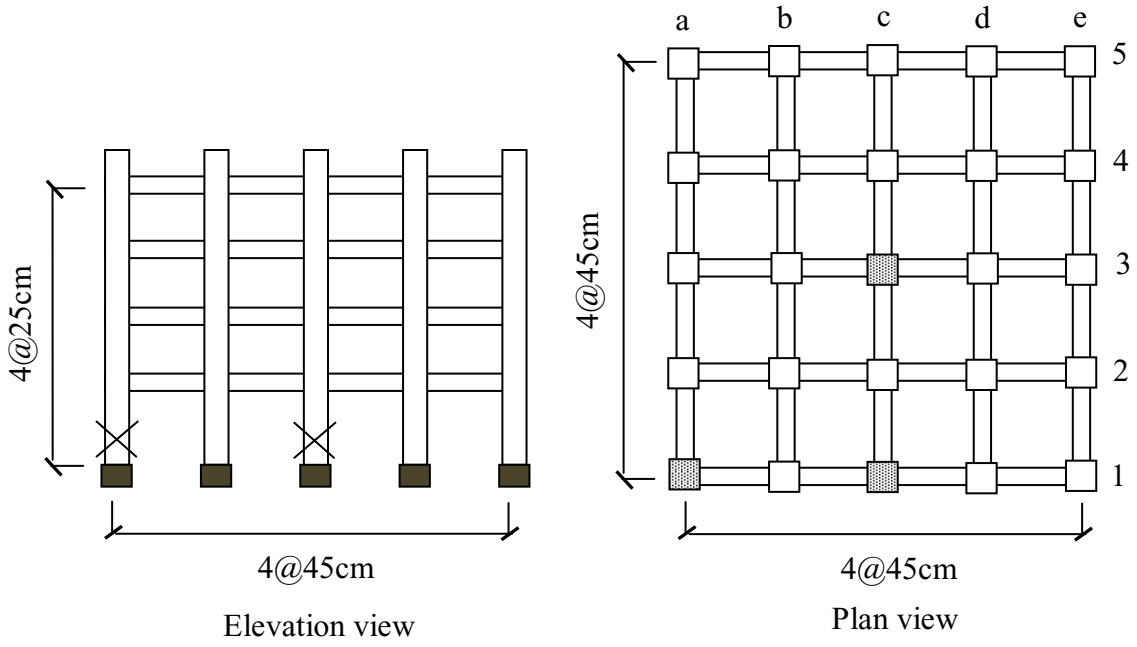

Figure 3.1 Building configurations (a) elevation view and (b) plan view

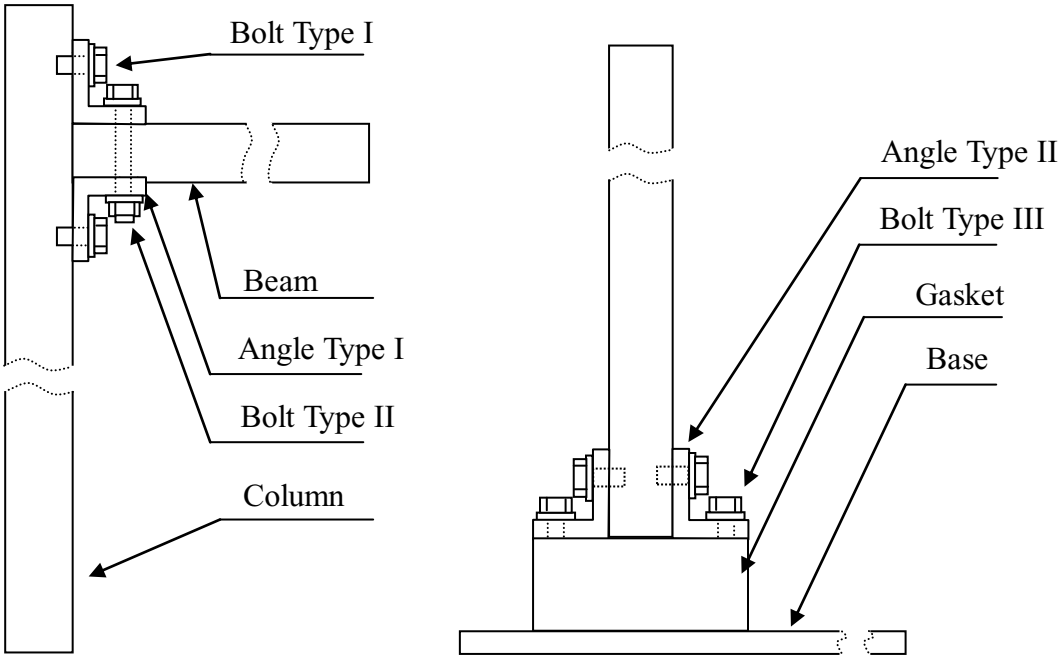

Figure 3.2 Connections details for (a) beam and column and (b) column, gasket, and base

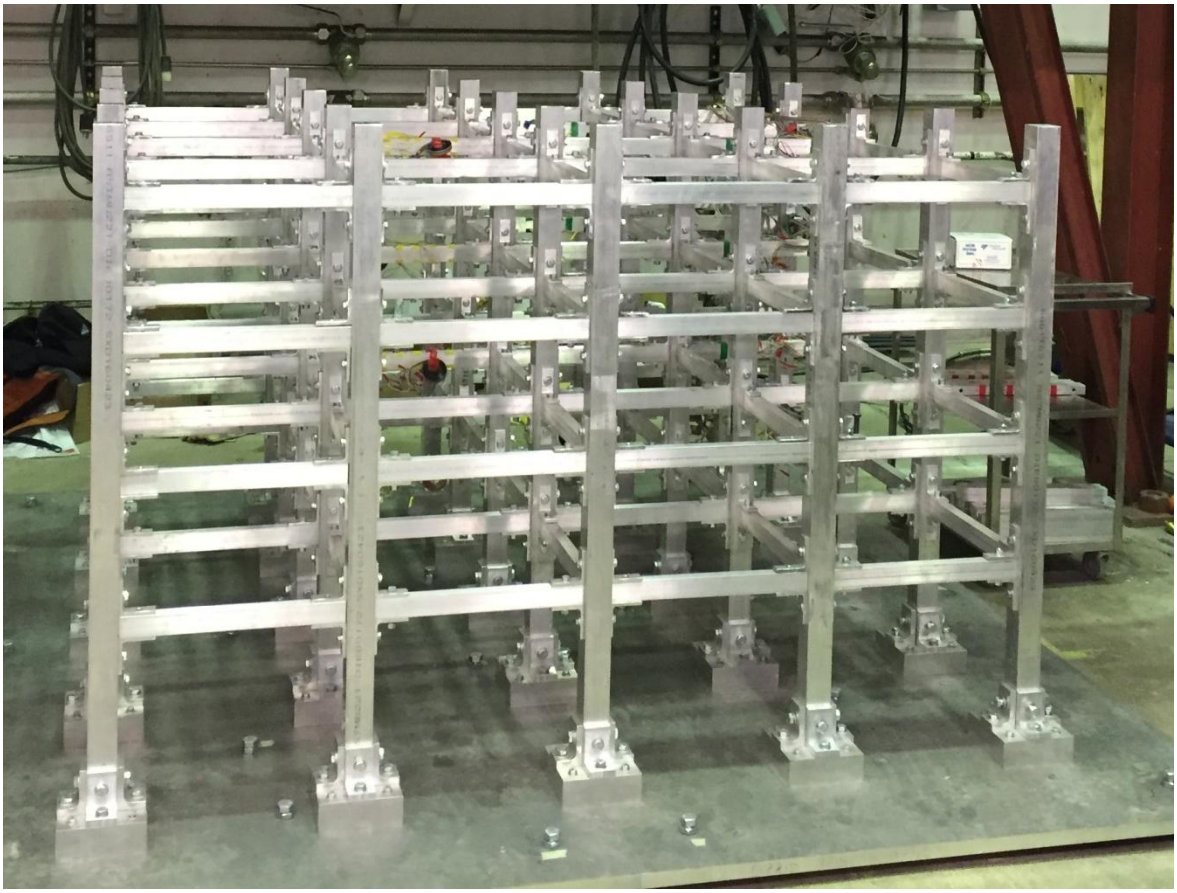

Figure 3.3 Experimental down-sized aluminum frame structure

3.2.2 Material

The beams, columns, gaskets and foundations, were made of T6061 aluminum. The material parameters, to include; yield strength (f_y), elastic modulus (E), ultimate tensile strength (f_u) and Poisson's ratio (v), are summarized in Table 3.1. The angles were constructed using high strength steel A36. Three specimens were selected to be examined using a tensile test in the lab. The results are presented in Table 3.2. The bolts used to connect the angles to beams and columns were made from Grade 9 aluminum. In order to determine the strength of the bolts, tensile tests were conducted on five samples. The tensile test results are provided in Table 3.3.

Table 3.1 Properties of the main members of frame building (T6061 aluminum)

Symbol ID	f_y(MPa)	f_u (MPa)	E(GPa)	v
S-1	241.26	308.78	68.81	0.30
S-2	240.23	312.33	69.24	0.34
S-3	242.19	315.16	68.65	0.33
S-4	239.26	309.11	69.41	0.31
Average value	240.74	311.35	69.03	0.32

Table 3.2 Properties of angles (Hot rolled steel A36)

Symbol ID	f_y(MPa)	f_u (MPa)	E(GPa)	v
A-1	258.19	532.18	197.25	0.26
A-2	259.03	532.45	199.14	0.28
A-3	258.67	533.67	201.27	0.27

Table 3.3 Properties of bolts

Grade 9	**#1**	**#2**	**#3**	**#4**	**#5**	**Average value**
f_u (MPa)	1241.12	1243.05	1239.87	1242.32	1245.12	1242.30

3.2.3 Setup of the Structure

The members of the frame building were fabricated in the laboratory according to the design given in section 3.2. The frame includes 160 beam pieces, 25 column pieces, 640 angle pieces, 25 plate pieces, and a 1-piece base. Figure 3.4 depicts the materials used in the project. Figure 3.5 presents the beams, columns, angles, and the base connections.

Figure 3.4 Aluminum raw materials

(a) beams (b) columns

(c) base

(e) the angles, (f) an assembled base plate.

Figure 3.5 Connection details of a column and the base

The assemblage of the frame was made in five steps:

Step 1: The base of the frame was placed beneath the supporting frame, and the horizontal level was adjusted using a measuring device before being fixed onto the floor with bolts. With a fastening torque of 515 N.m, the square plates were tightened onto the base, as illustrated in Figure 3.6.

Step 2: The frame of assembled columns and beams with bolts was fixed on the plates with a fastening torque of 68 N.m, as indicated in Figure 3.7.

Step 3: The strain gauges were then mounted on beams, columns, and angles, with B-502. Figure 3.8 reveals the electrical resistance strain gauges that were mounted on the beam of frame building (strain gauge, load device, and displacement instrument configurations are illustrated in detail section 3.5.

Step 4: A load device (hydraulic jack) was fixed on the top of the supporting frame, as shown in Figure 3.9, and was located directly above the prescriptive settling column.

Step 5: The data acquisition system was placed and connected to measuring instruments, which are divided into three categories: loading force, displacement, and strain. The test data acquisition system (DAS) used two systems in parallel. The loading force data acquisition used the DPM-3, and the displacement and strain used the BZ2205C acquisition system.

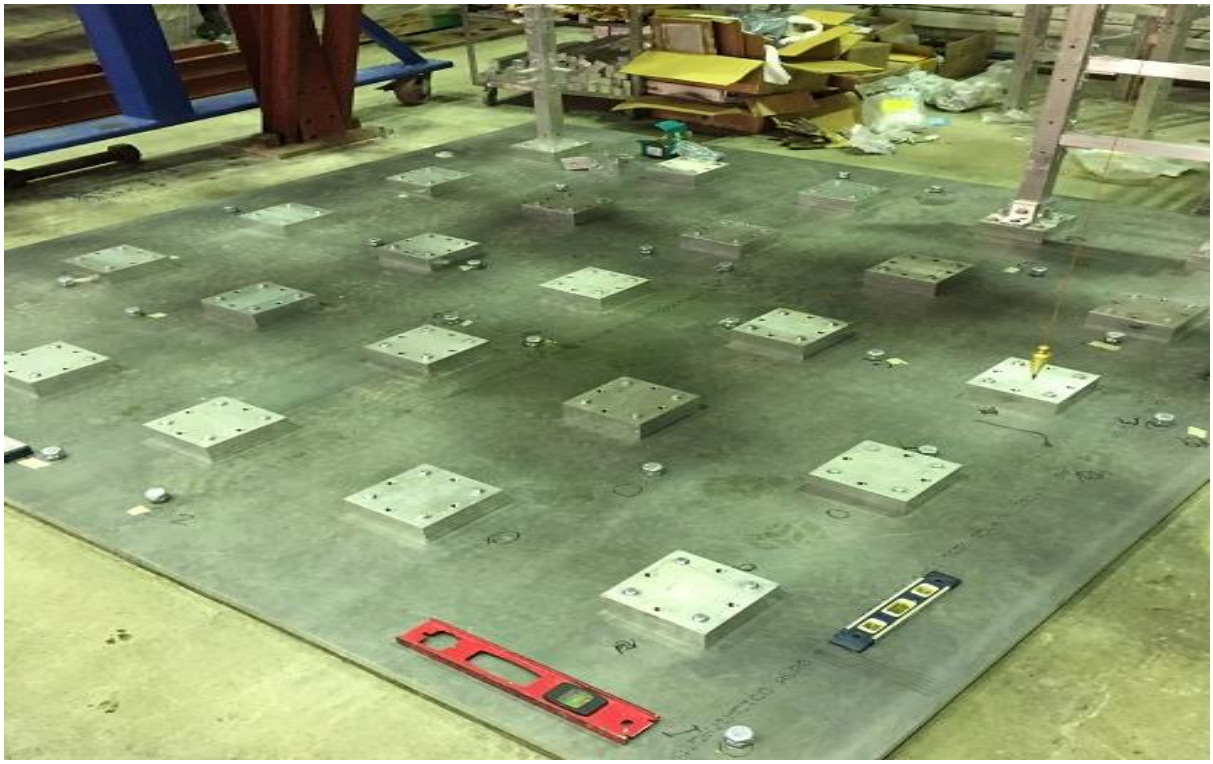

Figure 3.6 Base leveling

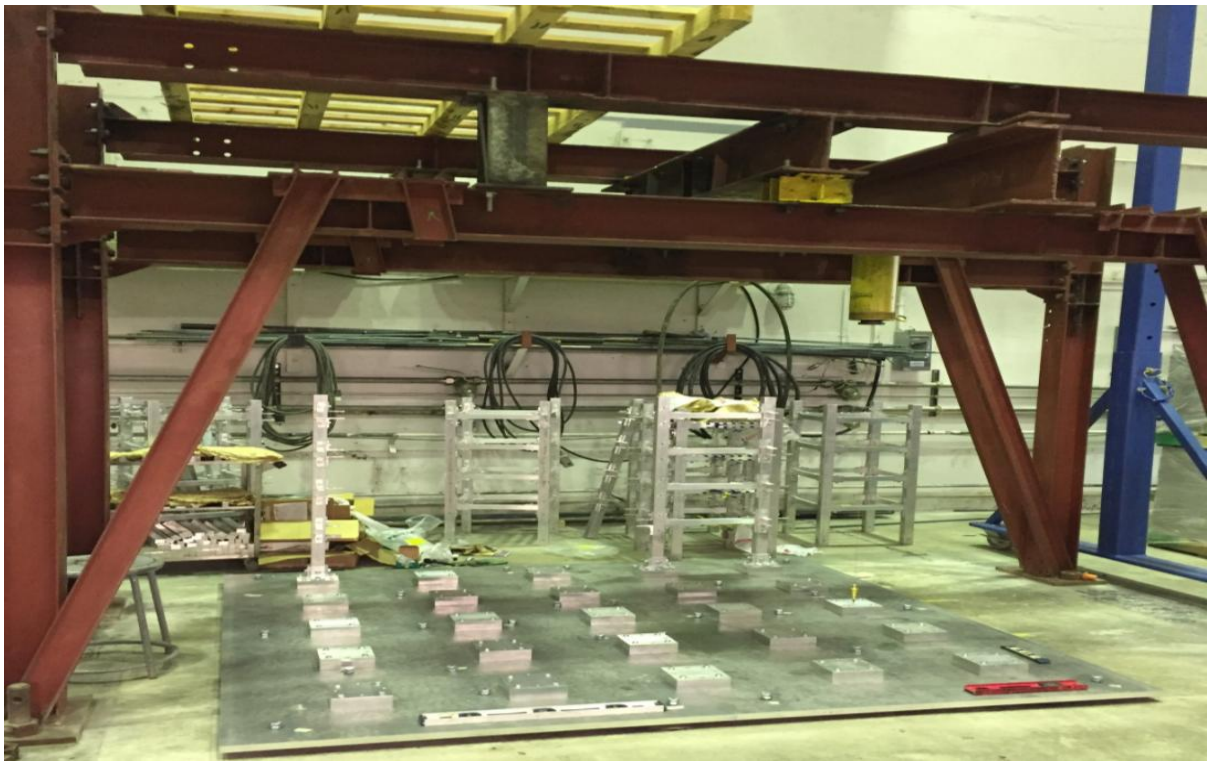

Figure 3.7 Assembling of columns and beams on the base

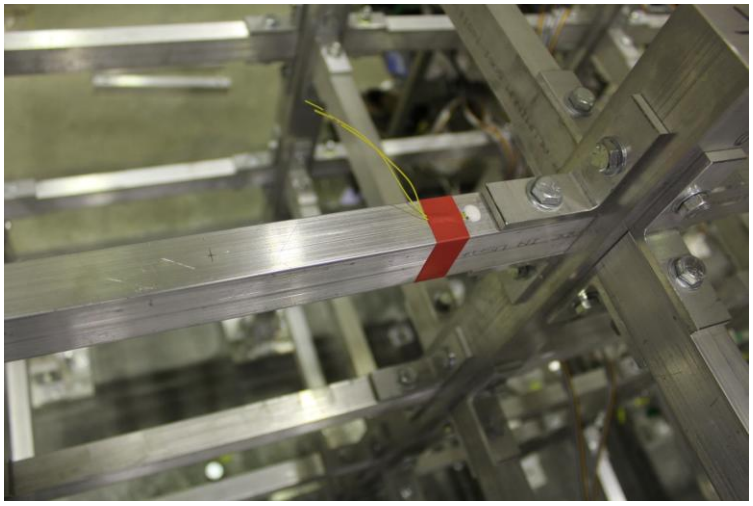

Figure 3.8 installation of strain gauge on a beam

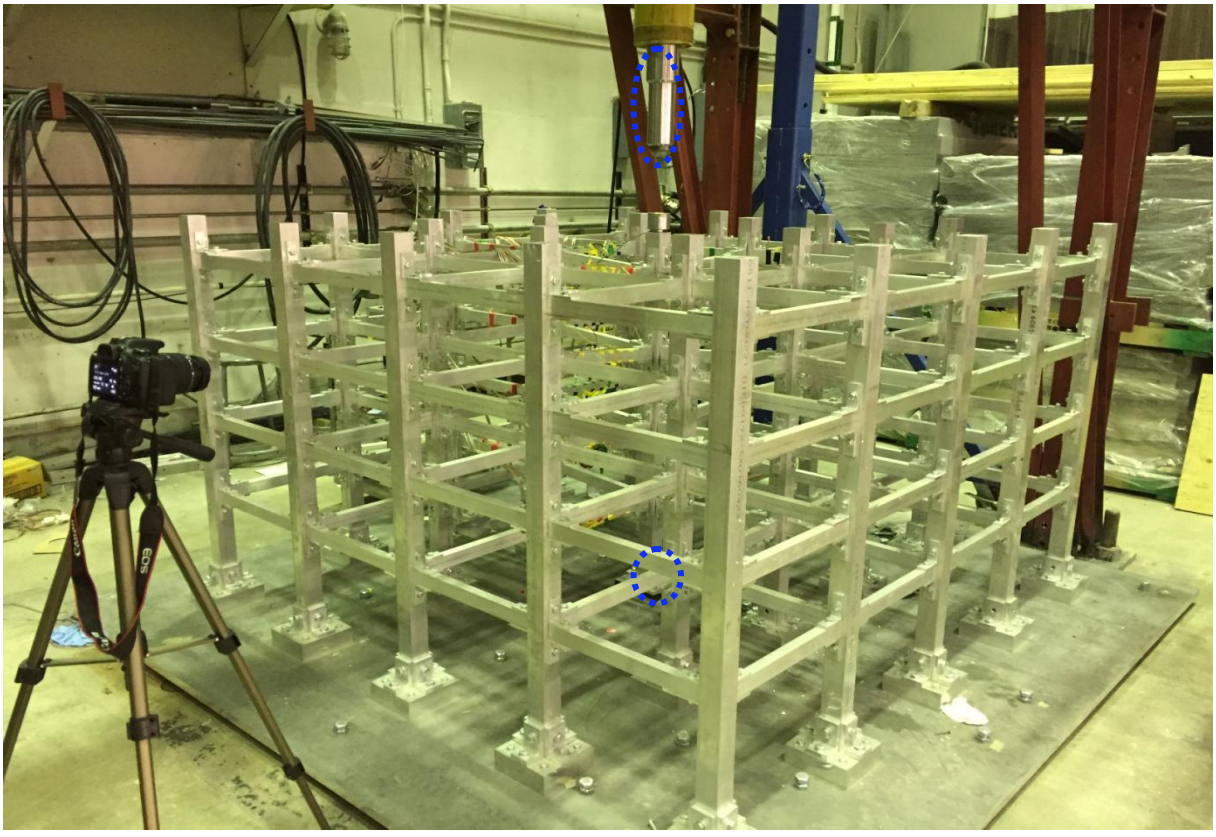

Figure 3.9 Final test setup

3.2.4 Measuring Devices

A load cell was placed on the top of the prescriptive settling column. The vertical displacement of the column was measured with a high precise Linear Variable Displacement Transformer (LVDT), which was placed beneath the settled column. To study the overall stress characteristics, the force transmission mechanism of the frame was recorded during testing. In order to measure the strain during the settlement of the column, resistance strain gauges were mounted at critical locations along the beams, columns, and angles.

The members of the frame were labeled with numbers, which are shown in Figure 3.10 and Figure 3.11. Figure 3.12 presents a diagram expresses the typical testing points and the loading location of column. In this figure, the red arrows show the loading location and the highlighted beams and columns are those tested for each case. Furthermore, the columns are named after the axis in both directions, and the beam were named as the distance between two columns.

Specifically: The c3 is the cross of the c frame and the 3 frames, and b3 is the cross of the frame b and the frame 3. The blue solid point is the testing point located in the end of beam b3c3 connecting to the column b3, which can be defined as b3c3. If the solid blue point located in the end of b3c3 connected to settling column c3, which will be defined as testing point c3b3. I, II, III, IV are the floor of the building. The solid green point is the testing point located in the column of c3 in IV floor, which sign should be IV-c3b3.

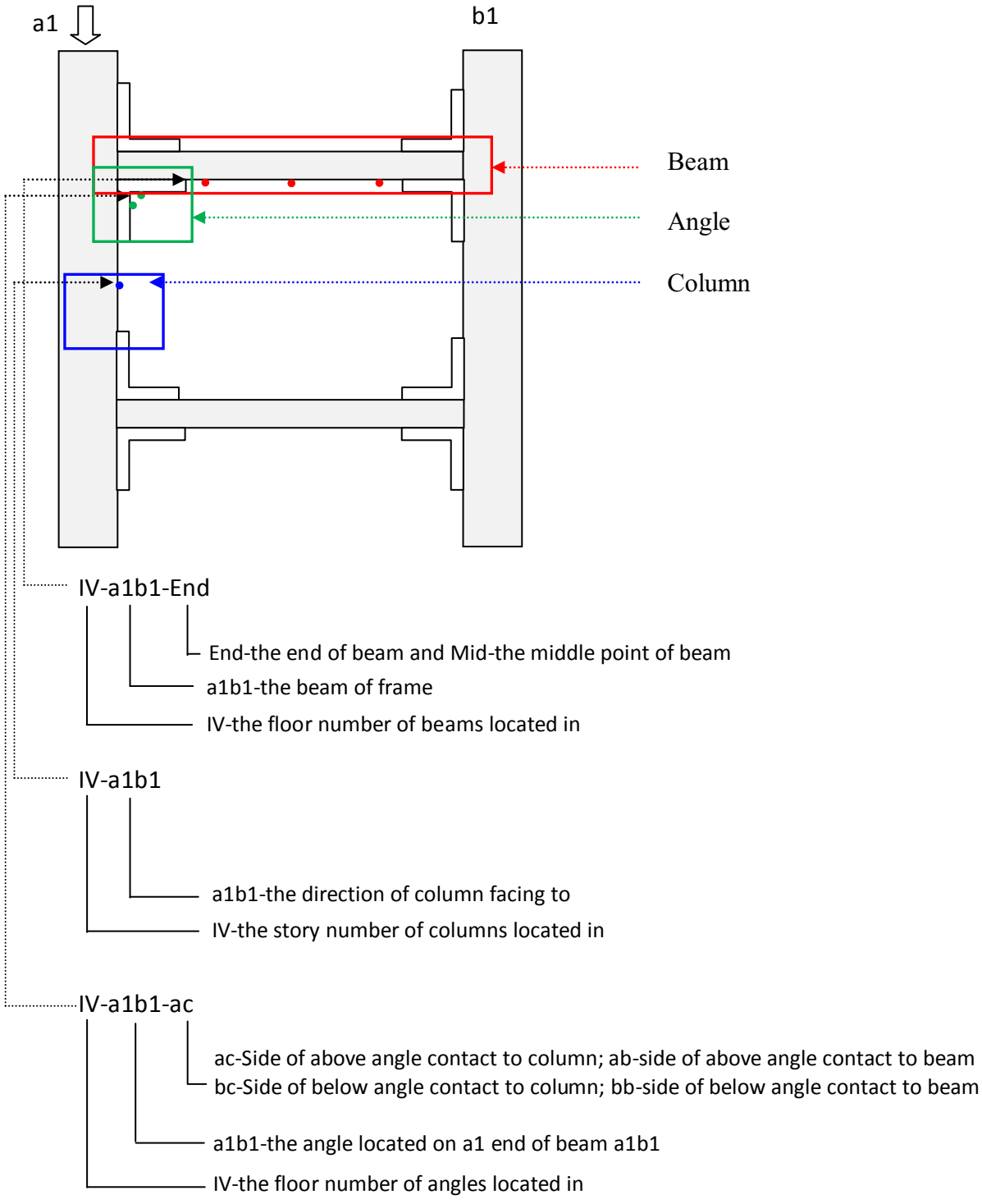

Figure 3.10 Definitions of testing point

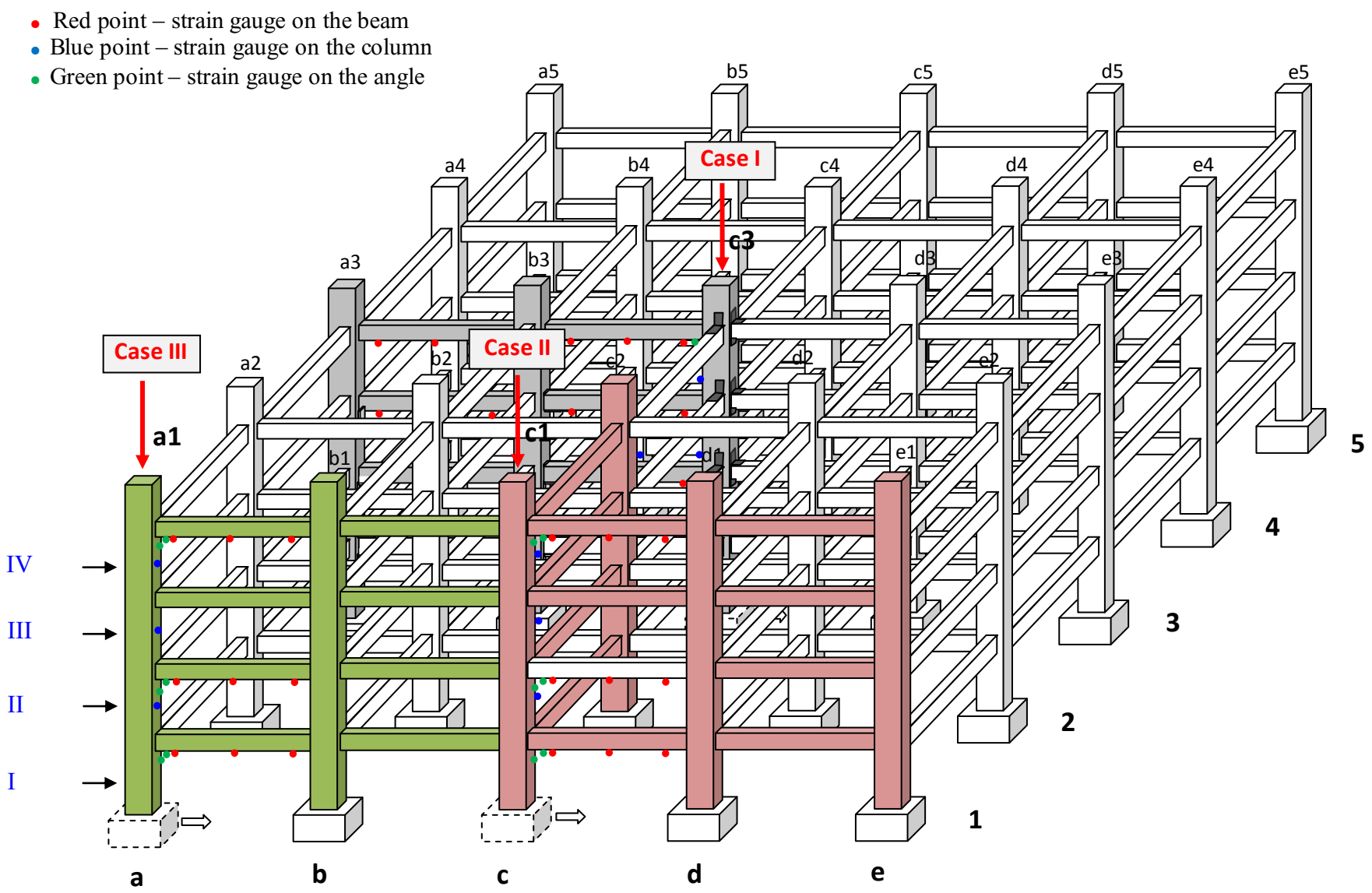

Figure 3.11 Sketch showing the highlighted testing beams and columns for three cases

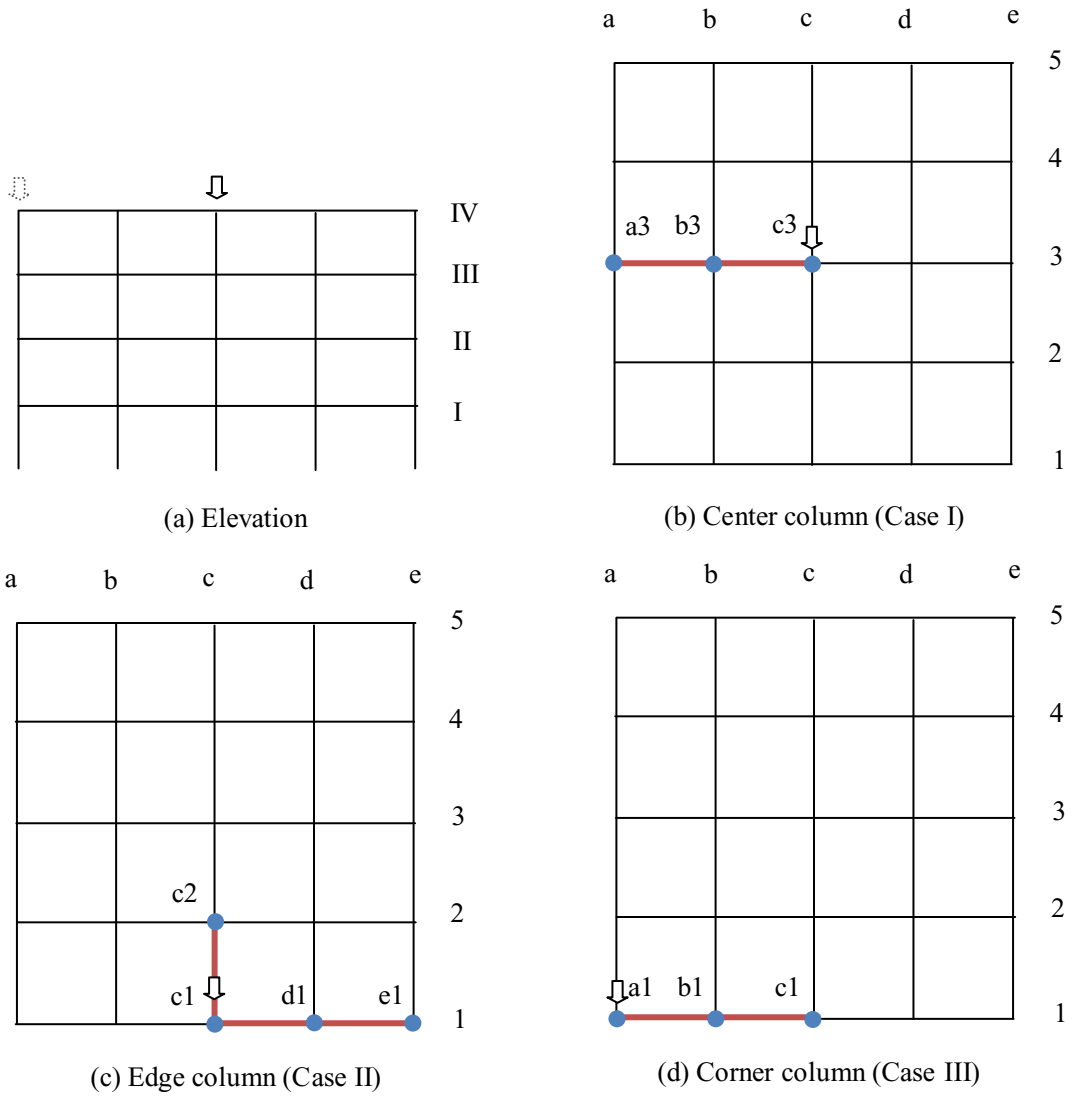

Figure 3.12 Sketch show the location of the three cases tested on elevation and top view

3.2.5 Test Procedure

In this investigation, three cases were tested, namely the settlement of the center column (Case I), edge column (Case II) and corner column (Case III). The test proceeded by removing the plates beneath the columns and the base for the assigned column to settle.

For Case I, the settlement of center column c3, which is indicated by the testing points listed

in Table 3.5, was measured. In Case II, the side settlement of column c1, which is represented by the testing points in Table 3.6, and for Case III, the settlement of the corner column a1, which is noted through the testing points listed in Table 3.7.

The tests were conducted by gradually applying the load to the top of the settling column on the frame. The loading was quasi-statically controlled (displacement control) by the loading system using a speed of 0.08 mm/s. The prescribed settling column moved downward until it reached a settlement of 50 mm. The loading process was recorded by a high-speed camera, which was fixed on a tripod that was placed on the floor near the frame. The strain, displacement, and loading force were measured and recorded during the loading process for the three cases tested in this investigation.

For the repeatability of the testing data, each test was conducted twice. All beams, angles, and bolts connected to the settling column were replaced with new ones after each test. In total, six tests were conducted in the laboratory.

3.3 Test Results and Analysis

3.3.1 Load-Settlement Curves

The load-settlement curves for three cases tested in this investigation are presented in Figure 3.13. Test results are summarized in Table 3.4, where δ_v is settlement of the column and f_v is the load applied on the top of settling column. It can be noted that for the center column, the relationship is linear (OA), then nonlinear (AB), beyond which the settlement will continue at no additional load. The nonlinear phenomenon of the relationship is due to the displacement of beams, which causes lateral force to resistant the loading force. Similar relationships were noted for the edge and corner columns. It also noted that the central column provides the highest

resistance to settlement, followed by the edge columns, and finally the corner columns.

In fact, the experimental frame is connected by beam to column connection with top and seat cleats angle. The deformation of the connection effects the forces developed in the structural element of the frame due to settlement of column. During the load-settlement curve, the above angle of beam starts to deform after the below angle of the beam. The beams and columns show no any deformation and keep its elastic properties. The settlement leads to beams down forward rotation and top of angle exceed the bearing capacity to deform. The top of above angle of beam bears the vertical load and the top of below angle of beam bears the lateral load, so the deformation in above angle of the beam is less than below angle of the beam.

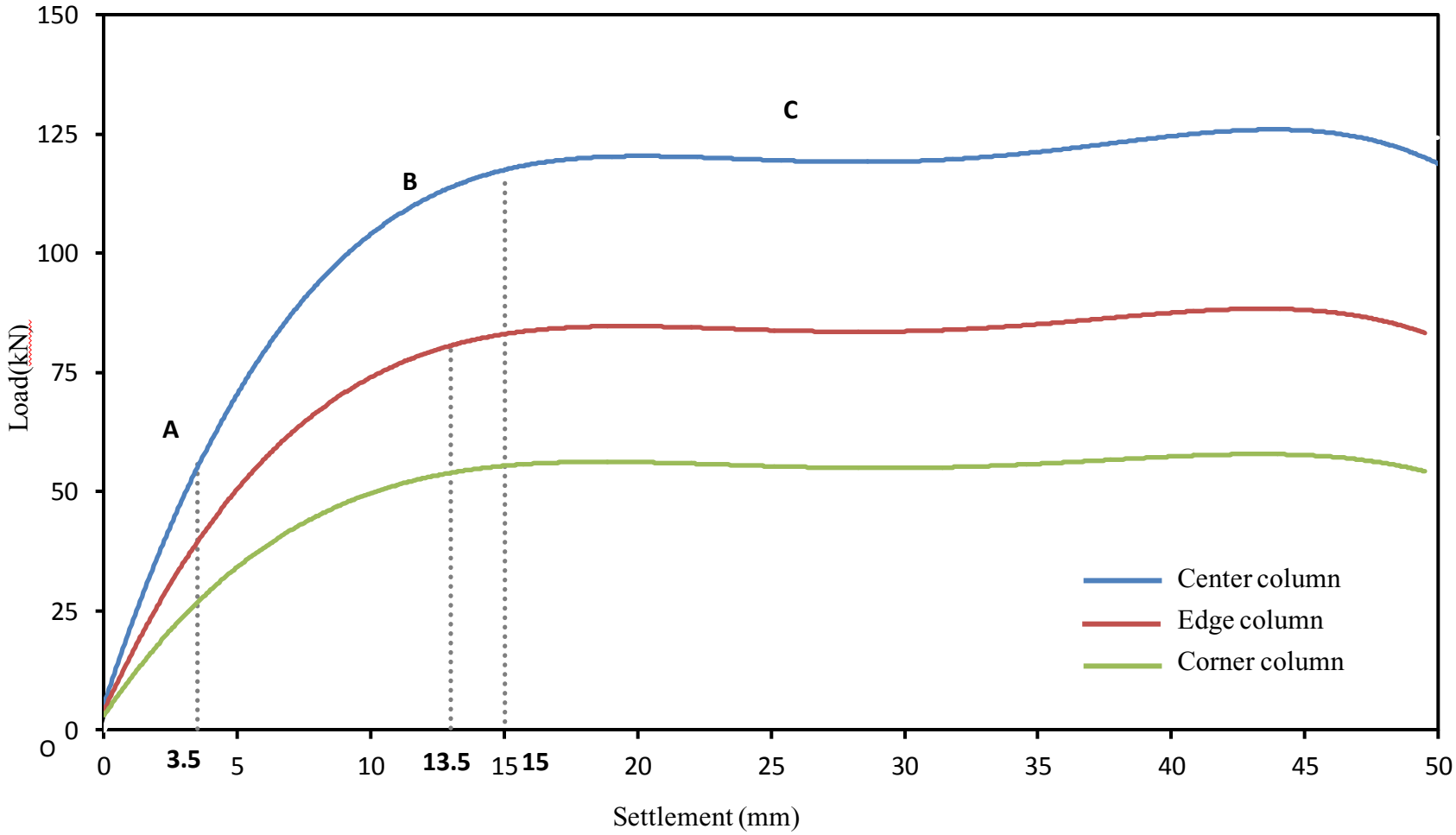

Figure 3.13 Load-settlement curves of three cases tested (Case I: center column; Case II: edge column; and Case III: corner column)

Table 3.4 Test results of the experimental investigation for the three cases tested

Items		Settlement (δ_v/mm)	Load (f_v/kN)	Fitting equation
Case 1	OA	0-3.50	0-55.817	$f_v = 15.859\delta_v + 1.618$, R^2=0.998
	AB	3.50-15.00	55.817-114.685	Nonlinear
	BC	15.00-50.00	114.658-124.264	$f_v = 0.2246\delta_v + 113.99$, R^2=0.811
Case II	OA	0-3.50.00	40.035	$f_v = 11.321\delta_v + 1.443$, R^2=0.997
	AB	3.50-13.50	40.035-80.284	Nonlinear
	BC	13.50-50.00	80.284-87.250	$f_v = 0.167\delta_v + 79.632$, R^2=0.778
Case 3I	OA	0-3.50.00	0-27.098	f_v=7.594δ_v+1.357, R^2=0.811
	AB	3.50-13.50	27.098-53.851	Nonlinear
	BC	13.50-50.00	53.851-57.435	f_v=0.076δ_v+53.507, R^2=0.653

3.3.2 Strain in Columns

Figure 3.14 presents the strain versus settlement for the center column c3. The positive and negative values present tensile and compressive strain, respectively. It can be noted that the settling column c3 is in compressive, while the neighboring column b3 and the edge columns a3 are also under compression, except for the columns in the first floor. The tension forces developed in column b3 and a3 are due to the axial forces developed by the beam in 2nd floor, which are higher than the compression forces applied on the column c3.

It is of interest to note that the maximum strain value was observed in column a3 in 1st floor, which explain the failure, which take place in exterior wall due to foundation settlement. Furthermore, the strain at column a3 was about 1/3 for the settling column c3 during the linear state. In additional, the free bottom end of Column c3 bears nearly no stress. Furthermore, the absolute value of the strain increases with the increasing of the floor level.

Figure 3.15 presents strain versus settlement due to 50 mm settlement assigned to the edge column c1. It can be noted that the strain values are negative for the tested points in the 2nd, 3rd and 4th floor, which has linear characteristic before settlement of 3.50 mm to 4.00 mm. The absolute amount of the strain in higher floors is larger than those for the lower floors. It is of interest to note that maxim strain recorded for the settling column c1 is about 2 times and 5 times of strain developed in Columns c2 and d1 respectively. Furthermore, the strain values for IV-c2c3 and II-d1c1 are positive during testing.

Figure 3.16 presents the strain versus settlement due to 50 mm settlement assigned to the corner column a1. It can be seen that the strain of IV-a1b1, III-a1b1 and II-a1b1 are negative. The relationship has linear characteristic up to settlement of 3.50 mm. And the strain of III-b1c1,

II-b1c1 and I-b1c1 are negative, but IV-b1c1 is positive. The maxim strain recorded for the settling column a1 is about 2 times of strain developed in Columns b1. But the maxim strain for settling column a1 is similar with strain developed in column b1 at the linear stage of settlement.

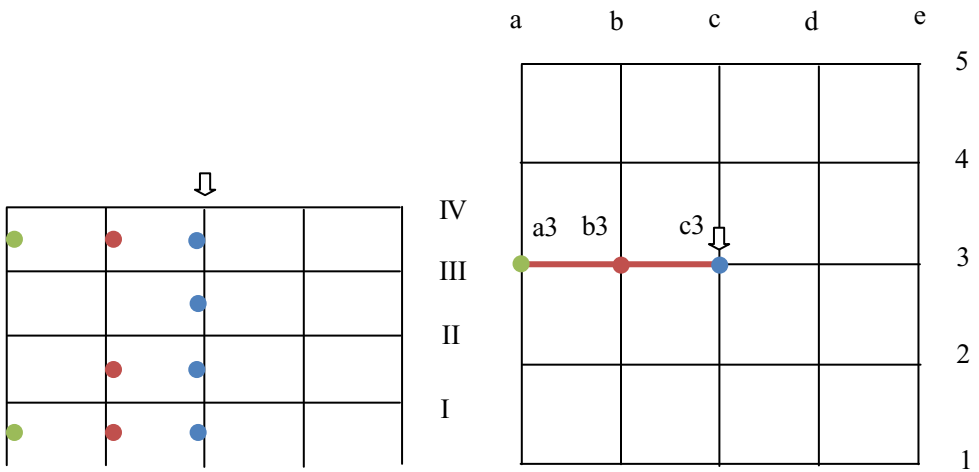

(a)

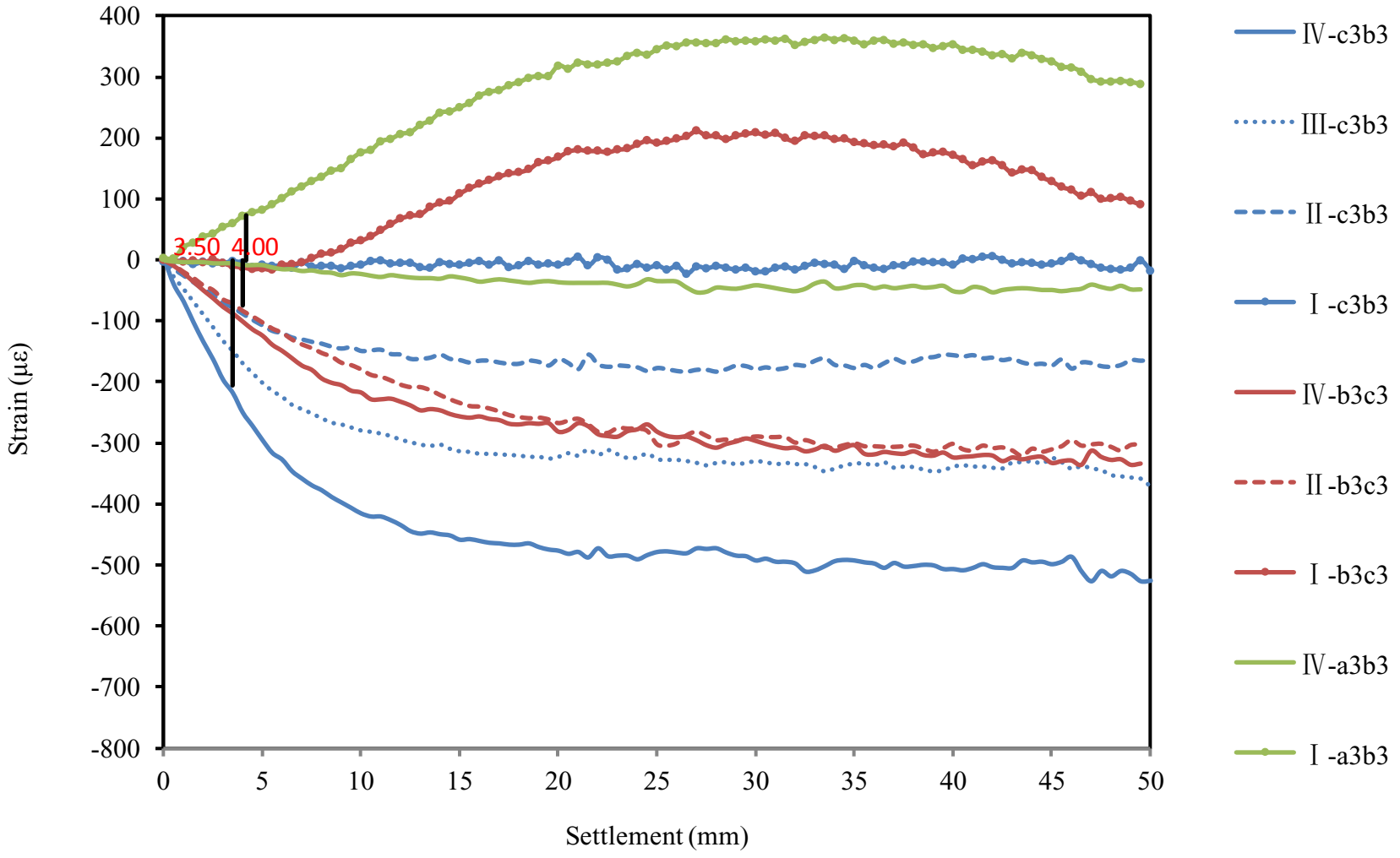

(b)

Figure 3.14 Strain vs. settlement curves for the center column c3 (Case I)

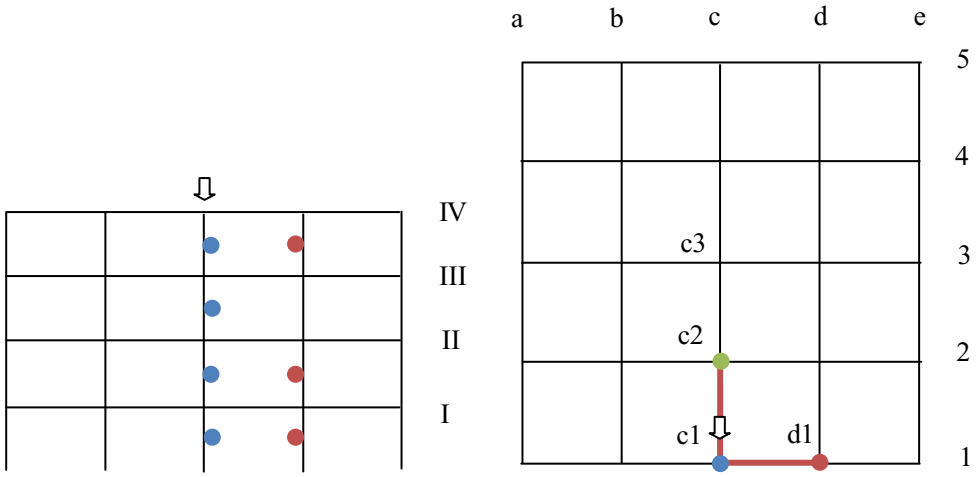

(a)

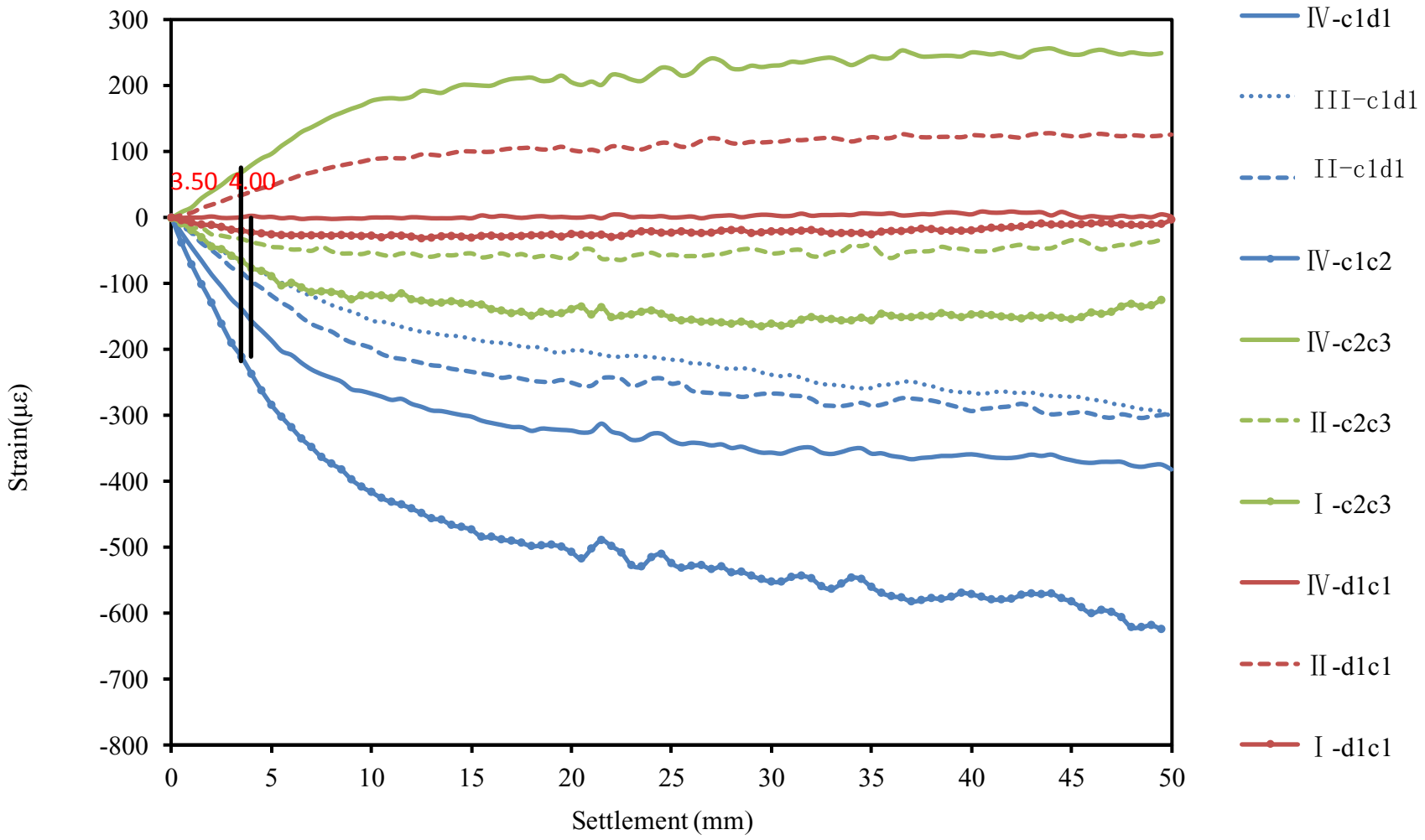

(b)

Figure 3.15 Strain-settlement curves at the middle points of the edge Column c1, c2 and b1 (Case II)

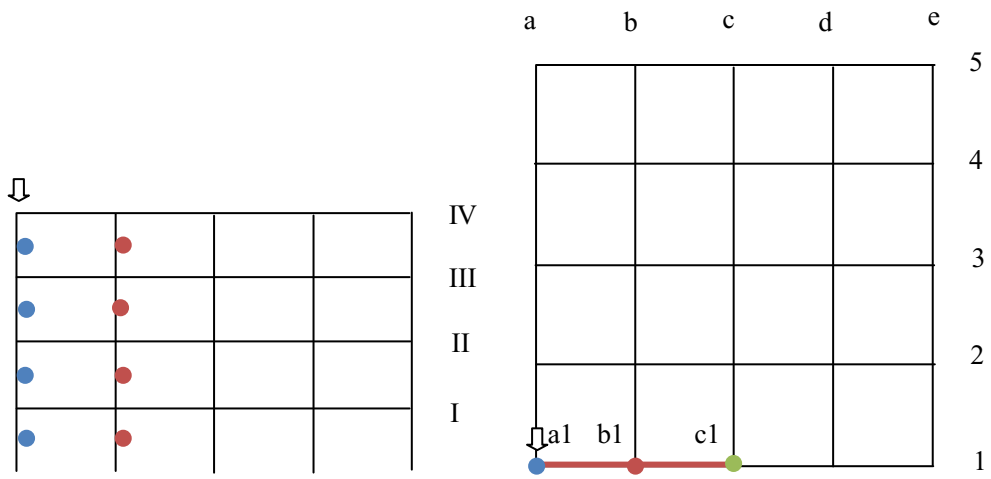

(a)

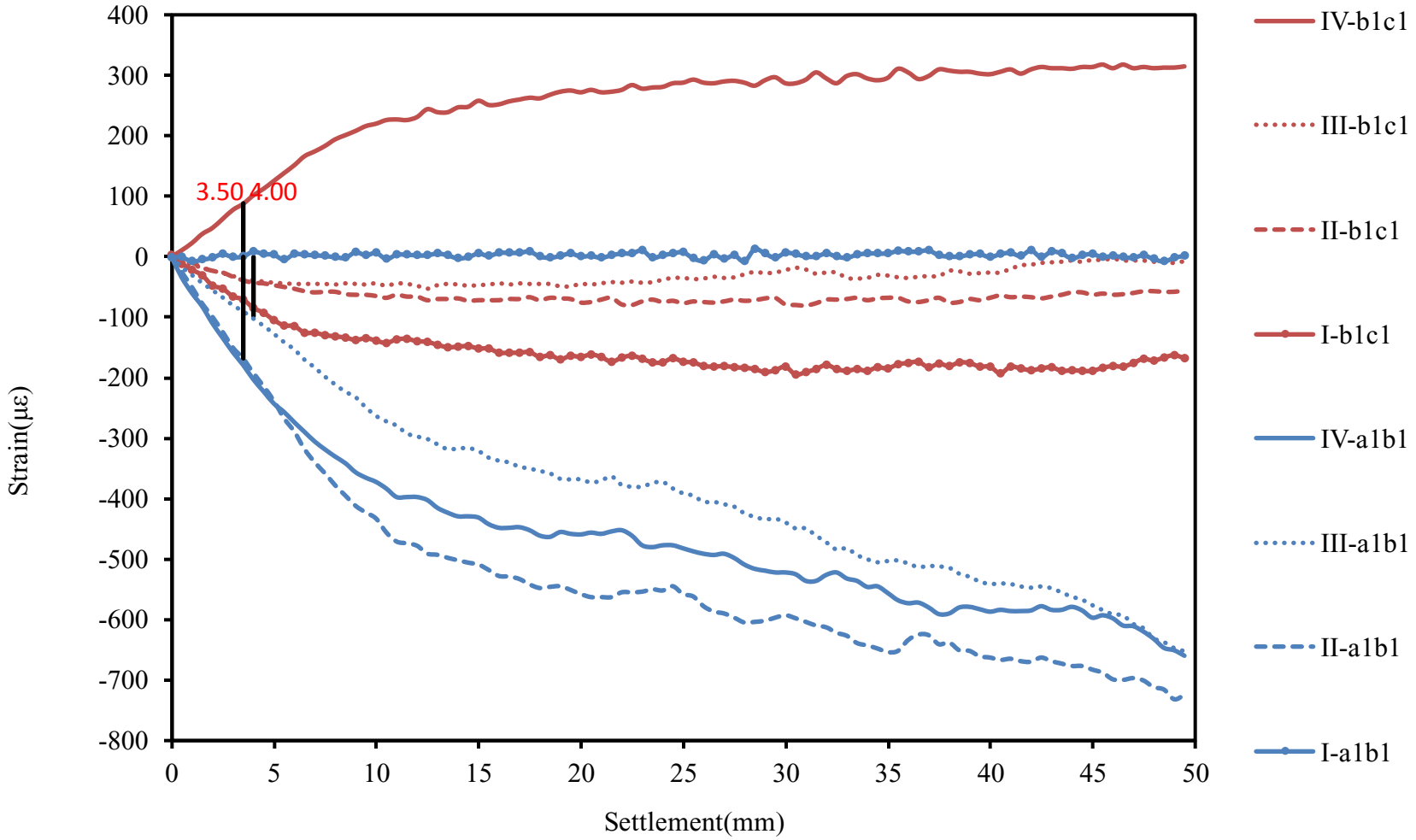

(b)

Figure 3.16 Strain-settlement curves at the middle points of the corner Column (Case III)

3.3.3 Strain in Beams

Figure 3.17 presents the strain developed below the surface of the beam due to the settlement of the column c3. The strain gages were installed below surface of both ends and the middle of beam c3b3, b3a3 and b3b4, as shown in Figure 3.17 (a).

It can be noted that the relationship is linear up to about 3.50 mm for the two ends of the beam, furthermore, the strain at the two ends of the beam are the same, with opposite signs. The maximum strain values on b3a3 are only around 1/5 of the strain on beam c3b3. The effect of settlement on beam b3a3 is negligible as compared to beam c3b3, especially during the linear state. In addition, it can be noted that the settlement of column c3 has almost no effect on beam b3b4.

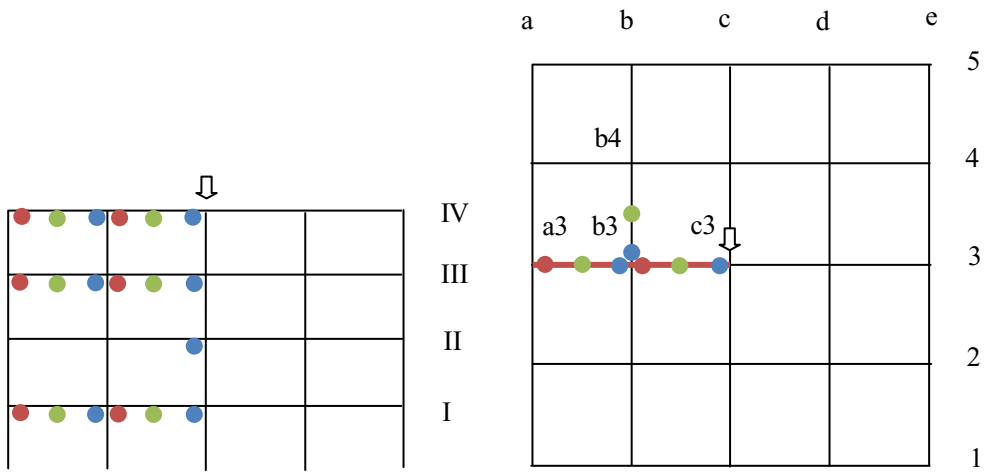
a
b
c
d
e
5
4
3
2
1
b4
a3
b3
c3
IV
III
II
I

(a)

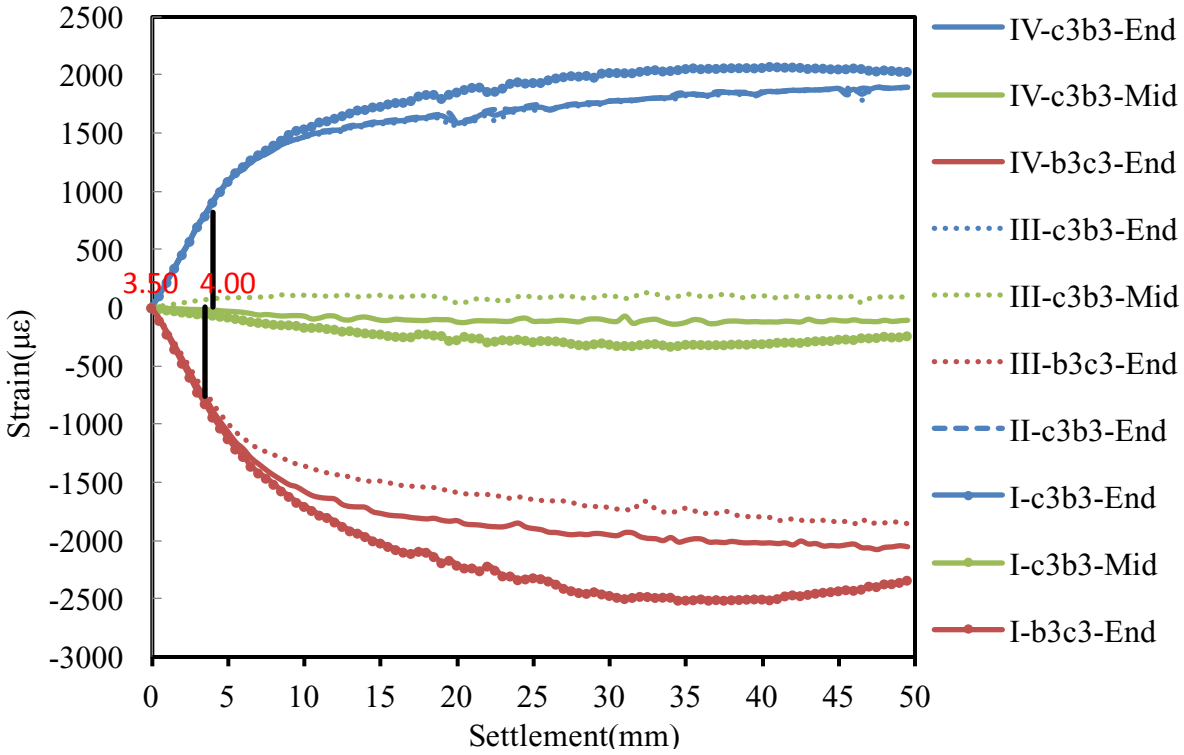
2500
2000
1500
1000
500
0
-500
-1000
-1500
-2000
-2500
-3000
3.50
4.00
Strain(με)
0
5
10
15
20
25
30
35
40
45
50
Settlement(mm)
IV-c3b3-End
IV-c3b3-Mid
IV-b3c3-End
III-c3b3-End
III-c3b3-Mid
III-b3c3-End
II-c3b3-End
I-c3b3-End
I-c3b3-Mid
I-b3c3-End

(b) beam c3b3

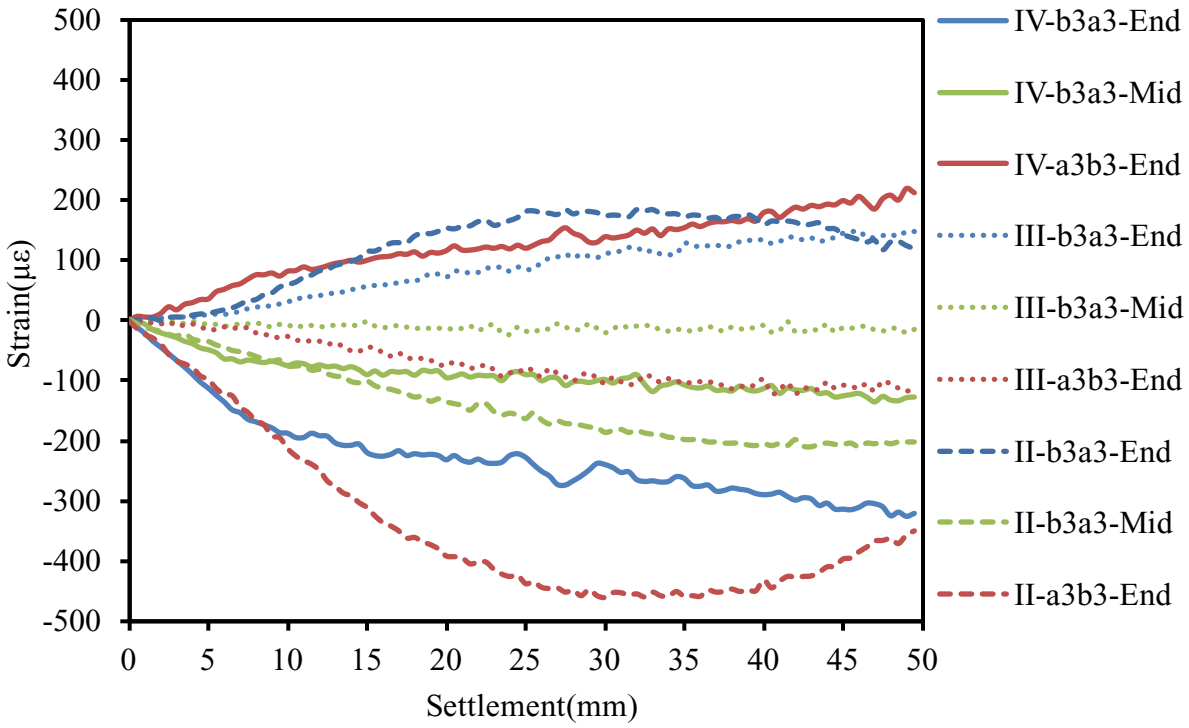

(c) beam b3a3

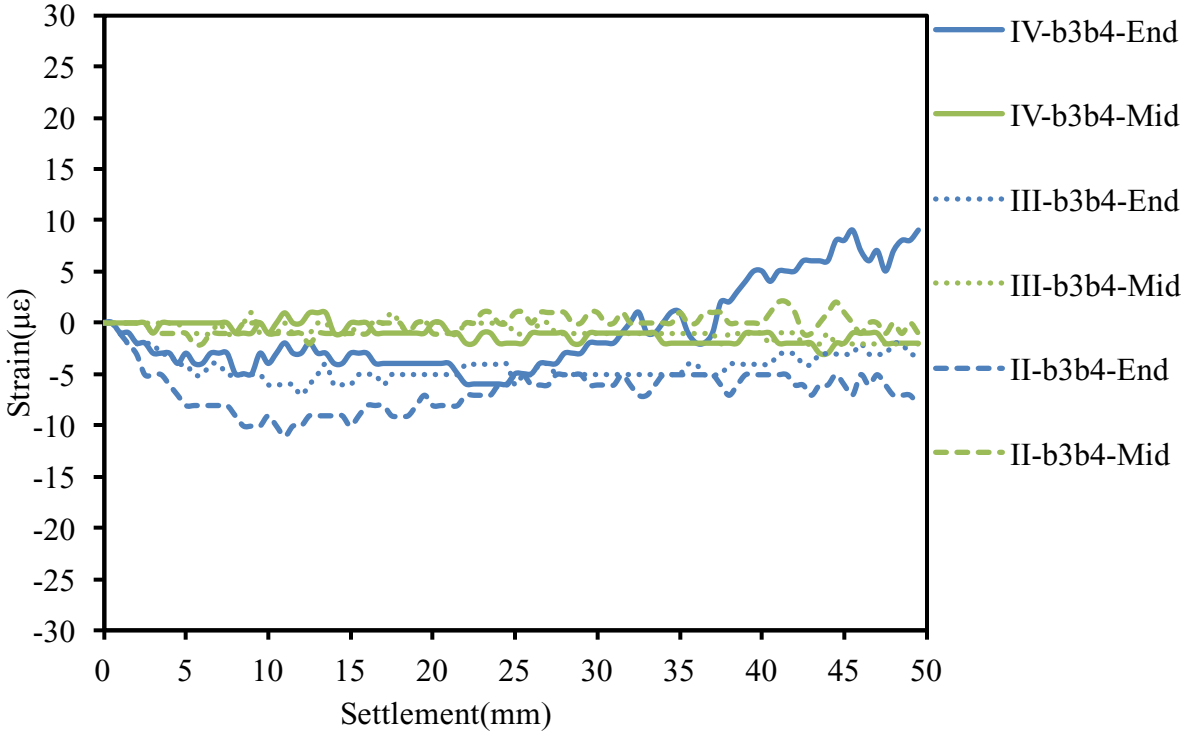

(d) beam b3b4

Figure 3.17 Settlement vs strain curves of the beam during the settlement of center column

(Case I)

Fig. 3.18 presents the strain developed in beams, due to the settlement of the edge column c1. Gages were installed at the surface of the two ends and at the middle beam c1c2, c1b1 and b1a1. It can be noted that the settlement of the edge column c1 on the two ends of the exterior beam c1d1 and interior beam c1c2 has basically similar strain values, with opposite signs. The relationships have a linear characteristic up to settlement of around 3.50 mm. In the non-linear stage, the strain value of the beam ends is higher in the bottom floor, followed by the top floor, then the third floor, and finally in the second floor. The strain values at the middle of the beam for all four floors are close to zero, which means that the maximum shear force takes place at the mid-section of the beams. Furthermore, the strain of the beam d1e1 are about 1/10 to 1/5, which can be negligible.

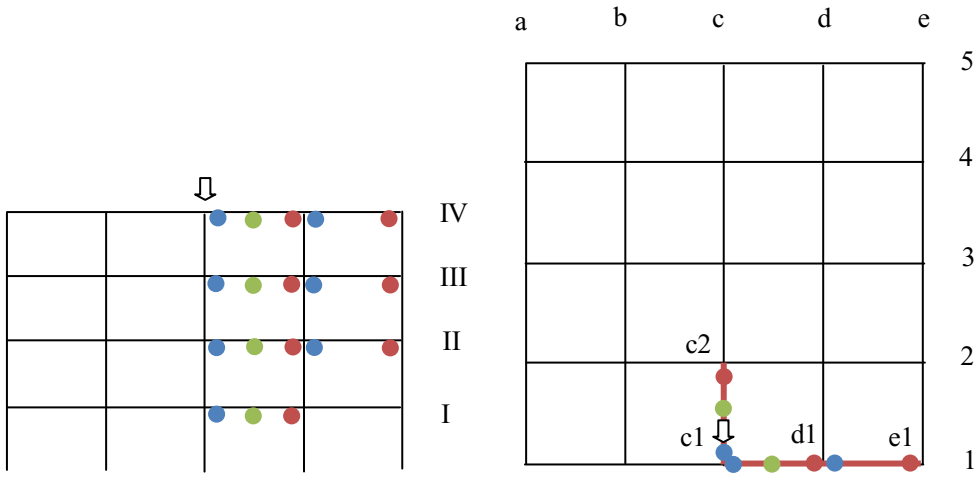

(a)

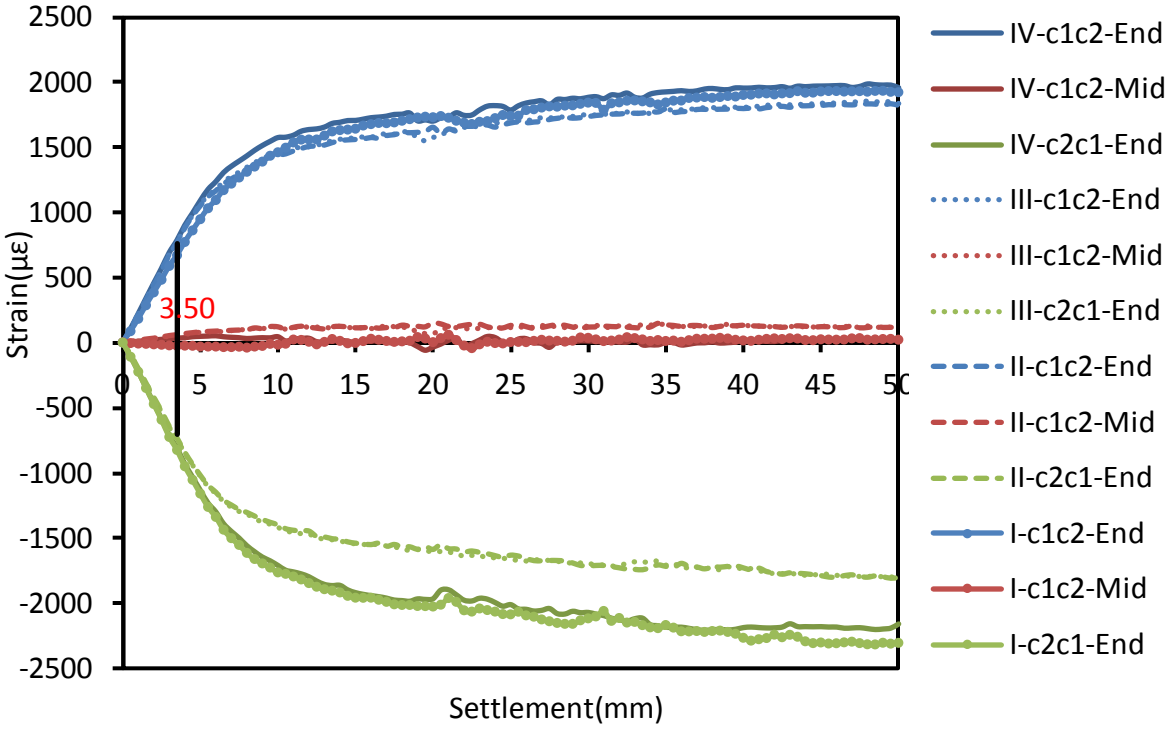
2500
2000
1500
1000
500
0
-500
-1000
-1500
-2000
-2500
Strain(με)
3.50
0
5
10
15
20
25
30
35
40
45
Settlement(mm)
IV-c1c2-End
IV-c1c2-Mid
IV-c2c1-End
III-c1c2-End
III-c1c2-Mid
III-c2c1-End
II-c1c2-End
II-c1c2-Mid
II-c2c1-End
I-c1c2-End
I-c1c2-Mid
I-c2c1-End

(b)

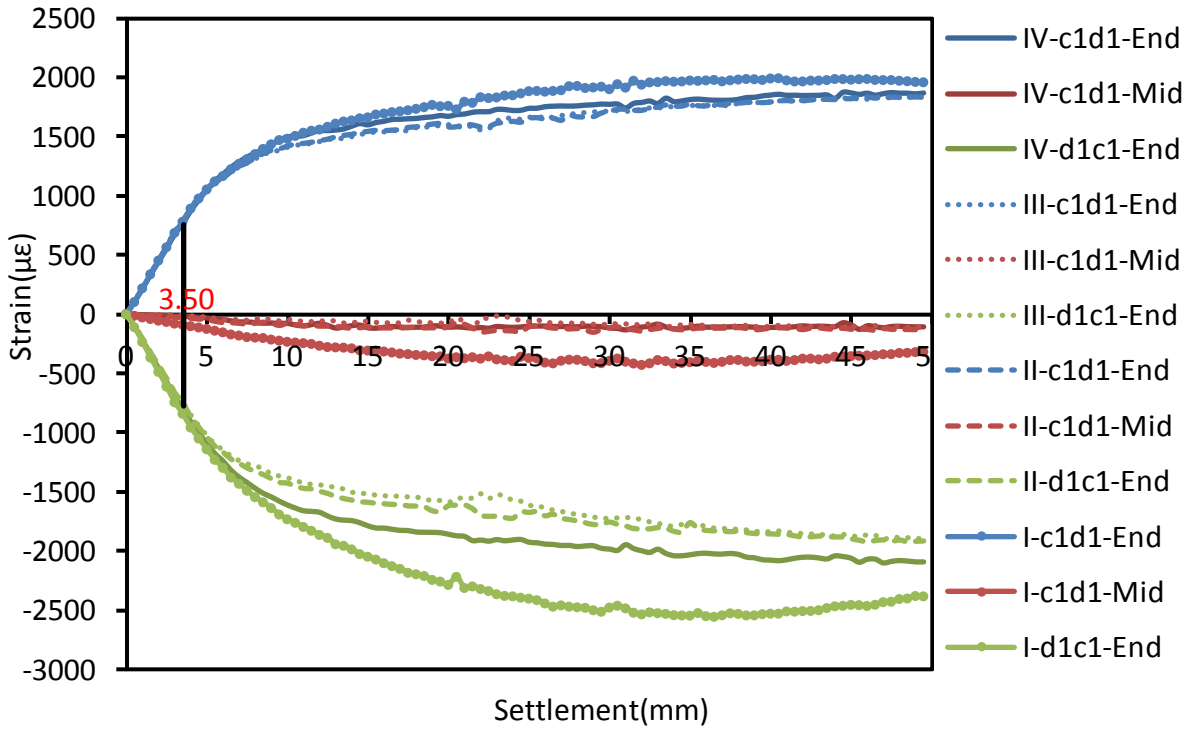
2500
2000
1500
1000
500
0
-500
-1000
-1500
-2000
-2500
-3000
Strain(με)
3.50
0
5
10
15
20
25
30
35
40
45
Settlement(mm)
IV-c1d1-End
IV-c1d1-Mid
IV-d1c1-End
III-c1d1-End
III-c1d1-Mid
III-d1c1-End
II-c1d1-End
II-c1d1-Mid
II-d1c1-End
I-c1d1-End
I-c1d1-Mid
I-d1c1-End

(c)

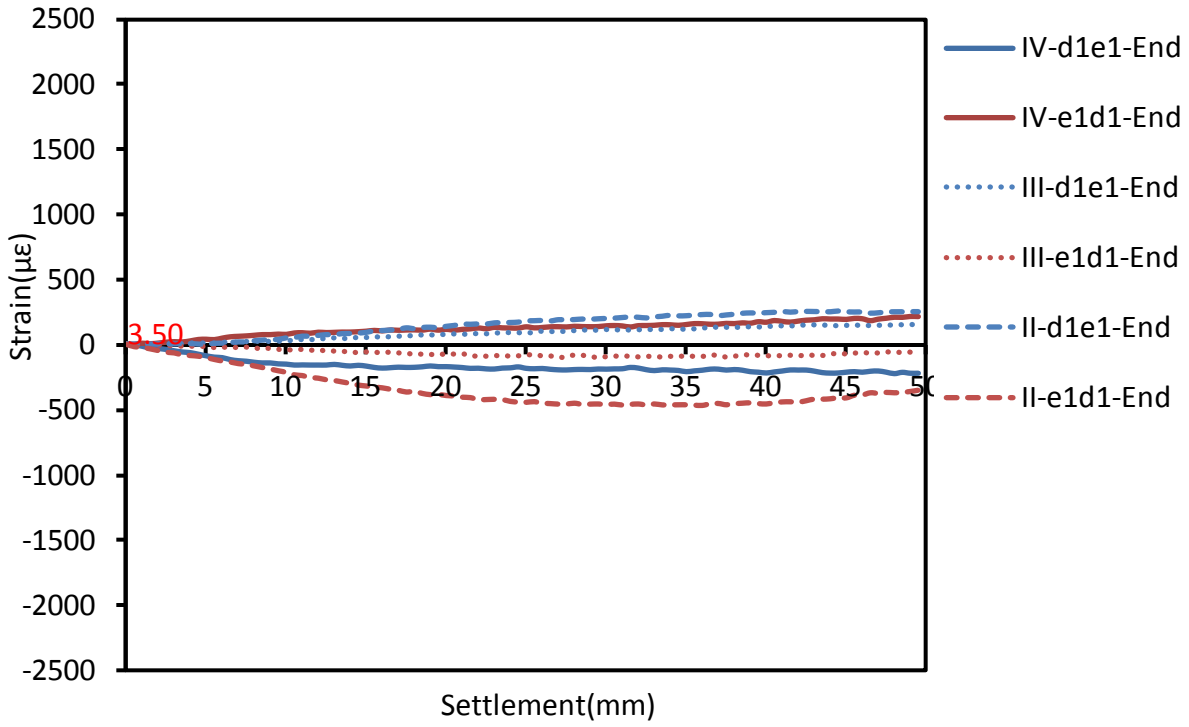

(d)

Figure 3.18 Strain testing point locations, Settlement-Strain curves of beam due to settlement of edge column (Case II)

Figure 3.19 presents the strains developed below the surface of the beams due to the settlement of the corner column a1, at the selected shown point. It can be noted that the nonlinear behavior was occurring at the settlement of around 3.50 mm for the two ends of the beam during the settlement process. The strain values of the two ends of the beam are similar with opposite signs. The maximum strain values on b1c1 were around 1/7 of the strain on beam a1b1.

Furthermore, the effect on the beam b1c1 is negligible as compared to beam a1b1, especially in the linear state of the curve (the value only around 1/10 compared to beam a1b1).

A comprehensive comparison of the effects of the three cases tested in this investigation shows that at the linear relationship stage, the strains generated are basically similar in the first floor, while for the center column at the linear stage, the strain generated by the beams on different floors does not change much. But for the edge and corner columns, the strain produced by beams on different floors varies greatly.

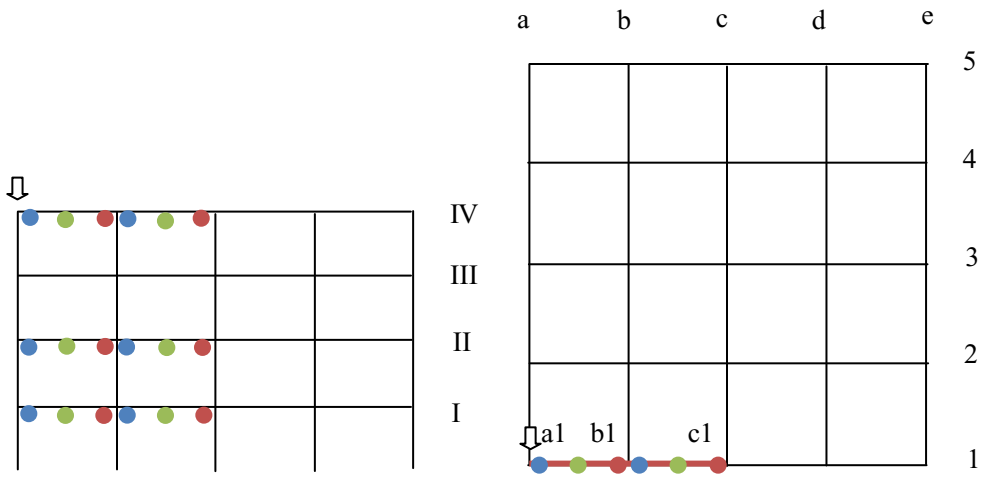
a
b
c
d
e
5
4
3
2
1
IV
III
II
I
a1
b1
c1

(a)

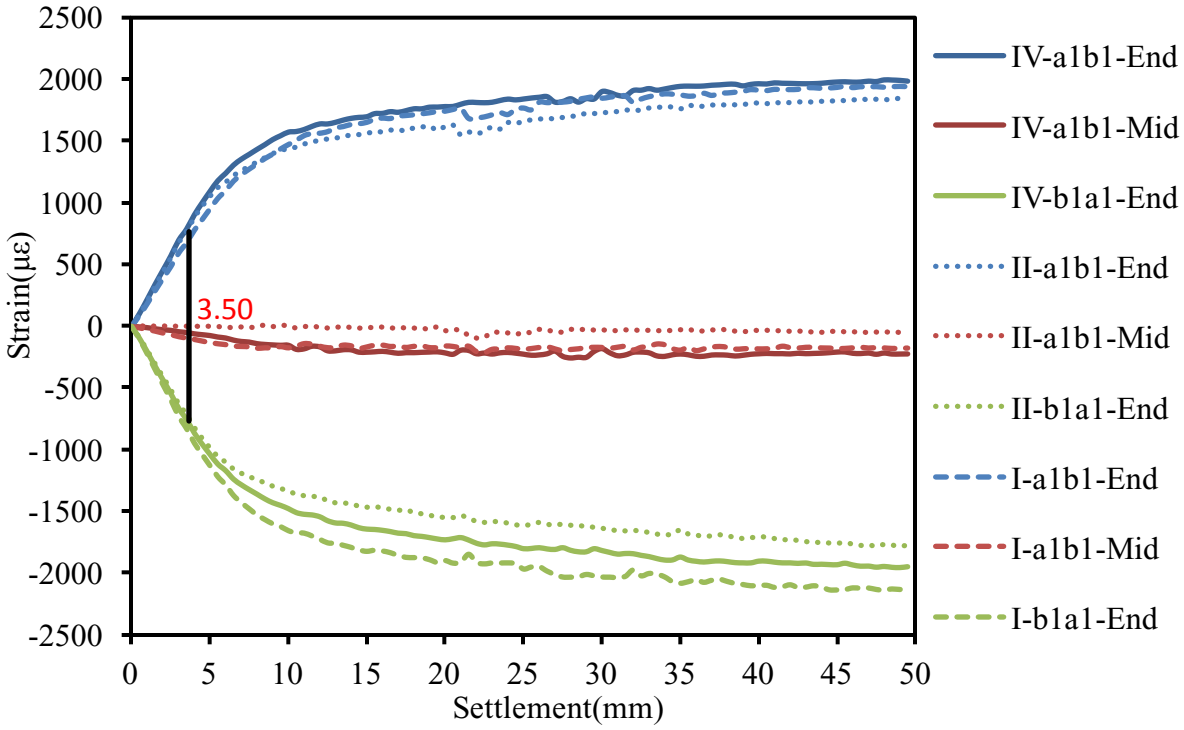
2500
2000
1500
1000
500
0
-500
-1000
-1500
-2000
-2500
Strain(με)
3.50
0
5
10
15
20
25
30
35
40
45
50
Settlement(mm)
IV-a1b1-End
IV-a1b1-Mid
IV-b1a1-End
II-a1b1-End
II-a1b1-Mid
II-b1a1-End
I-a1b1-End
I-a1b1-Mid
I-b1a1-End

(b)

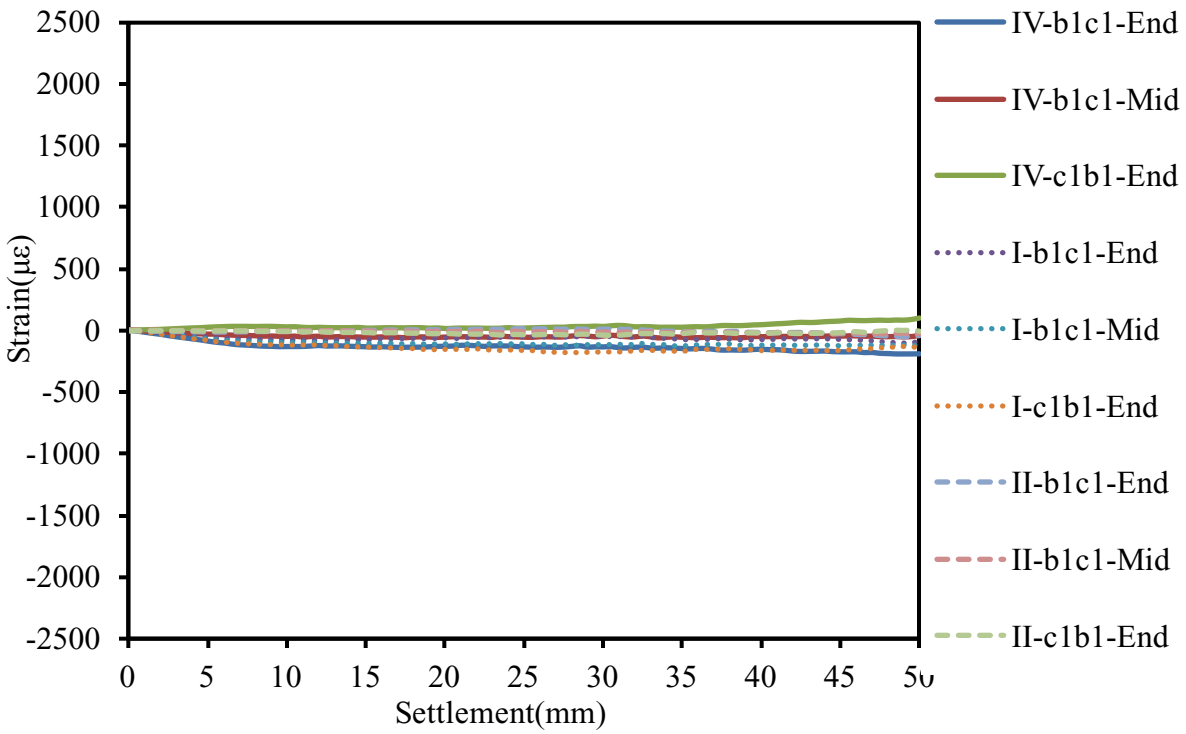

(c)

Figure 3.19 Location of strain gages in the building, Settlement-Strain curves of beam due to settlement of corner column (Case III)

3.3.4 Strain in Angles

Figure 3.20, presents the strain developed in the angles connecting the beam with column. It can be noted that the angles were in the state of tensile stress during the settlement process. At the initial stage, the stress values are basically the same. Due to the increase of the settlement, the angle at the top of the beam bears significantly more force than the angle at the bottom of the beam. In addition, angles at different floors bear basically similar behavior, however stresses increase with the increase of floor level. It can be noted that the strain increases slowly after the settlement of 3.50 mm, then rapidly increases. The change from linear to nonlinear is due to failure of bolts, which start when settlement starts, then the failure continued in angles at higher settlement first the top angles, then at the bottom angles. Fig. 3.21 and Fig. 3.22 produce the same conclusion.

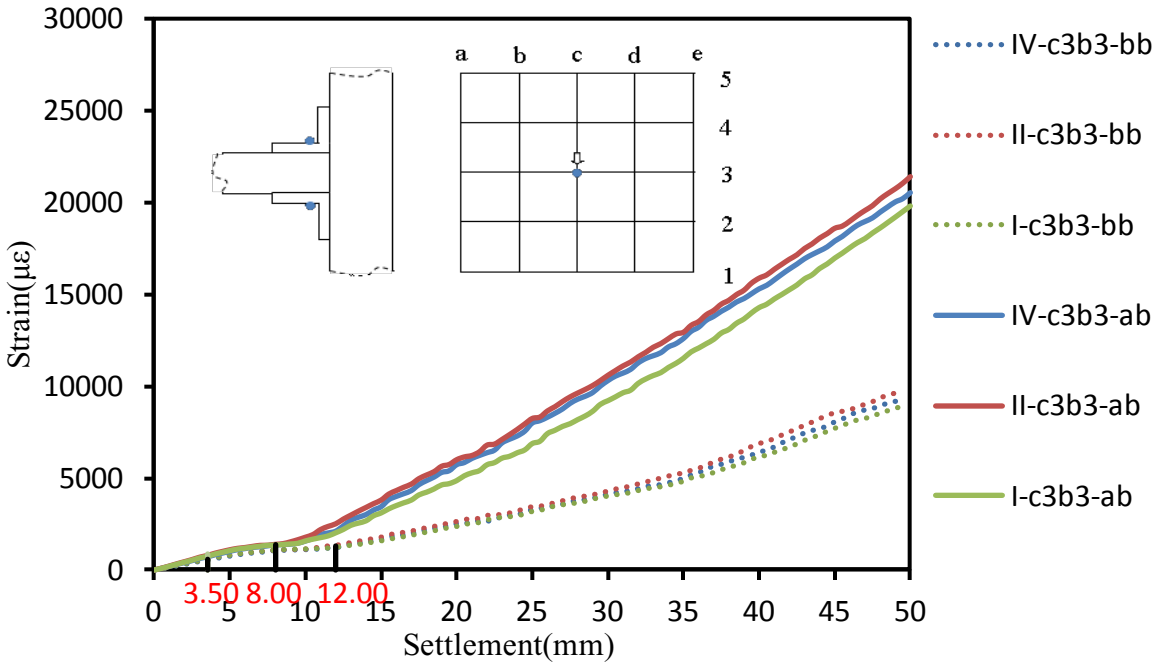

Figure 3.20 Strain versus settlement curves at the selected points at the top and the bottom angles for column c3 (Case I)

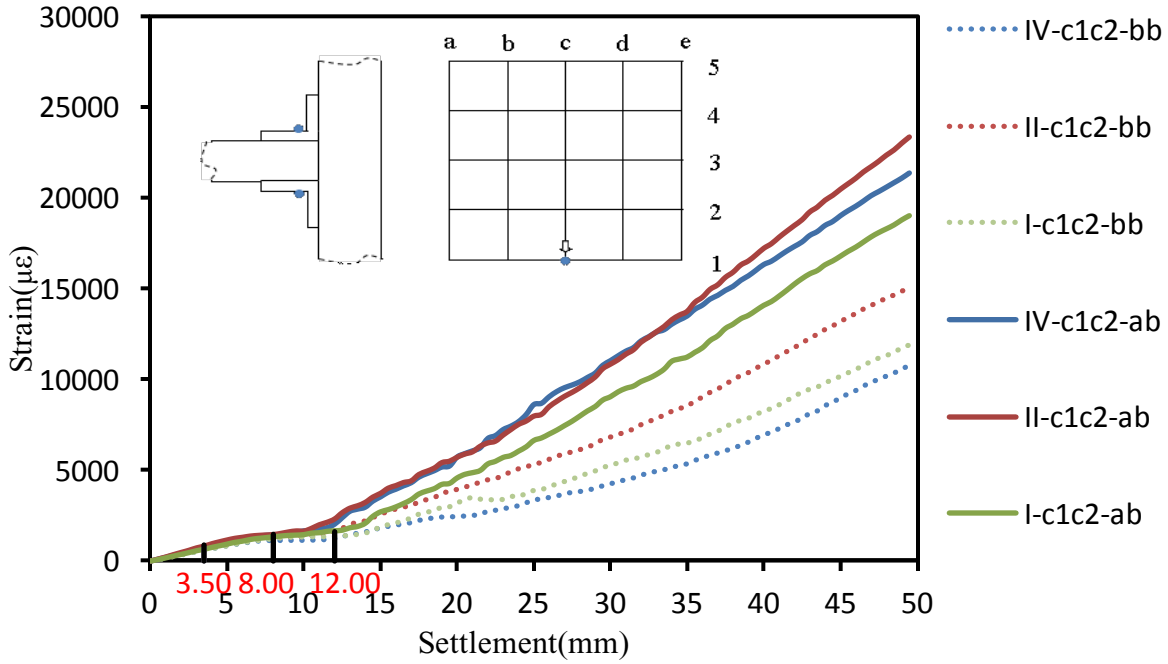

Figure 3.21 Strain versus settlement curves at the selected points at the top and the bottom angles for column on column c1 (Case II)

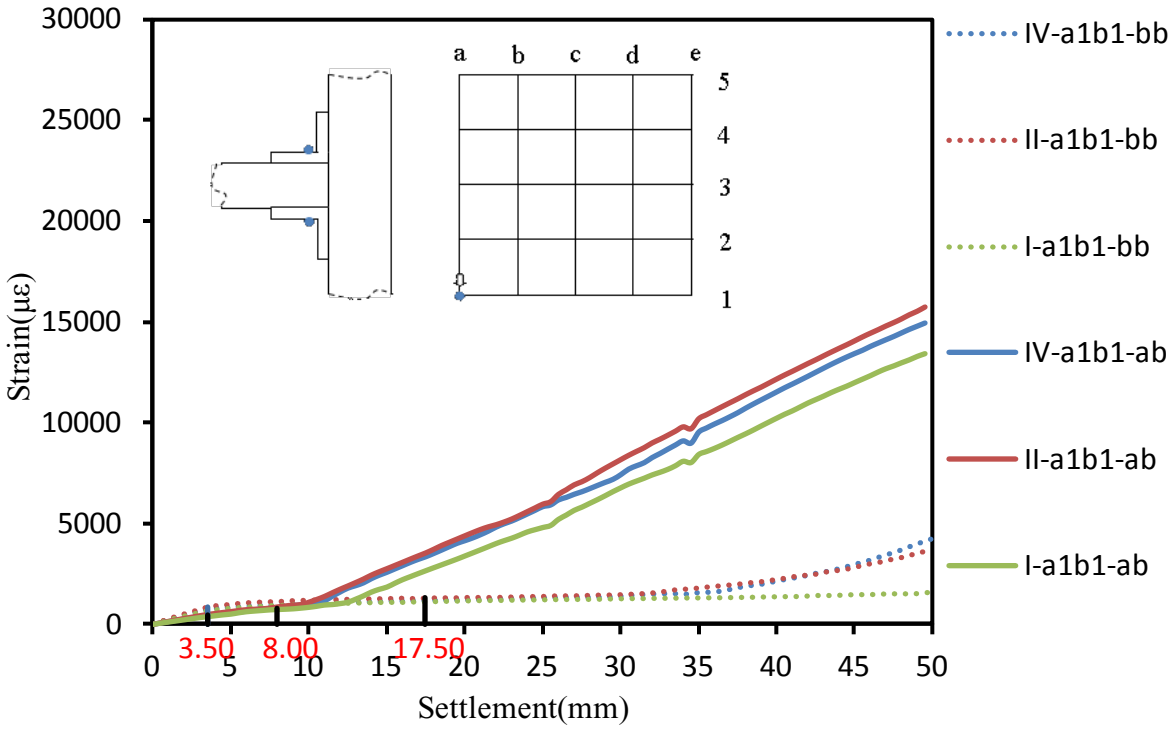

Figure 3.22 Strain versus settlement curves at the selected points at the top and the bottom angles for column a1 (Case III)

3.4 Summary

Based on the experimental results obtained, a structural response was recorded during the settlement of the center, edge and corner columns. The failure modes for these three cases, showed that the beams and columns did not undergo obvious plastic deformation, nevertheless, they showed downward rotational displacement. In fact, the damage was concentrated at the connecting angles and bolts.

The angle at the top of the beam bears the vertical load, while the angle at the bottom of the beam bears the lateral load, accordingly, the deformation in the top angle experienced less than the one at the bottom. Furthermore, the deformation caused by the settlement of the central column is the largest, followed by the edge columns, then the corner columns. Therefore, from the perspective of the structure's integrity to resist settlement, the central column provides the greatest resistance, followed by the edge columns, and finally the corner columns.

The vertical load-settlement curve takes place in three stages: linear, nonlinear and then linear. In these tests, all elements begin at the linear elastic state, then move to the elastic-plastic, then plastic deform, where the vertical load changes from a linear relationship to a nonlinear stage. Due to the continuous increase of the settlement, the beam will provide the lateral resistance, in order to maintain the rigidity of the beam-column connection, resulting in a quadratic linear state.

Chapter 4

Numerical Modeling

4.1 General

3-D numerical models are developed to examine the non-linear performance of the material and the geometry of the four-floor four-bay frame structure, using the software "ABAQUS" program (6.14, 2010). In this analysis, modeling of column, beams, bolts, nuts and angles, meshing, boundary conditions are presented. The experimental results presented in Chapter 3 were used to calibrate the models developed herein. After model validations, the model was used to produce results for a wide range of parameters.

4.2 Finite Element Models

4.2.1Material Properties

The tested 3-D structure consists of aluminum beams and columns as well as steel angles and bolts. The modulus of elasticity, yield strength, and the ultimate strength for the aluminum were as 69 GPa, 241 MPa, and 311 MPa, respectively, while for the steel were 200 GPa, 259 MPa, and 533 MPa, respectively (see *Table 3.2* and *Table 3.3*). For nonlinear simulation, the aluminum tangent modulus is set as 27 GPa.

An eight-node solid hexahedral element, C3D8R elements, was used for modeling of beams, column, bolts, nuts, and angles. These elements have the capability to model plasticity of strain hardening, which has large deflection and strain behavior, and use relatively less integration method. The element is defined by eight nodes having three translational degrees of freedom at

each node in the nodal x, y and z directions, as shown in Figure 4.1. The meshing C3D8R element provides a high level of accuracy and less computation time results (ABAQUS, Release 6.14, 2010).

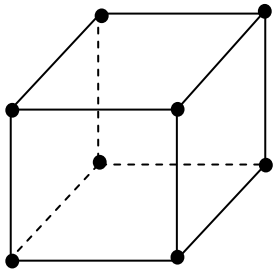

Figure 4.1 C3D8R solid element (ABAQUS, Release 6.14, 2010)

4.2.2 Geometry, Loading, and Boundary Conditions

The general layout of the structure tested in this investigation is presented in figure 4.2. The structure has beams and columns lengths in the x-y direction and the depth in the z-direction. The structure was made of 25 columns, 160 beams, 640 top and seat cleats angles, and 1280 bolts. A mesh convergence study was carried out on the connections in order to determine the appropriate mesh density, which is used for beams and angles. For the cross section, the beam consisted of 48 and 40 elements respectively, as depicted in Figure 4.3. While the numbers of elements across the beam length for the case 1, 2, 3, and 4 were 30, 40, 50, and 80 elements respectively. Figure 4.4 presents the results of the mesh convergence for the four cases examined. It can be noted that the response in cases 1 and 2 was the same as for the cases 3 and 4. Based on the above results, and in order to reduce the computational time, case 3 and a beam with 50 mesh elements were selected as typical for further analyses.

Furthermore, in order to simulate the connections in the experimental investigation, a convergence study was made to examine different friction coefficients. Friction coefficients

ranging from 0.05 to 0.2 in increments of 0.05 were tested. Figure 4.5 presents the results of the friction convergence for the central column. Based on this study, a friction coefficient of 0.15 was chosen for the present analysis.

As for the loading protocol, the quasi-static load of 0.08 mm/s was applied gradually on the top faces of the assigned locations of the central, exterior, corner columns until the perspective column settlement reached 50 mm. To simulate the testing conditions, only the tested column was allowed to settle, while the other columns remained fixed during loading. Figure 4.6 presents a simplified description of boundary conditions for the central column settlement. The total number of elements after mesh is 1282835.

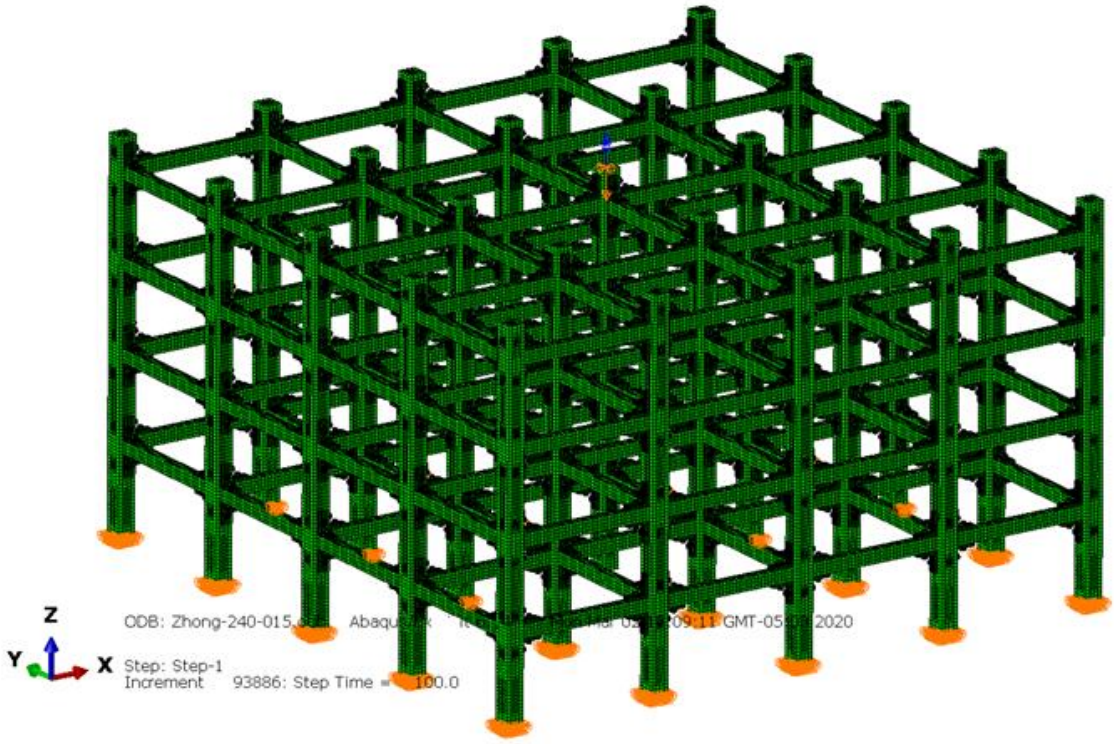

Figure 4.2 The FE model of tested structure

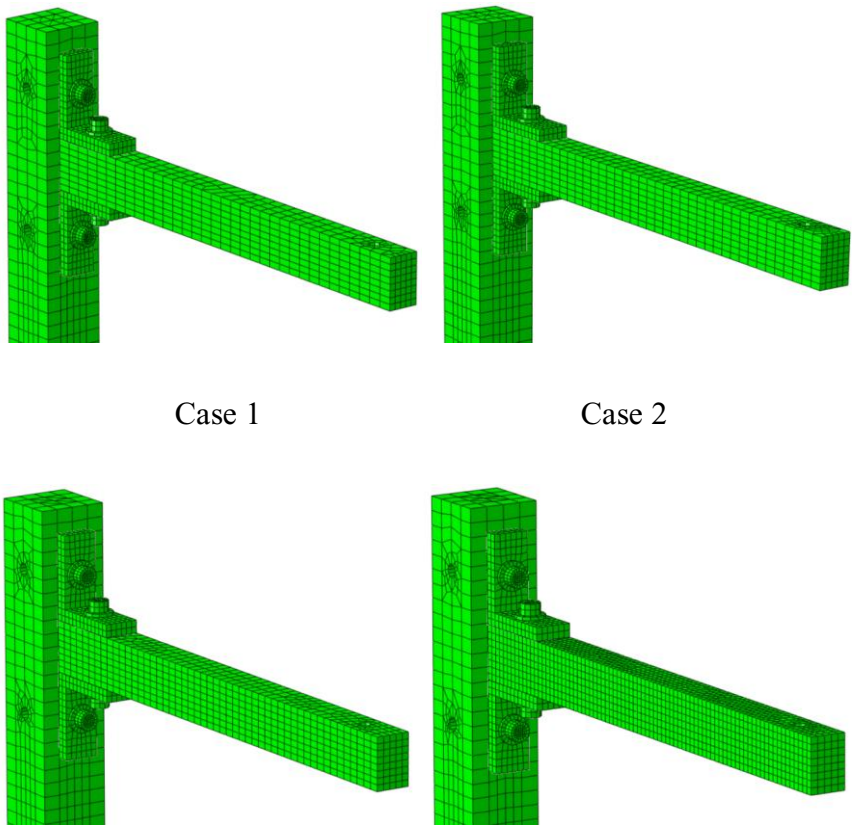

Figure 4.3 Mesh convergence for the cross section and the beam models

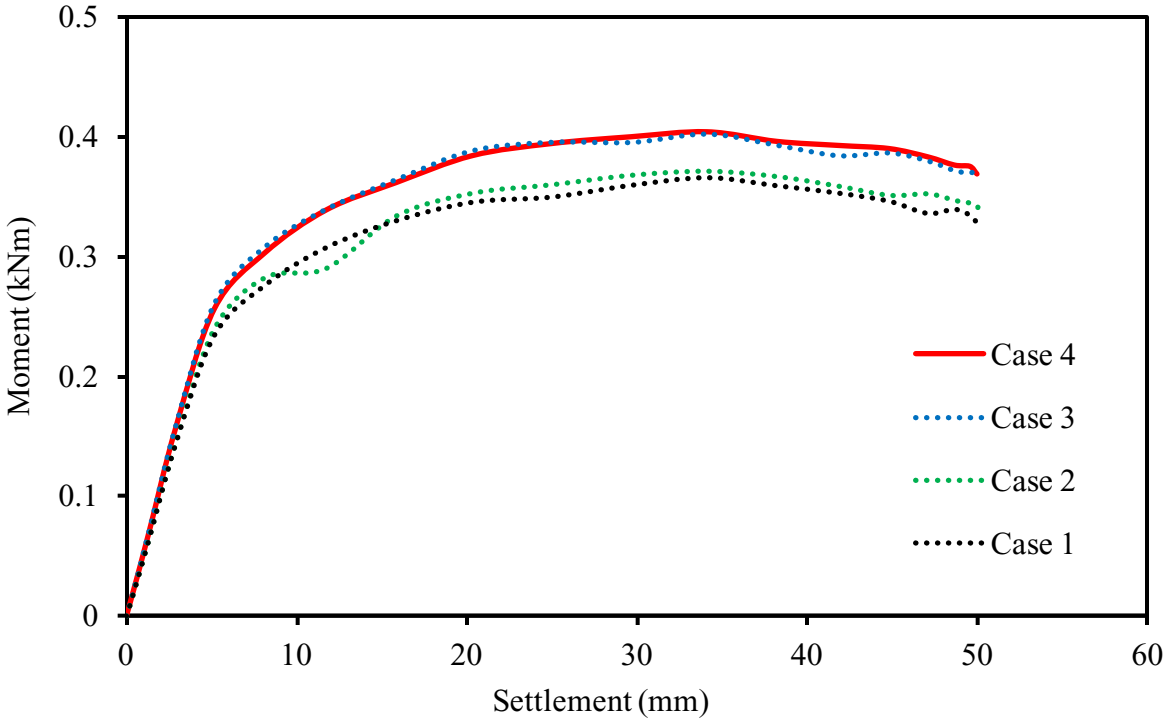

Figure 4.4 Results of mesh convergence for the cases examined (Case 1: 30; Case 2: 40; Case 3: 50 and Case 4: 80)

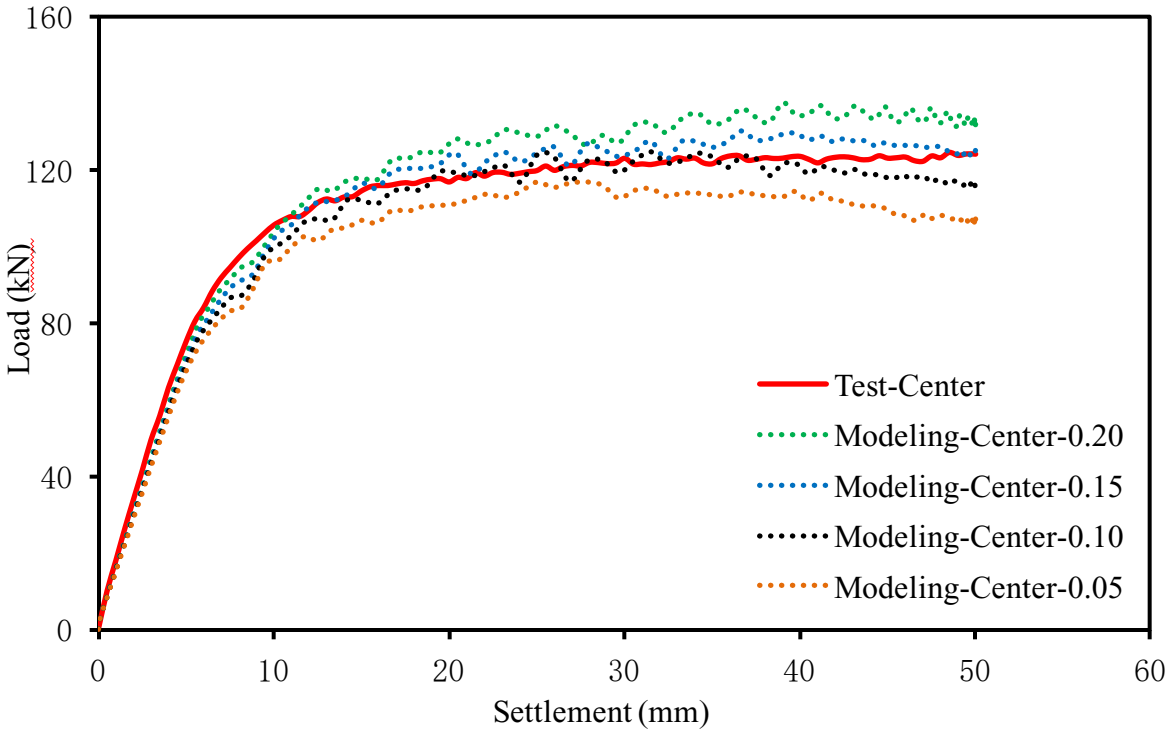

Figure 4.5 Results of the friction convergence study for the central column

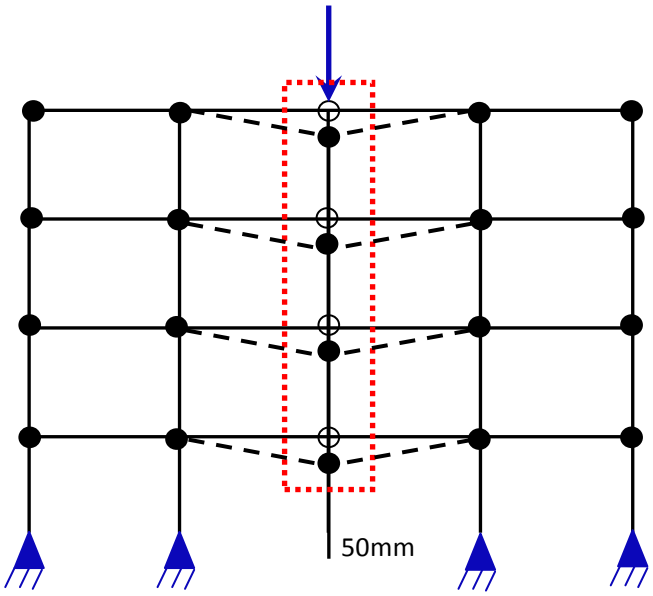

Figure 4.6 Boundary and loading conditions for the central column during loading / settlement

4.3 Validation

Figure 4.7 presents the numerical and experimental results of the load-settlements curves for the central, edge and corner columns. It can be noted that in order to achieve the same settlement, the maximum load was 130 kN for the center column, while it was 92 kN for the edge column and 64 kN for the corner column. Furthermore, a good agreement was obtained between the numerical and experimental results, with an error of 10%, 12%, and 15% for the central, edge and corner columns respectively.

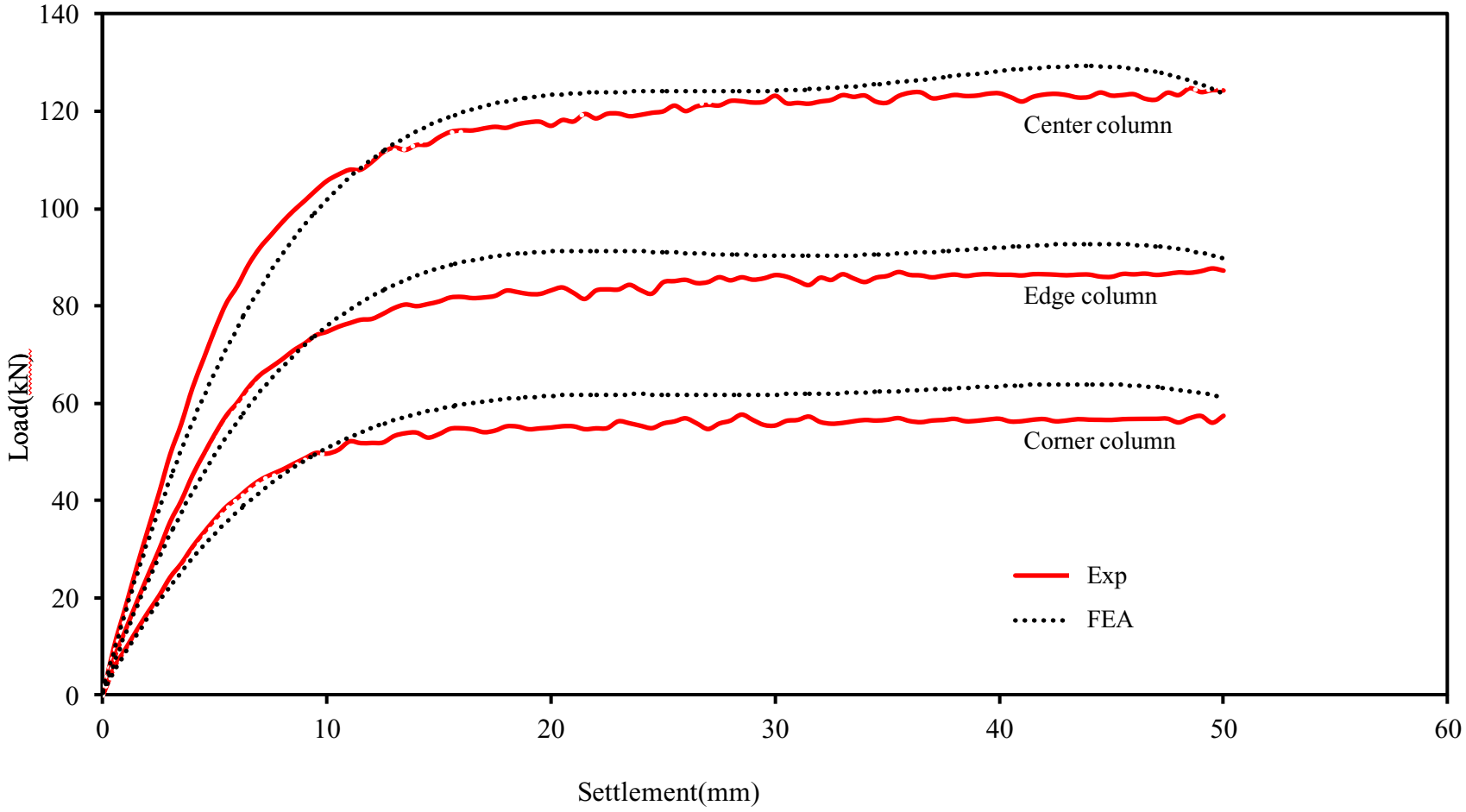

Figure 4.7 Load-Settlement curves for the center, edge and corner columns

Figures 4.8 and 4.9 present the numerical and experimental strain-settlement relationships for beams and columns. In this analysis, the beam chosen for the comparison is marked in red on these figures. It can be noted that the strain-settlement curves for the beams are similar for those of the center column, edge column and corner column. As expected the relationship is linear until it reaches a peak, then changed to nonlinear. Furthermore, the strain values are the same for the two points at the end of the beam with opposite signs. In the linear stage, the experimental and numerical results are almost the same for the three scenarios of settlement. And in the nonlinear stage, the maximum difference of experimental and numerical results is 19% for the settlement of corner column. It is an 18% difference between experimental and numerical results for edge column settlement and 12% for center column settlement.

Furthermore, the comparison between the numerical and the experimental results in terms of strain-settlement relationships on column, showed a good agreement at the linear stage. The numerical results are slightly higher for the nonlinear stage. The maximum difference is 13% between experimental and numerical results for settlement of center column and edge column. It is 8% for settlement of corner column. In general, it can be reported that the numerical model compared well with the experimental results of the present investigation.

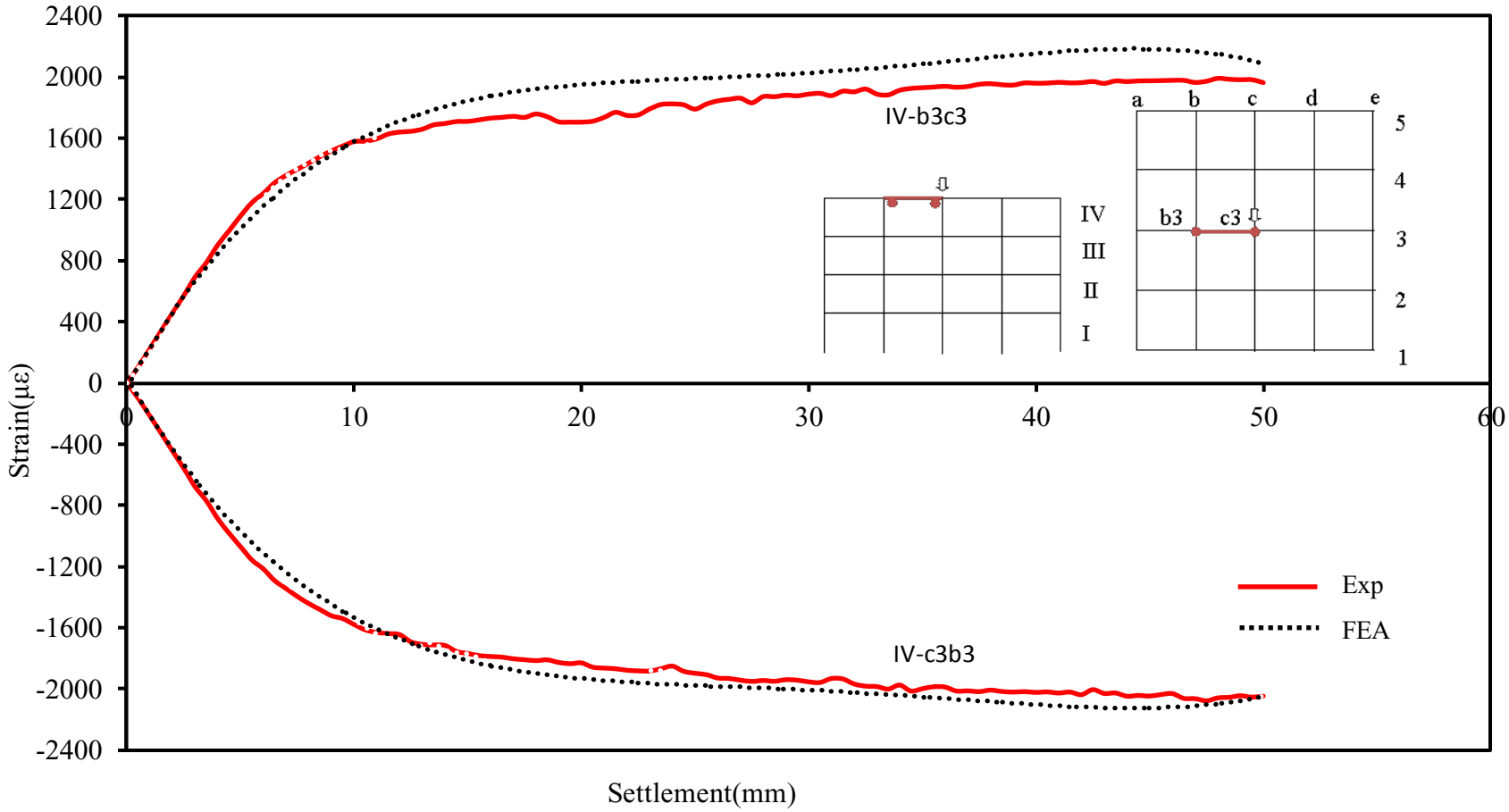

(a) Center column

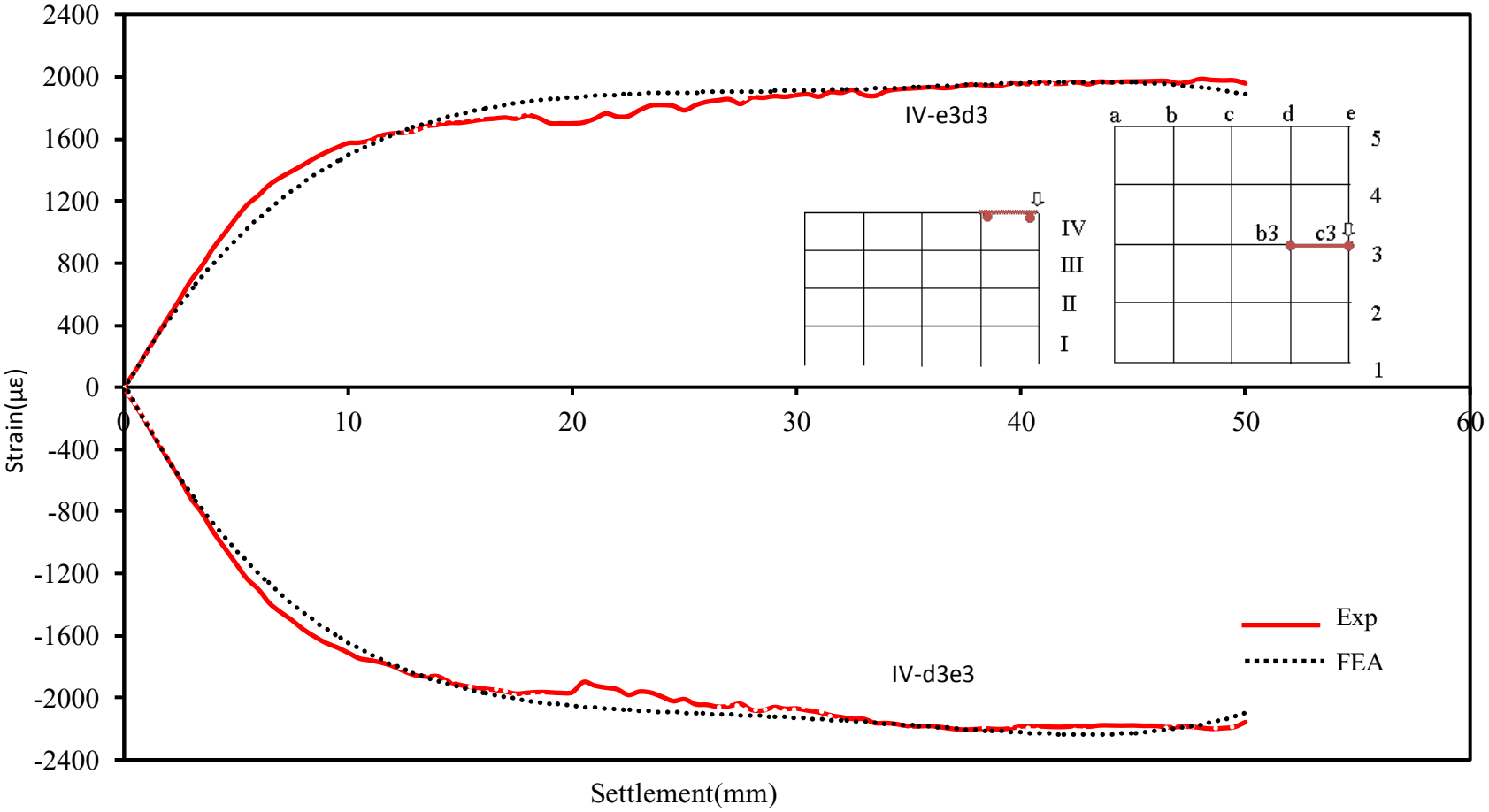

(b) Edge column

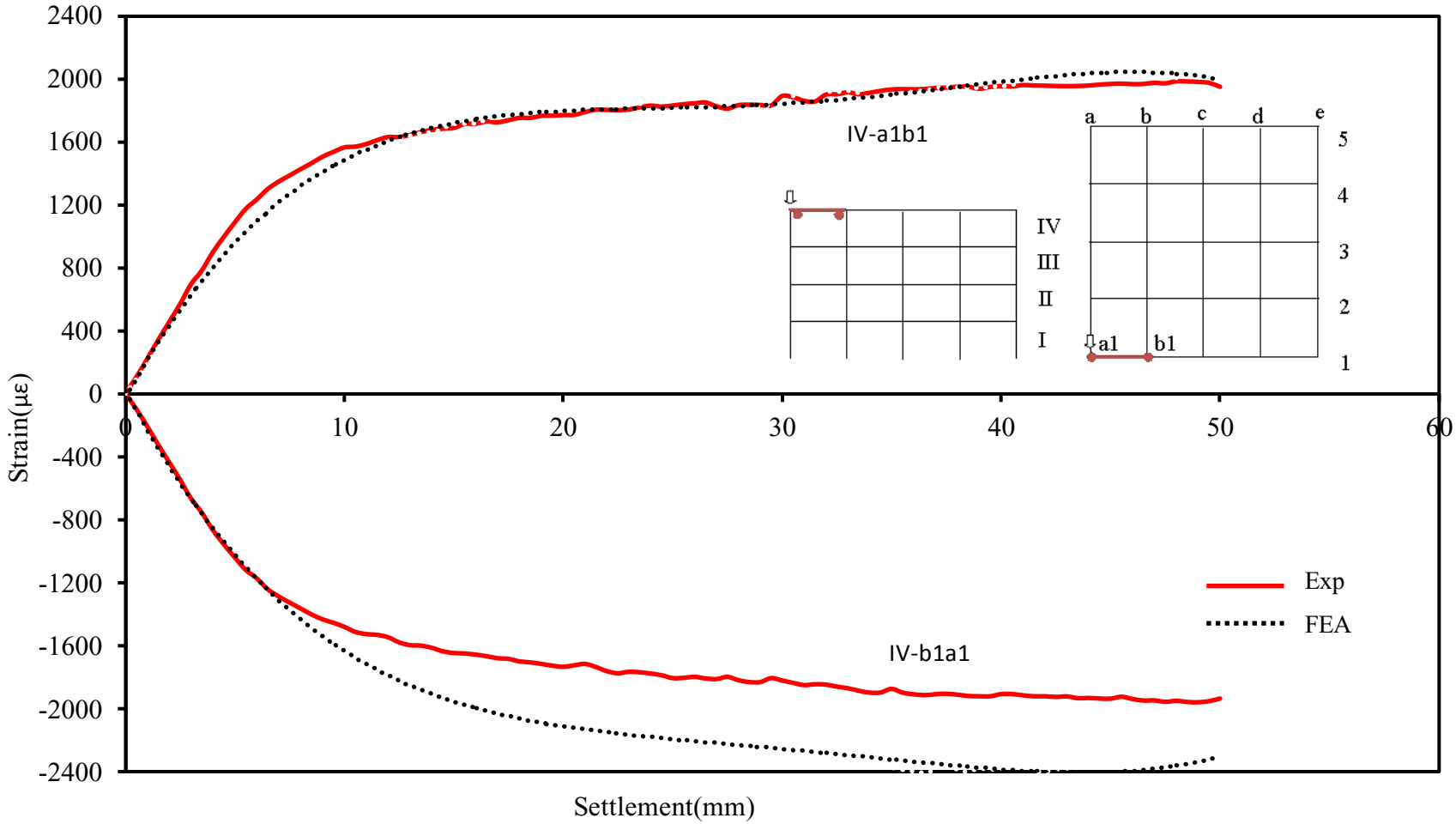

(c) Corner column

Figure 4.8 Strain versus settlement for beam ends

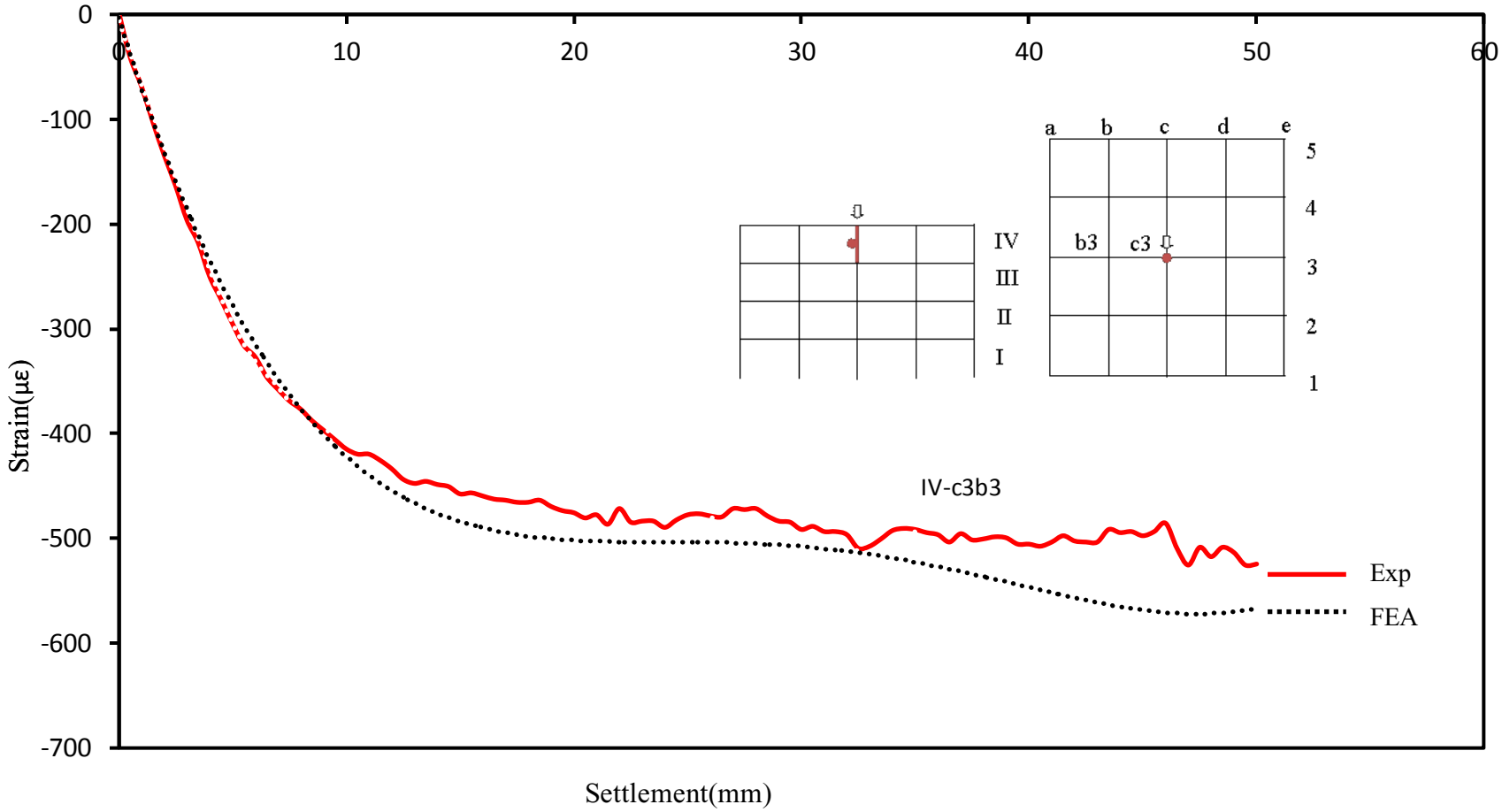

(a) Center column

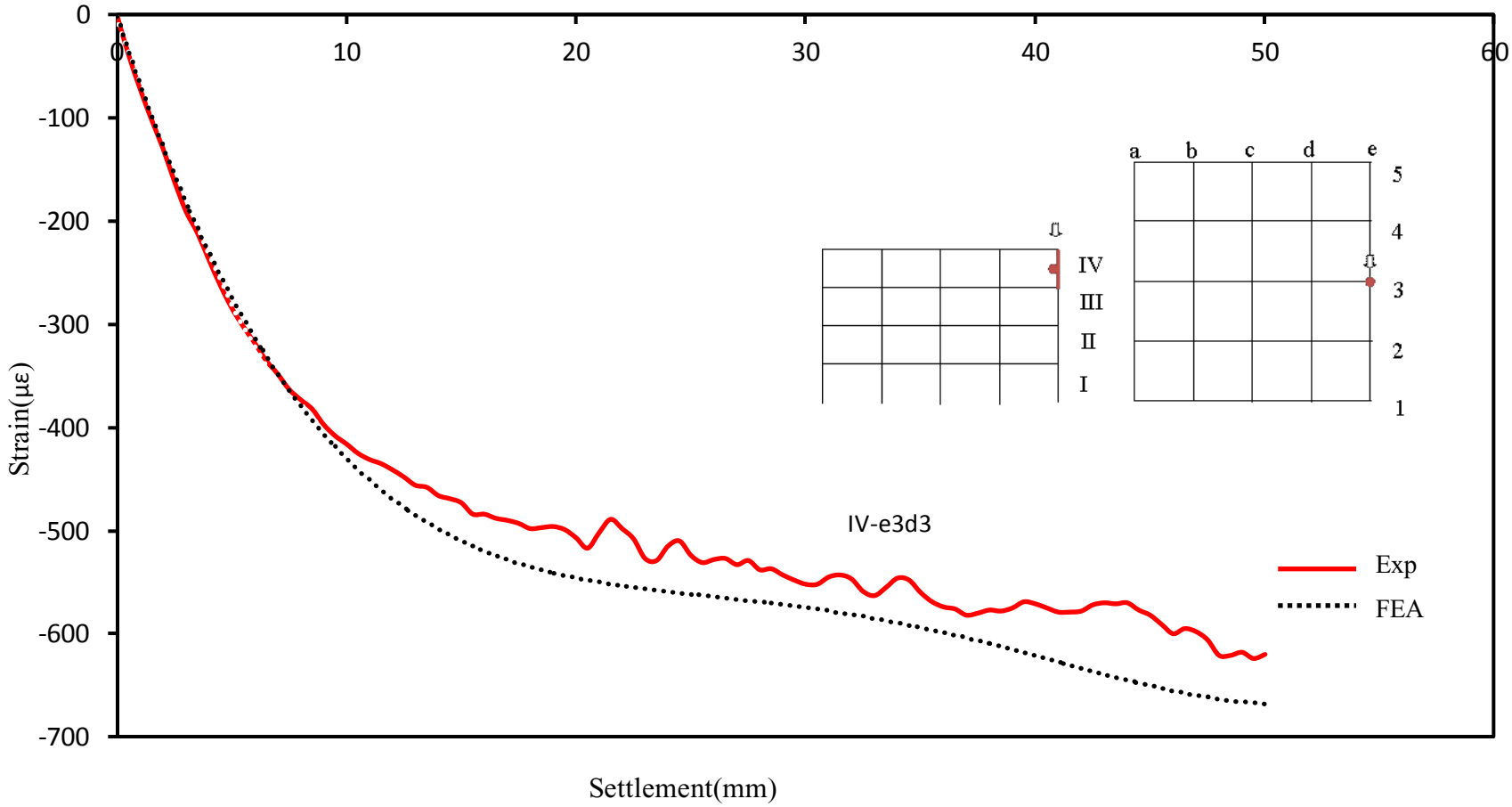

(b) Edge column

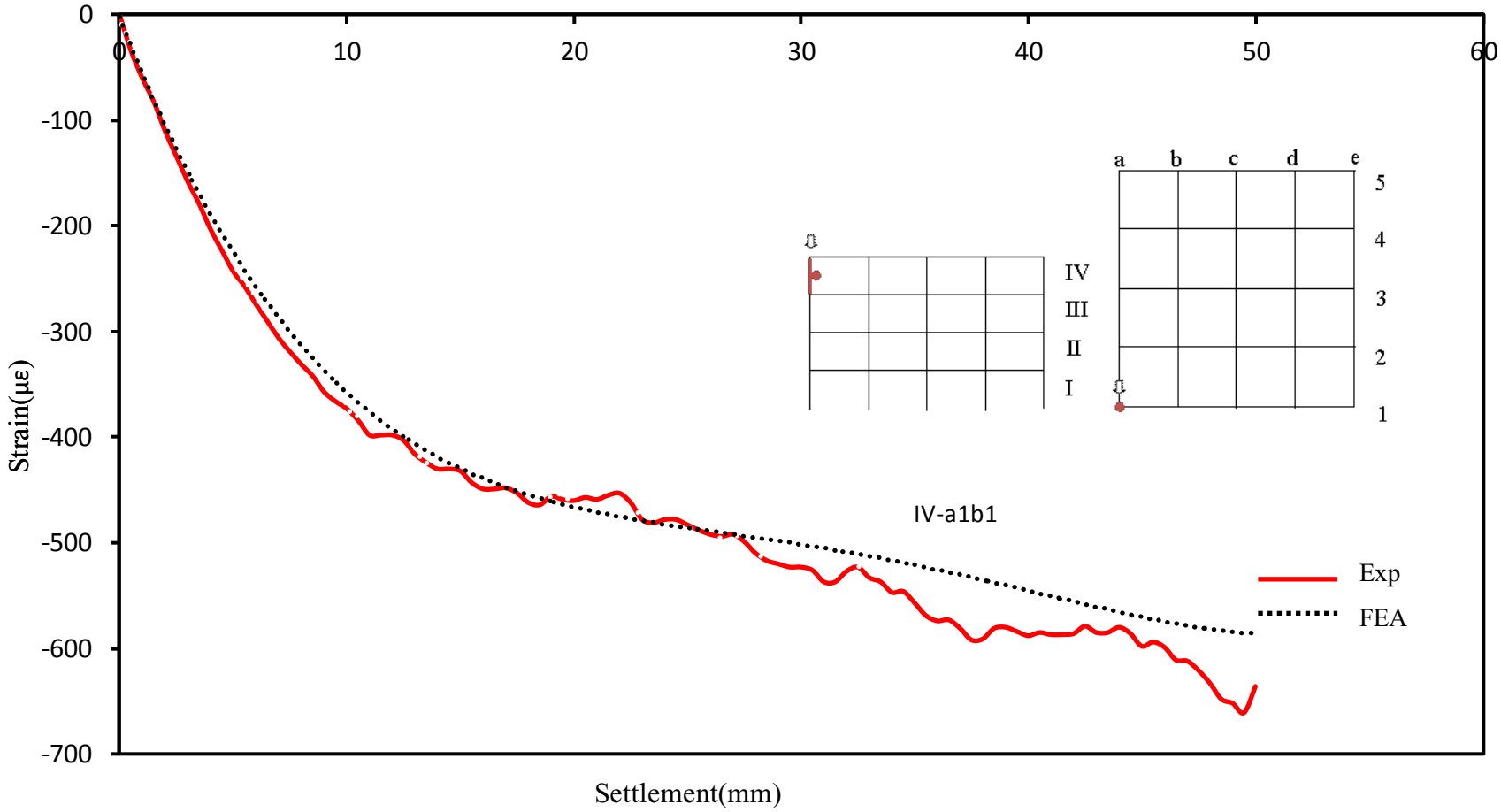

(c) Corner column

Figure 4.9 Strain versus settlement on the middle floor

In order to facilitate the experimental operation, the simulated foundation settlement in the laboratory is realized by applying load from the top of the column. In fact, settlement generally occurs at the foundation level. In the numerical simulation, the load causing the settlement can be set at the bottom end of the column. The following section compares the simulation results of the bottom loading settlement with the experimental results of top loading settlement.

Figure 4.10 presents the load versus settlement curves for columns subjected to prescribed settlement at the bottom. It can be noted the produced curves are overlapping and almost identical. Figure 4.11 presents settlement versus strain curves on the beam ends for column loading on the top and by prescribed settlement at the foundation level.

Figure 4.12 presents that the strains on columns are the same value with opposite sign for the case of loading top and bottom of column. The main reason is that different loading mode lead to compression for top loading and tension for bottom loading. It is important to report herein that in this investigation, the analysis was not accounted for columns due to the fact that the building was designed to resist seismic loads, i.e., the seismic design satisfied the criterion for "strong column-weak beam" (Lan Lin et al. 2015). So this model and its setting can be used to conduct parametric study.

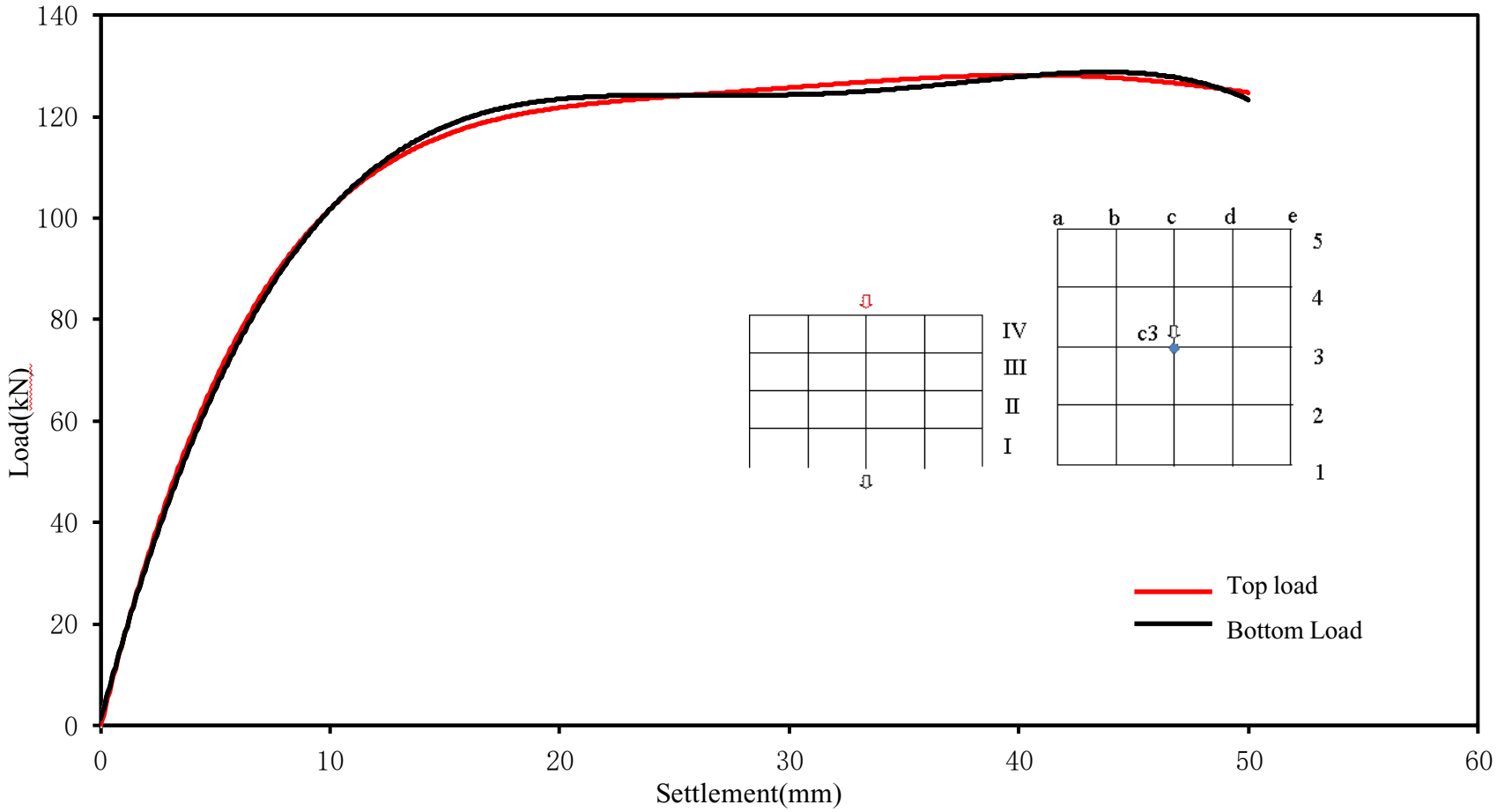

Figure 4.10 Load versus settlement curves for the top and the bottom of the center column

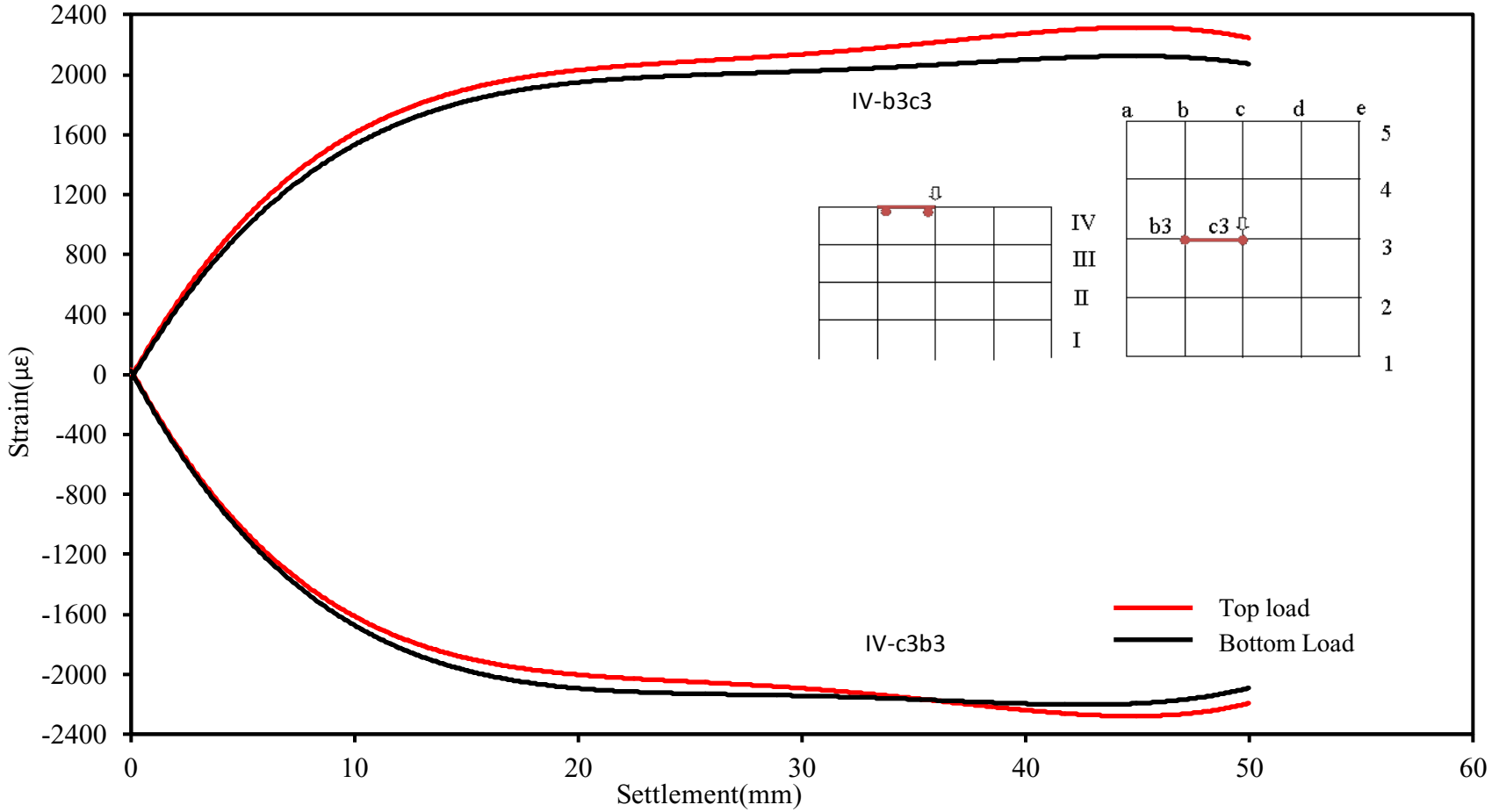

Figure 4.11 Settlement versus strain curves for the beam ends of b3 column top loading and bottom loading

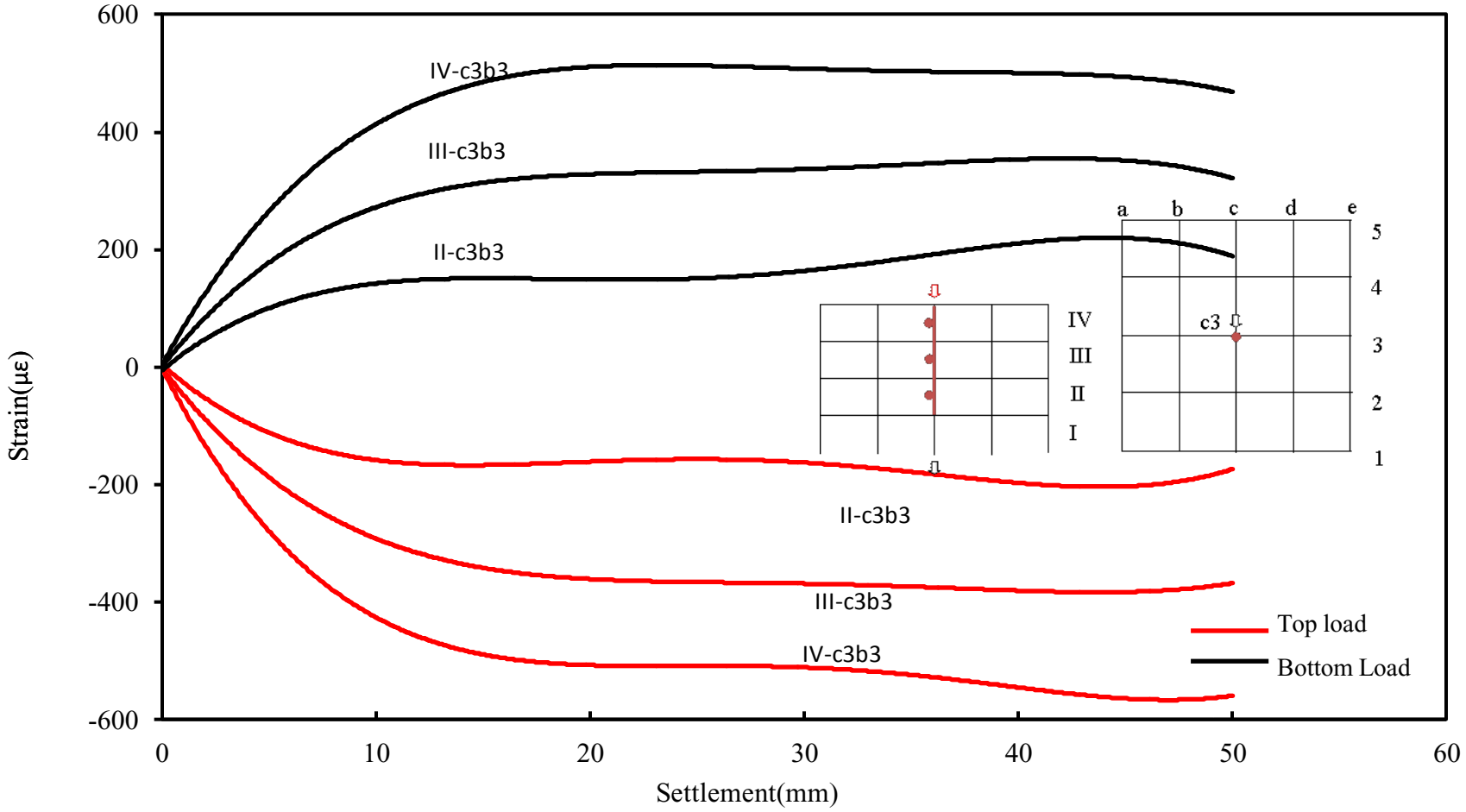

Figure 4.12 Settlement versus strain curves on the middle point of column for each floor loaded from the top and from the bottom of column

4.4 Summary

ABAQUS software was selected to simulate the responses of structure due to settlement. The 50-mesh elements of a beam were selected as typical model based on the mesh convergence study. A friction coefficient of 0.15 was chosen for the numerical model from the convergence study of friction coefficient.

Comparison results between numerical and experimental of load-settlement relationship, strain-settlement in beams and strain-settlement in columns for three scenarios settlement, show that the maximum differences are 15%, 19% and 13%, which is acceptable for validation of numerical modeling.

Comparison of the simulation results of the bottom loading settlement with the experimental results of top loading settlement shows that two curves are overlapping and almost identical for the same measured point on the beams. Yet, the strains on columns are the same value with opposite sign for the case of loading top and bottom of column as different loading mode lead to compression for top loading and tension for bottom loading.

Chapter 5

Analysis of Steel Structures

5.1 General

In this chapter the 3-D numerical models developed in this investigation was used to analyze a 9-floor steel structure subjected to the settlement of the center, edge and corner columns. The structural responses due to these settlements were evaluated in terms of damage propagation in beams, displacements, axial forces, lateral drifts in columns and bending moments in beams. The relationship of moment and settlement was proposed with a chart and equations based on the rigidity of connection. The parameter study was investigated for structural responses of settlement of foundation.

5.2 Building Description

5.2.1 Building Properties

A 9-floor steel structural building was selected for this study, having the layout and member dimensions of the prototype building designed by Kirby (1997). The building was built with 4×4 spans of 6 m and 9 floors of 4 m (Figure 5.1). All the primary beams were taken as 356×171×51 UB (Universal beam) and the columns were taken as 305×305×198 UC (Universal column) which are given in Table 5.1 and presented in graphical form in Figure 5.2. No secondary beam was used in the model. The properties of the steel used are given in Table 5.2.

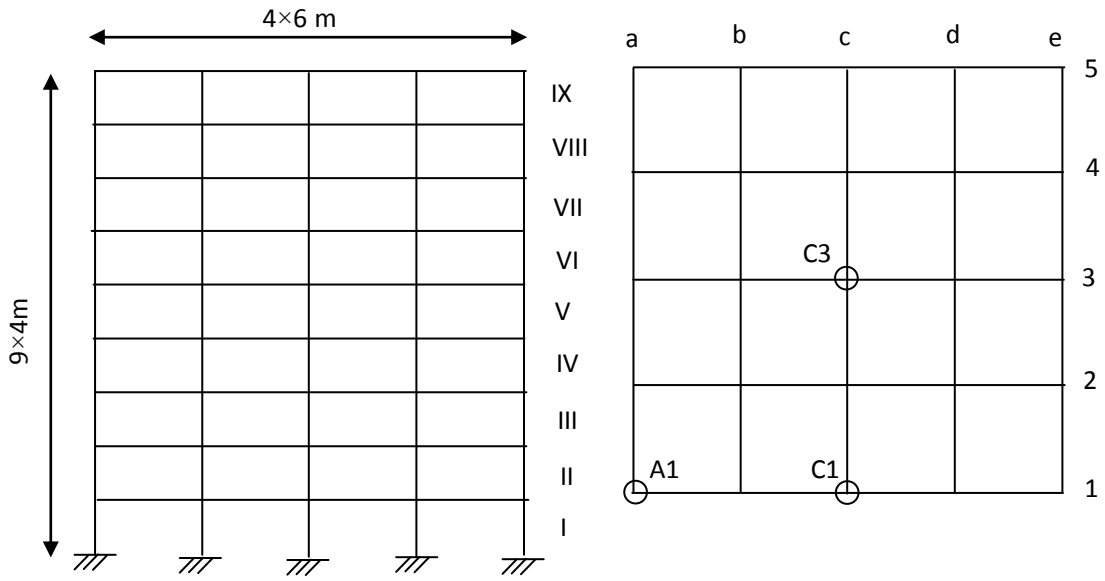

Figure 5.1 Geometrical configuration of the building

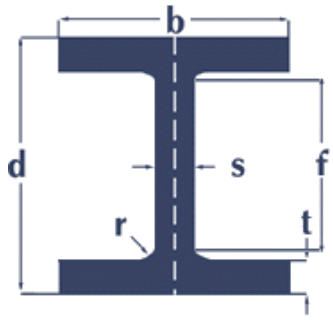

Figure 5.2 properties of the I Section

Table 5.1 Dimensions of beam and column

Item	**Type**	**Depth** ***d (mm)***	**Width** ***b (mm)***	**Web** ***s (mm)***	**Flange** ***t (mm)***	**Root Radius** ***r (mm)***	**Depth between fillets** ***f (mm)***
Beam	356×171×51 UB	355.6	171.5	7.3	11.5	10.2	311.6
Column	305×305×198 UC	339.9	314.5	19.1	31.4	15.2	246.7

Table 5.2 Properties of Materials

Item	**Young's Modulus** ***E(GPa)***	**Tangent Modulus** ***E_t (GPa)***	**Yield strength** ***f_y (MPa)***	**Ultimate strength** ***f_u (MPa)***	**Poisson's Ratio**
Beam	200	81	355	483	0.3
Column					

5.2.2 Beam to Column Connections

The beam-column connections in steel frame structures are categorized according to their flexural behavior as: flexible, semi-rigid and rigid. Figure 5.3 presents a schematic sketch for the moment-rotation of those connections. It can be noted that the relationship of the flexible structure is nearly horizontal, which represent a simple connection, however, a small moment develops at the connection due to rotation. Accordingly, the moment at the middle of a simple beam is maximum where both ends of the beam withstand zero moment and maximum shear force. Furthermore, in case of lateral load acting on a simple beam connection, braces are required to stabilize the structure.

Whereas, the moment-rotation relationship of a rigid structure is almost vertical, which represent a rigid beam-column connection, where nearly no rotation occurs between beams and columns due to the increase of the moment. The maximum bending moment occurs at the connection, which is transferred to the columns. However, in practice, it is impossible to achieve a fully rigid steel connection.

The semi-rigid connection is the most popular; however, the moment-rotation relationships vary with the degree of its rigidity. This type of connection leads to lighter beams and columns as the moments at both ends of the beam and the column connection become balanced. The secant stiffness, *Ks*, at service load is considered as an index property for these connections, as

$$K_s = \frac{M_s}{\theta_s} \tag{5.1}$$

Where, M_s= moment at service loads, (kN.m);

θ_s=rotation at service loads, (in radial).

It should be made clear herein that the difference between rigid and semi-rigid connections is the degradation of the connecting stiffness, which is expressed by the deformation of its components. The deformation in rigid connections takes place in the connected beams, while in the semi-rigid connection, the deformation mainly take place in the bolts and angles connecting the beam to column.

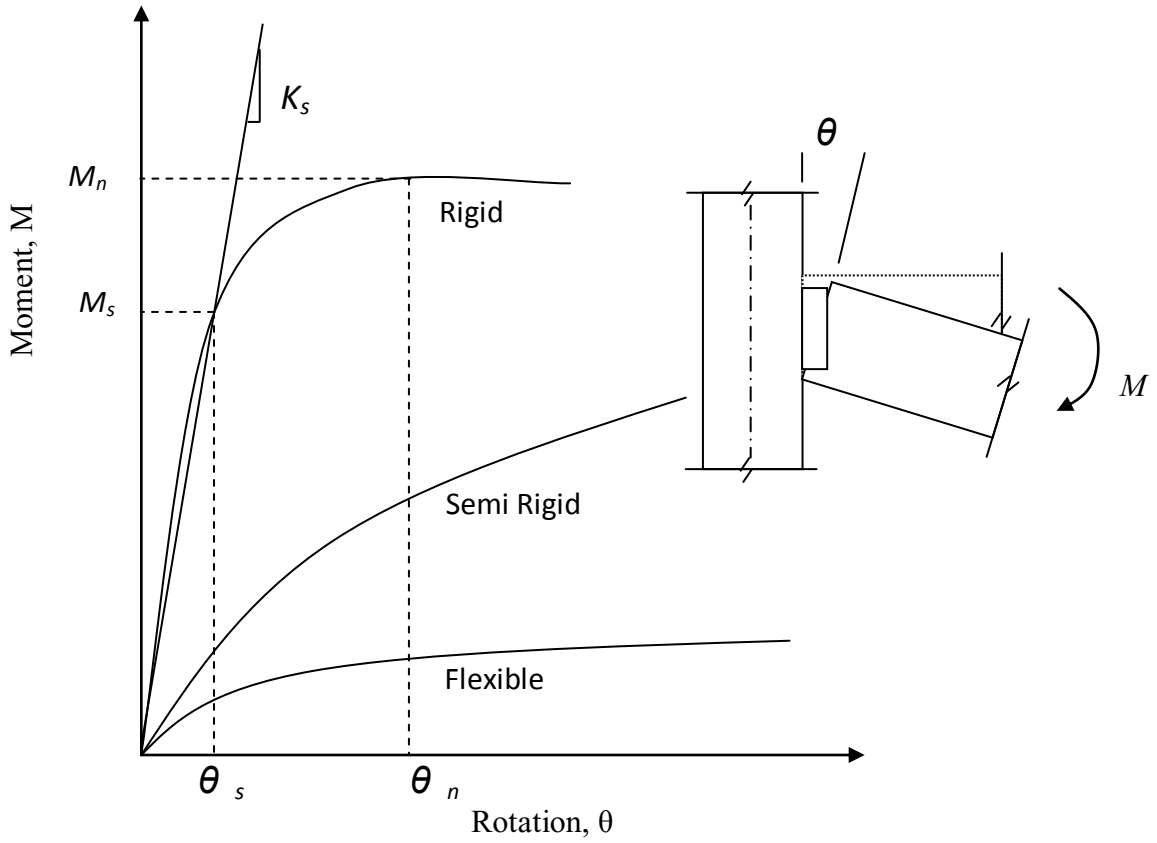

Figure 5.3 Moment-rotation of different types of connections

5.3 Numerical Modeling

The three-dimensional nonlinear finite element models developed in this investigation was

used to model beams, columns and angles. In this analysis, based on a mesh convergence study, more elements in the mesh will lead to higher accuracy. However, since the full-scale building structure of 9-floor 4span involves more construction, the gridding of its numerical model takes up a lot of hard disk space. Therefore, this model optimizes the mesh number of the beam structure. The mesh element number of a beam is 2508 and a column is 14560. The total number of mesh element in the whole structure model is 2016400 for the connection of beams and columns with the web angle (K1), 1774480 for top and seated angle connection with web angle (K2) and 1290640 for welded connection (K3), respectively. Figure 5.4 presents the possible connections, namely rigid connection, and two semi-rigid connections. The boundary condition of the model is that all columns are fully fixed to the foundation, except for the columns with prescribed settlement. A prescribed 500mm downward displacement is respectively loaded on bottom of the center column (c3), the edge column (c1) and the corner column (a1). Three connection type models are developed separately and a total of 9 times of modeling were simulated.

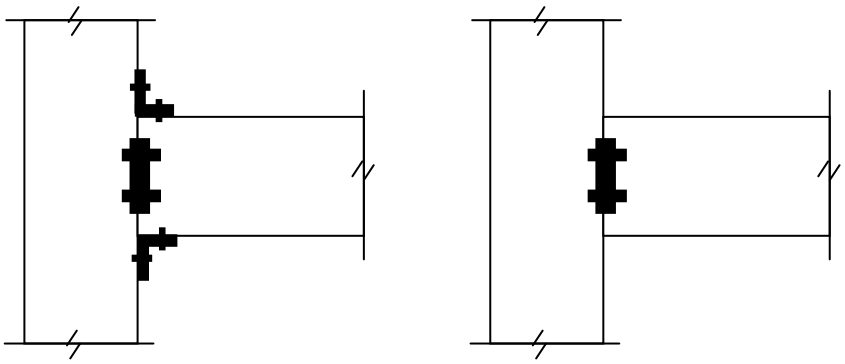

(a) Top and seated angle connection with web angle (Semi rigid-K2) and Single web angle connection (Semi rigid-K1)

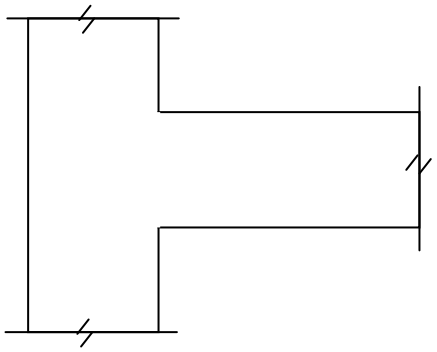

(b) Welded Connection (Rigid-K3)

Figure 5.4 Connection types

5.4 Response of Structural Elements to the Settlements

For steel structures, beam-column connections are designed as rigid connections. However, for facilitating the installation and disassembly, beam-column connections are generally composed of angle irons, bolts and webs, which makes the beam-column connection less than rigid, or rather semi-rigid connection. Depending on the field connection different of stiffness will be achieved, and accordingly the level of rigidity will vary.

This section will deal with beam-column welded structure, which is regarded as rigidly connected. However, some results were produced for the case of semi-rigid connection for the purpose of comparing the failure mode and identifying the critical elements.

5.4.1 Moment, Settlement and Rotation Relationships of Rigid and Semi Rigid Connections

Figure 5.5 presents the moment rotation curves for a rigid connection (welded connection) for the center column (c3) settlement. It can be noted that the moment reached a maximum value, beyond which the rotation continues to increase without any increase in the moment. Furthermore, the relationship for all floors is almost similar, except for top floor which showed slightly lower moment. This is due to the fact that the top floor has only five degrees of freedom fixed; while other floors have six (see typical top floor connection A and another floor B shown in Figure 5.5).

The similar observation was reported for semi-rigid connection in Figure 5.6, which the curves of moment-rotation for every floor are very similar, except for the top floor. The difference with the rigid connection is that the slope of the representative connection stiffness curve of semi-rigid connection is smaller than that of a rigid connection. Furthermore, it can be

noted that the moment reached a maximum value, beyond which the rotation continues to increase without any increase in the moment, these besides as noted for rigid connections, the relationship is similar for all floors except for top floor, which showed slightly lower moment. The reason is also that there are 5 freedoms fixed for top connection and for others there are 6.

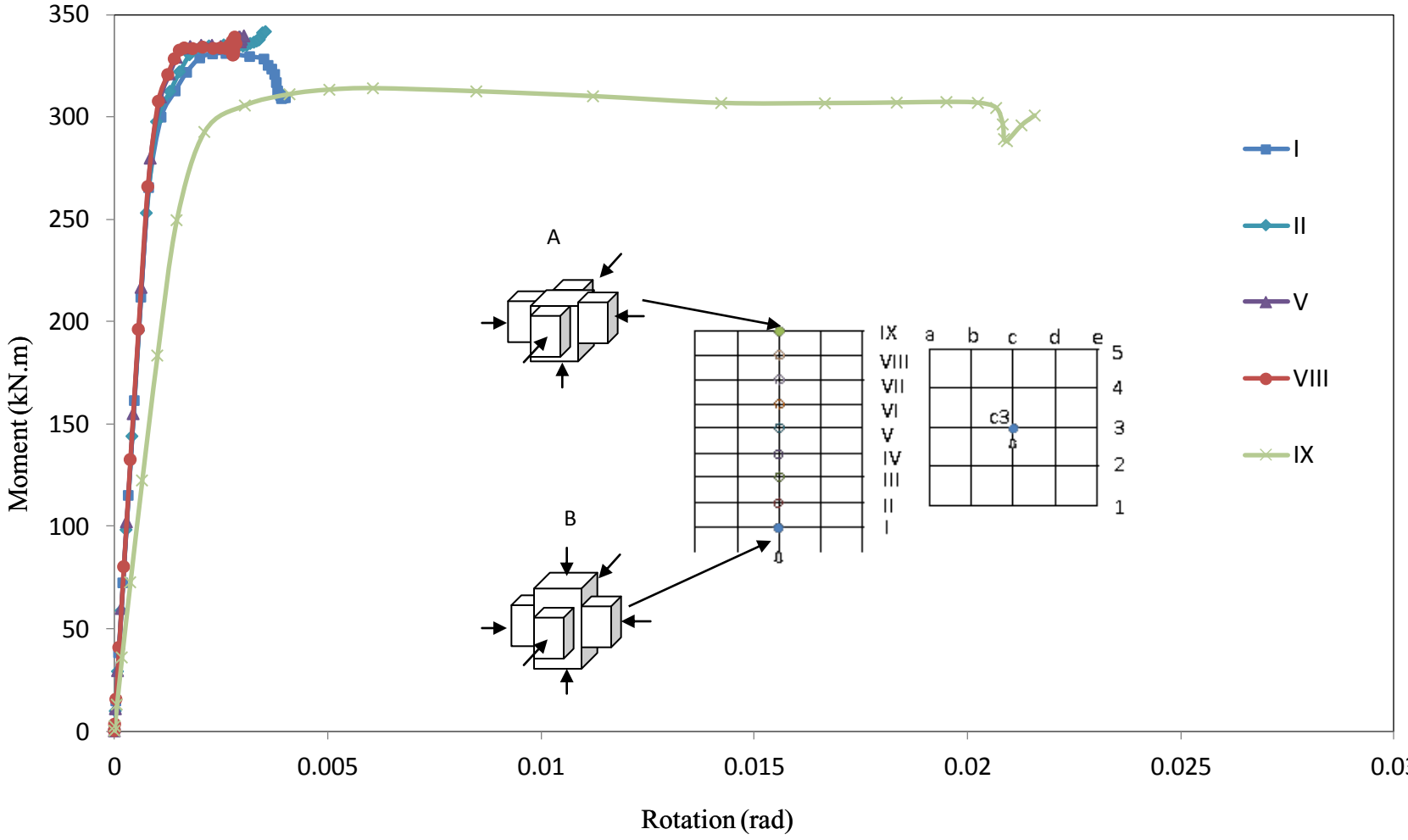

Figure 5.5 Moment rotation curves for the 9 floors steel structure having rigid connection

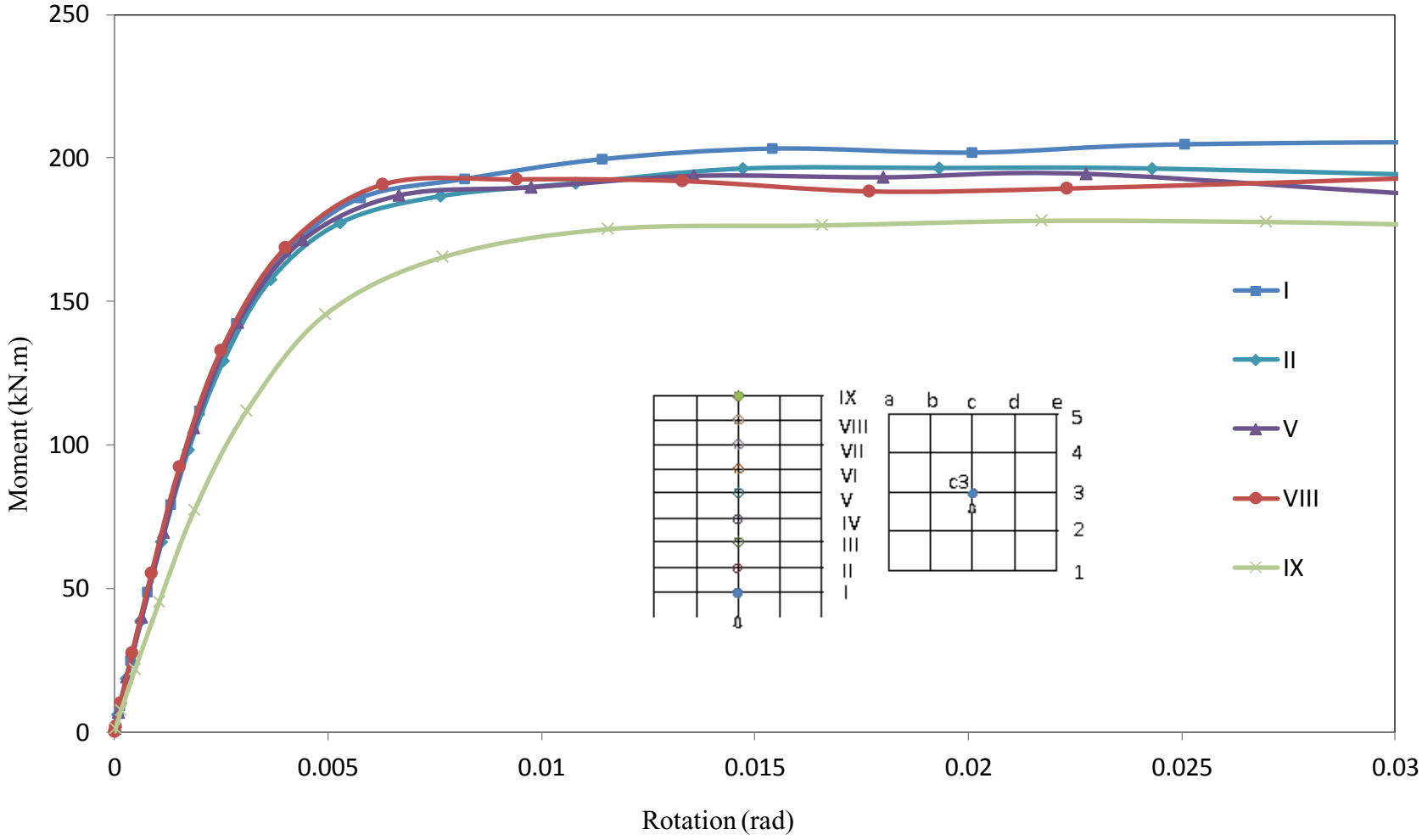

Figure 5.6 Moment rotation curves for the 9 floors steel structure having semi-rigid connection

Figure 5.7 presents moment - rotation relationships of three types of connection (rigid and semi-rigid), which measured at the connections of the first floor, where the moment is the maximum at the center column (c3). It also shows that the moment-rotation curve is closer to its double tangents with increase of stiffness of connections, which expressed with the size of arrows in the figure. Smaller of arrow, it is closer to the double tangents of moment-rotation curve. In fact, the moment and rotation curve of connection obey a semi analytical model proposed by Kishi and Chen (1990) as equation 5.2. This equation expressed the curve of moment and rotation of connection with a shape parameter *n*.

$$M = \frac{K_i \theta_r}{\left[1+\left(\frac{\theta_r}{\theta_o}\right)^n\right]^{\frac{1}{n}}} \qquad Eq.\ 5.2$$

Where $K_i\ is$ initial connection stiffness, θ_r is rotation, $M_u\ is$ ultimate moment capacity and *n* is a shape parameter, which controls the curve closing to the tangents. The three-parameter power model is mathematically represented by the following equation whose general shape for different values of *n* is shown in the Figure 5.8. The larger the *n*, the closer the curve is to the tangent line and the ultimate bending moment line.

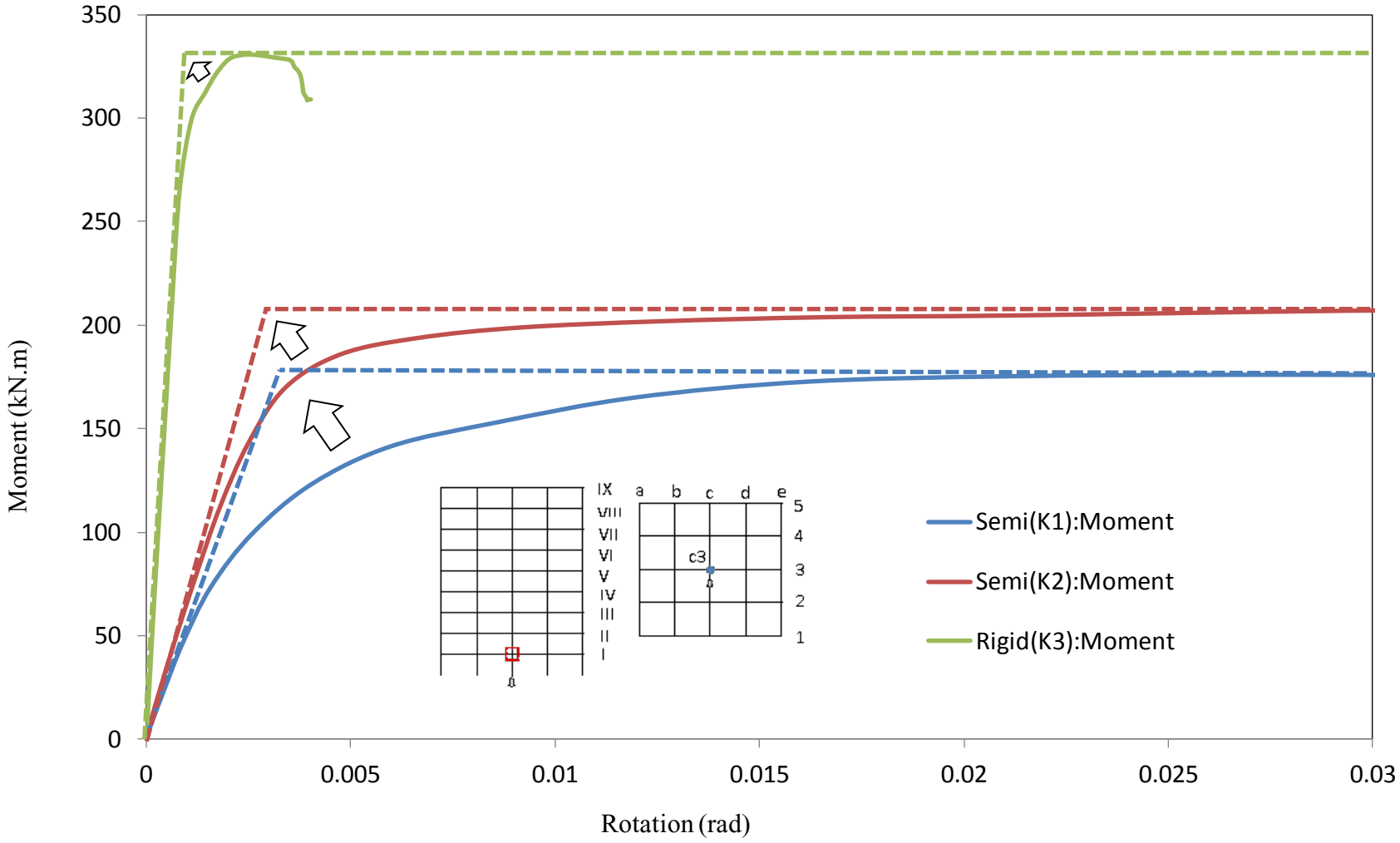

Figure 5.7 Test results: Moment-rotation curves at the first floor for three types of connections at the center column settlement

In order to calculate the moment of beam induced by settlement, a chart is proposed to express the relationship between moment, rotation and settlement. Figure 5.8 gives the relationship between moment-rotation and settlement-rotation curves for the stiffness of K1. The solid red line is the curve of moment-rotation and the solid black line is the curve of settlement-rotation. According to the Eq. 5.2, tangent line equation can be gained while $n = \propto$ as follows,

$$M = K_i \theta_r \qquad \text{Eq. 5.3}$$

So, the tangent line of curve of moment-rotation and M_u line can be drawn in Figure 5.8 as blue lines. The curve of settlement-rotation looks like linear curve, and the equation of settlement-rotation can be expressed as Eq. 5.4.

$$\theta_r = \text{Arctan}(\frac{\delta}{L}) \qquad \text{Eq. 5.4}$$

Where, L is the length of the beam connected to the settling column; δ is the settlement of foundation. The equation of moment M and settlement δ was derived with Eq. 5.2 and Eq. 5.4.

$$M = \frac{K_i \times Arctan(\frac{\delta}{L})}{\left[1+\left(\frac{Arctan(\frac{\delta}{L})}{Arctan(\frac{\delta_0}{L})}\right)^n\right]^{\frac{1}{n}}} \qquad \textit{Eq. 5.5}$$

For three cases of *K1, K2* and *K3*, the parameter n of shape can be gained by the curve of moment and rotation with equation 5.2 and 5.3, which is listed in Table 5.3. And the table gives the parameter comparisons of cross point on initial tangent and ultimate line of moment between $n = \propto$ and the real shape parameter n of curve. It can be seen that the value of $\frac{M}{\delta}$ from calculation with simple idea curves ($n = \propto$) is bigger than the value of $\frac{M}{\delta}$ from original curves (*n=2 for K1 case; n=3 for K2 case and n=6 for case K3*). From the frame resistant to settlement

aspect to analysis, when the curve is closer to idea curves the connections are more efficient for the structure, which means more good design of connections. Equation 5.5 can be used to guide design for engineers.

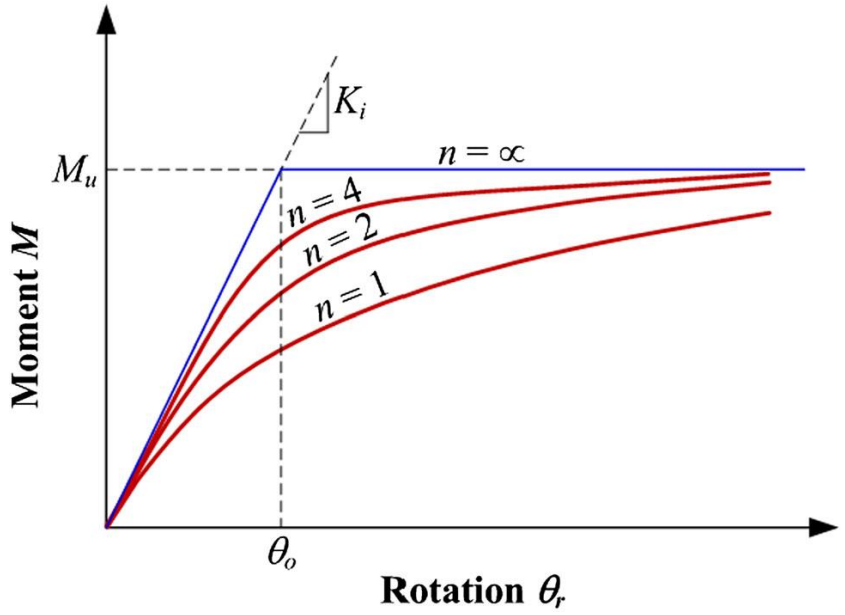

Figure 5.8 $M - \theta_r$ curves for three-parameter power model (Kishi and Chen, 1990)

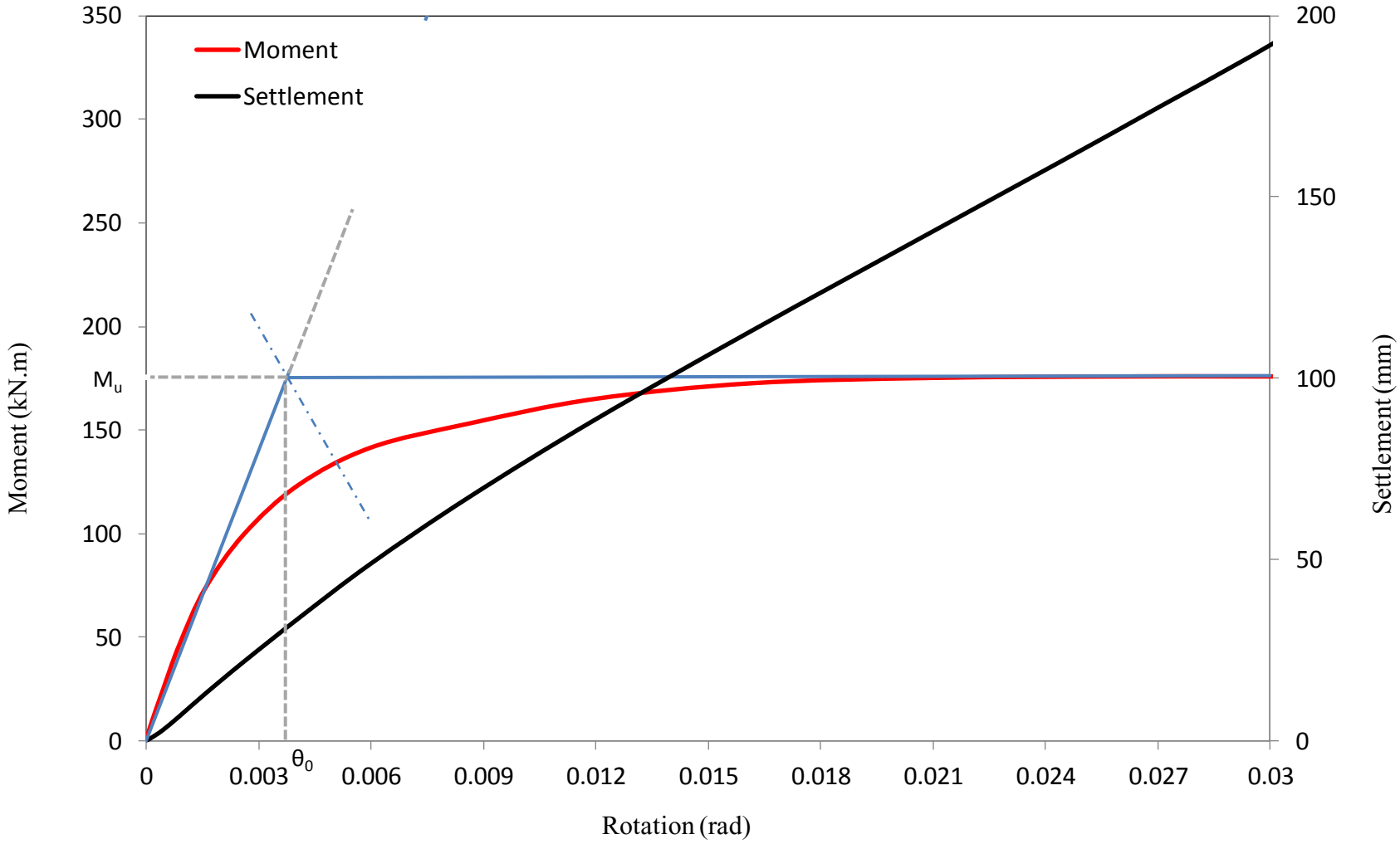

Figure 5.9 Chart for predicting moment and settlement for *K1* case

Table 5.3 Comparison of M, θ_r *and* δ for *K1, K2 and K3*

	Semi (*K1*)		Semi (*K2*)		Rigid (*K3*)	
Shape *n*	n=∝	n=2	n=∝	n=3	n=∝	n=6
Moment *M (kN.m)*	175	136	205	179	330	315
Rotation θ *(rad)*	0.0037	0.0051	0.0032	0.0041	0.0012	0.0015
Settlement δ *(mm)*	30	42	33	52	45	64
$\frac{M}{\delta}$	5.83	3.24	6.21	3.44	7.33	4.92

5.4.2. Settlement of Steel Structure with Rigid Connections

In order to describe the structural responses due to foundation settlement for rigid connection structure, the settlement of center, edge and corner column with 32 mm (elastic stage), 80 mm (maximum end of elastic plastic stage, the cross of moment-rotation and settlement-rotation curves) and 196 mm (maximum moment) in the following sections. In this model, the stiffness of connection *Ks* is 210000, which connections are welded beam to column.

5.4.2.1 Plastic Strain versus Settlement

Based on the results obtained, it can be reported herein that the deformation takes place mainly below the beam ends, which is connected to the settling columns, as shown in Figure 5.10. (a). Figure 5.10 (b), (c) and (d) presents the plastic strain (irrecoverable deformation) developed in beams connected to the settling column in each floor. It can be noted that the damage starts at the first floor at 39 mm, 45 mm and 49 mm settlement for the center, edge and corner column respectively. Then the damage propagates to the higher floors until it reaches the top floor, at 59 mm, 63 mm and 49 mm for center, edge and corner column settlement, respectively. It is of

interest to note that the plastic strains for the top floor is the lowest for the case of center column, and slightly higher for the edge column, and then it reaches a relatively higher value for the corner column. As described earlier, is due to the degree of freedom (rigidity) of the column connections to the adjacent beams.

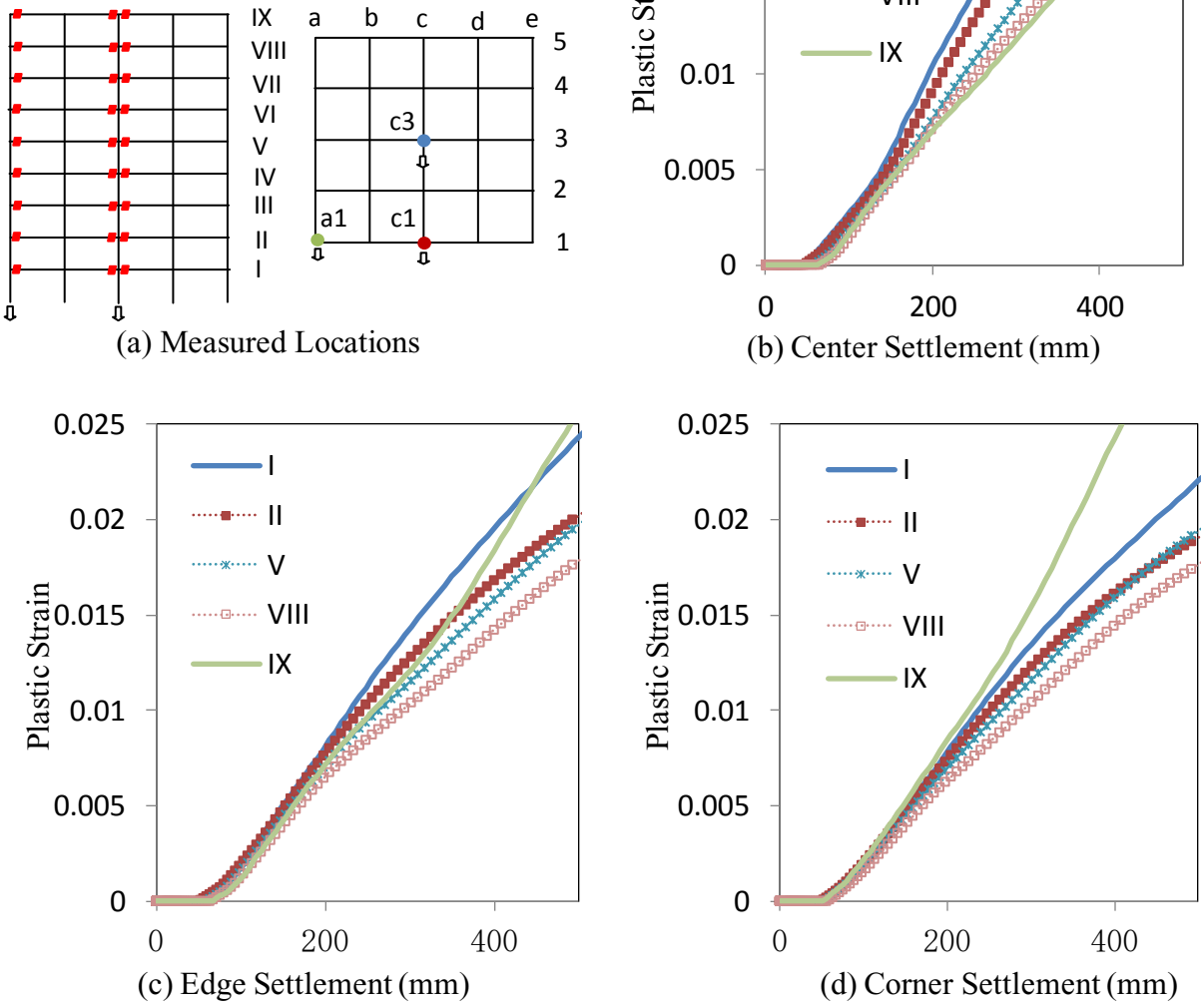

Figure 5.10 plastic strain versus settlement of beam ends connected to the settling column

5.4.2.2 Vertical Displacement of Columns vs Settlement

Figure 5.11 (a) is the measurement location of structure. Figure 5.11 (b) presents the vertical displacement (compression) of columns versus floor level, due to the settlement assigned to the center column c3. It can be noted that the displacement decreases with the increase of the floor level.

Figure 5.11 (c) presents the vertical displacement in the neighbor column b3 (one panel away from the settling column (c3). It can be noted that the column (b3) experienced compression for low values of the settlements up to 80 mm, and then it was reversed to tension, when the settlement reached 196 mm. This is due to the uplift force acted on column b3 while increasing the settlement on column c3.

Figure 5.11 (d) presents the vertical displacement in the neighbor column a3 (two panels away from the settling column (c3). It can be noted that all columns were subjected to compression. This can be explained by the fact that the beams c3 - b3 – a3 are acting as continuous beam, thus while b3 is under tension, the columns in a3 will be subjected to compression.

It is of interest to know that while column c3 was experiencing compression during settlement, column b3 was fist subjected to compression at low settlements then reversed to tension for higher values, column a3 was subjected to compression at all values of the settlements. Furthermore, the relative vertical displacement between the first floor and top floor for the column c3 is 26 mm for settlement of 196 mm, 32 mm for settlement of 80 mm and 22 mm for settlement of 32 mm, which show nonlinear behavior.

Similar analyses were performed for edge and corner columns c1 and a1, where similar

observations were noted, (Figure 5.12 and Figure 5.13). Table 5.4 summarizes these results, which presents vertical displacement versus floor level for the settlement of the center, edge and corner columns.

It can be reported herein that the center column represents the most critical case for the structure, followed by the edge column then the corner column. Furthermore, the maximum vertical displacement takes place in the first floor for all three columns.

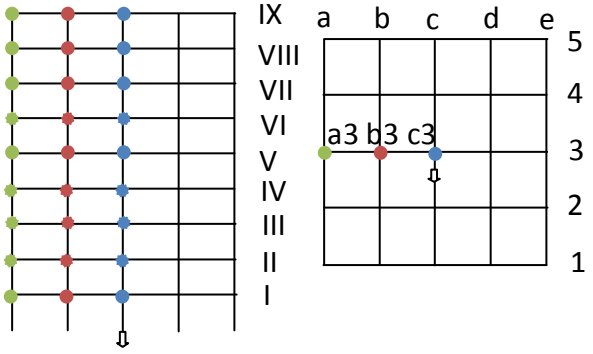

(a) tested locations

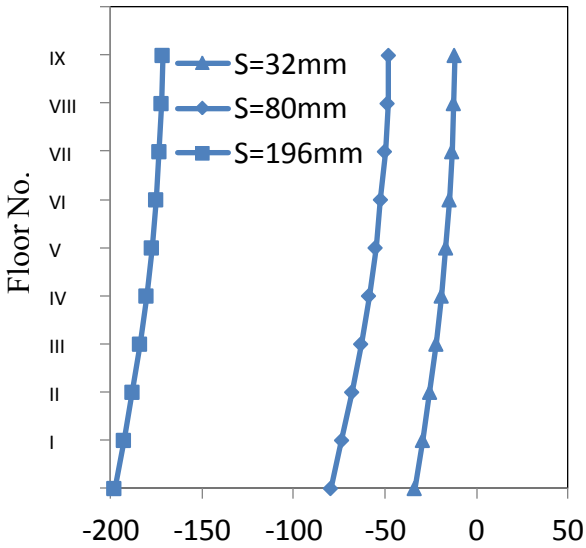

(b) Displacement (mm) (Center column c3)

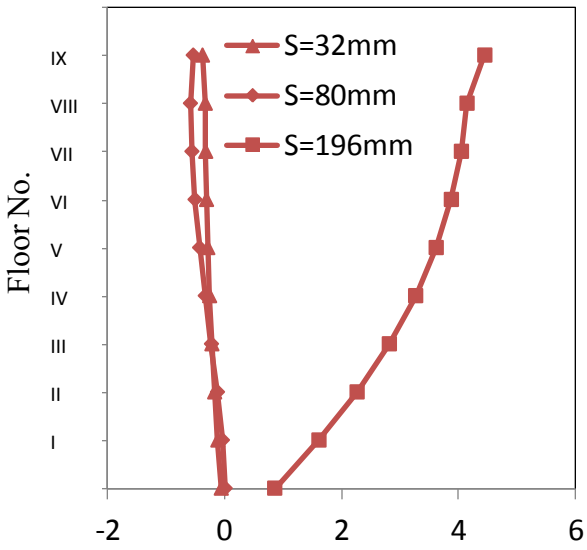

(c) Vertical displacement (mm)(Column b3)

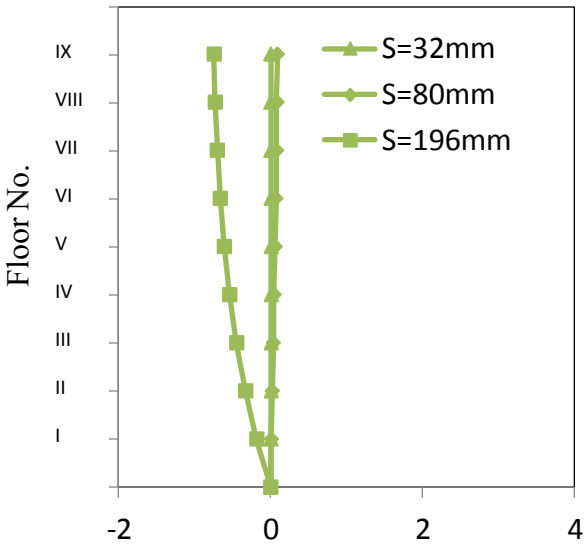

(d) Verticl displacement (mm)(Column a3)

Figure 5.11 Vertical displacements of columns c3, b3 and a3 versus Floor level during the settlement of center column c3

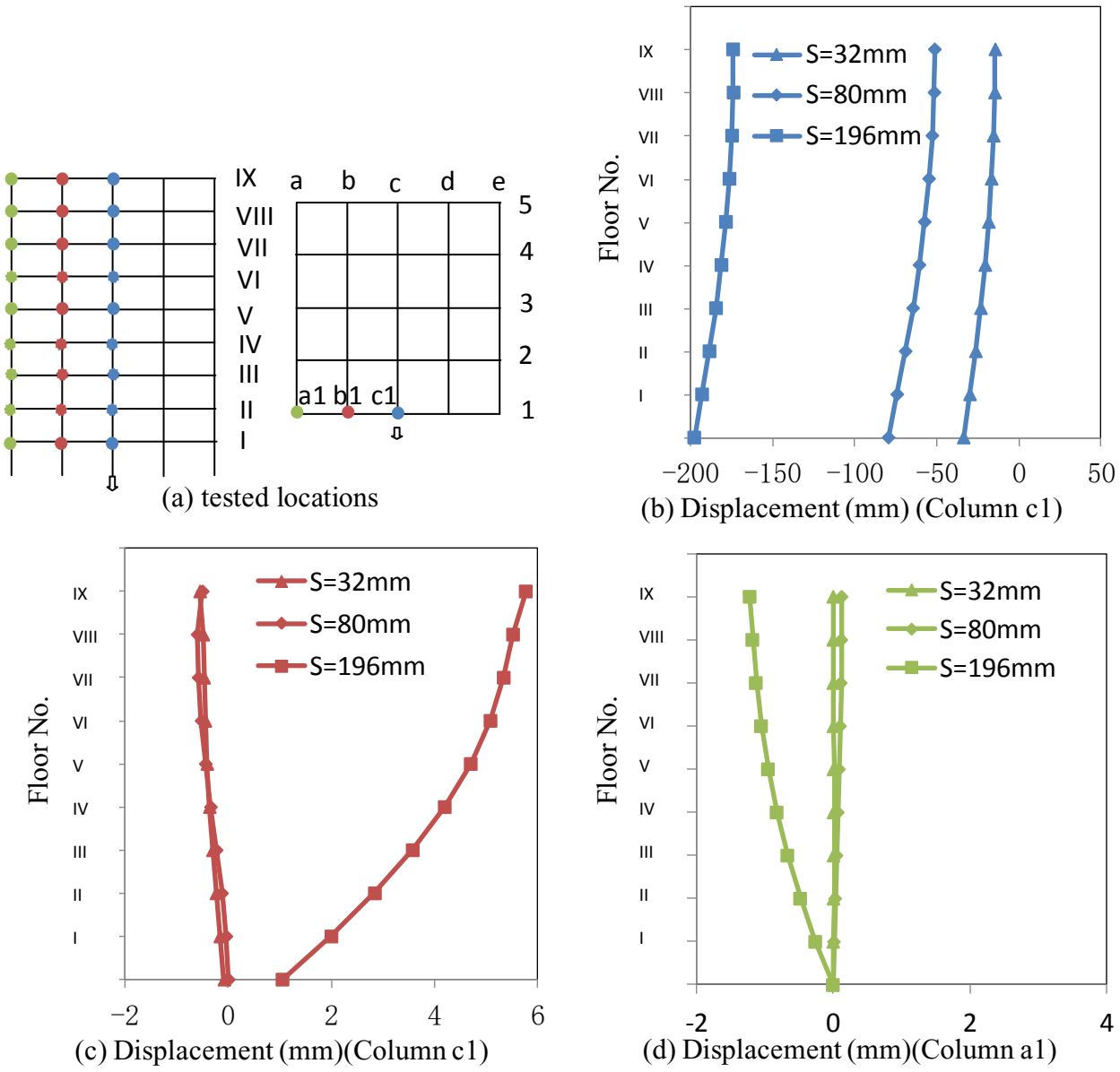

Figure 5.12 Displacement of columns c1, b1 and a1 versus Floor level during the settlement of column c1

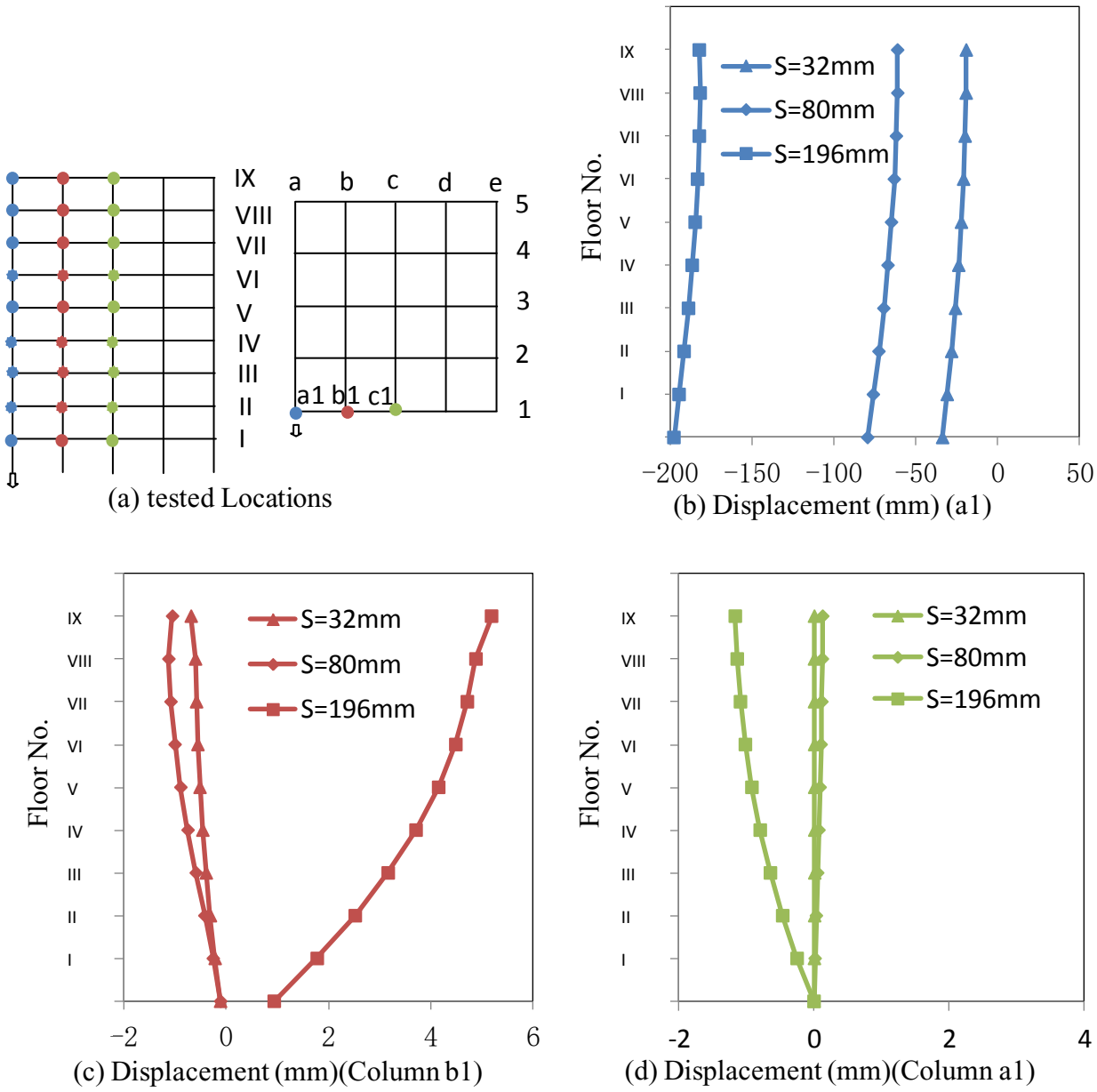

Figure 5.13 Displacement of columns a1, b1 and c1 versus Floor level during the settlement of column a1

Table 5.4 Summary of vertical displacement of column comparison for center, edge and corner at settlement of 32 mm, 80 mm and 196 mm

Settling on the column	Measured on column	*Vertical displacement at Settlement of 32 mm	Vertical displacement at Settlement of 80 mm	Vertical displacement at Settlement of 196 mm
Center (c3)	c3	#(+)26mm	(+)32mm	(+)22mm
	b3	(–)3.2×10^{-1}mm	(–)5.5×10^{-1}mm	(+)3.6mm
	a3	(+)4.6×10^{-4}mm	(+)8×10^{-2}mm	(–)7.4×10^{-1}mm
Edge (c1)	c1	(+)18mm	(+)29mm	(+)22mm
	b1	(–)5.6×10^{-1}mm	(–)5.1×10^{-1}mm	(+)4.3mm
	a1	(+)6.3×10^{-3}mm	(+)1.3×10^{-1}mm	(–)1.2mm
Corner (a1)	a1	(+)13mm	(+)19mm	(+)14mm
	b1	(–)5.8×10^{-1}mm	(–)1.2mm	(+)4.3mm
	c1	(+)6.2×10^{-3}mm	(+)1.3×10^{-1}mm	(–)1.2mm

* Vertical displacement of column is the relative displacement of the bottom floor and the top floor.

(+) means tension displacement and (-) means compression displacement

5.4.2.3 Horizontal Displacement in Columns vs Settlement

Deferential settlement between foundation elements in a structure generates horizontal displacement of the settling column (drift), which is materialized in the form of horizontal forces acting on the structure. These horizontal forces are often ignored during the design of the structure, especially for steel structure for the design of the bracing.

Figure 5.14 presents the horizontal displacement versus the settlement for the center, edge and corner columns. It can be noted (Figure 5.14.a) that column c3 did not experience any horizontal displacement, mainly due to the similarity of the column location within the building. Furthermore, the neighboring column b3 and edge column a3 showed similar behavior at all floor. The value of horizontal displacement of column increases with the level of the floor.

Figure 5.14 (b) and (c) present the settling at c1 and a1 where similar behavior was observed. Both settling columns are inclined towards the interior of the building for all floors, while the top column is opposite. The value of displacement decreases with the increase of floor level except for the top floor. It has the opposite rule for the neighboring columns, which is the value of displacement increases with the level of floor. The maximum horizontal displacements of column happened in neighboring columns of settling center column (b3), in settling edge column (c1) and in settling corner column (a1).

Figure 5.15 presents the tested location of horizontal displacement of column and the horizontal displacement versus floor level at the settlement of 32mm and 196mm of Center column, edge column and corner column, respectively. It can be seen that the horizontal displacement is close to zero at settlement of 32 mm. When settlement reaches 196mm the displacement increases a lot. There are similar displacements for the floors between top and

bottom floor. And the largest relevant horizontal displacement first happens in the top floor for three settlement cases and then in the second floor.

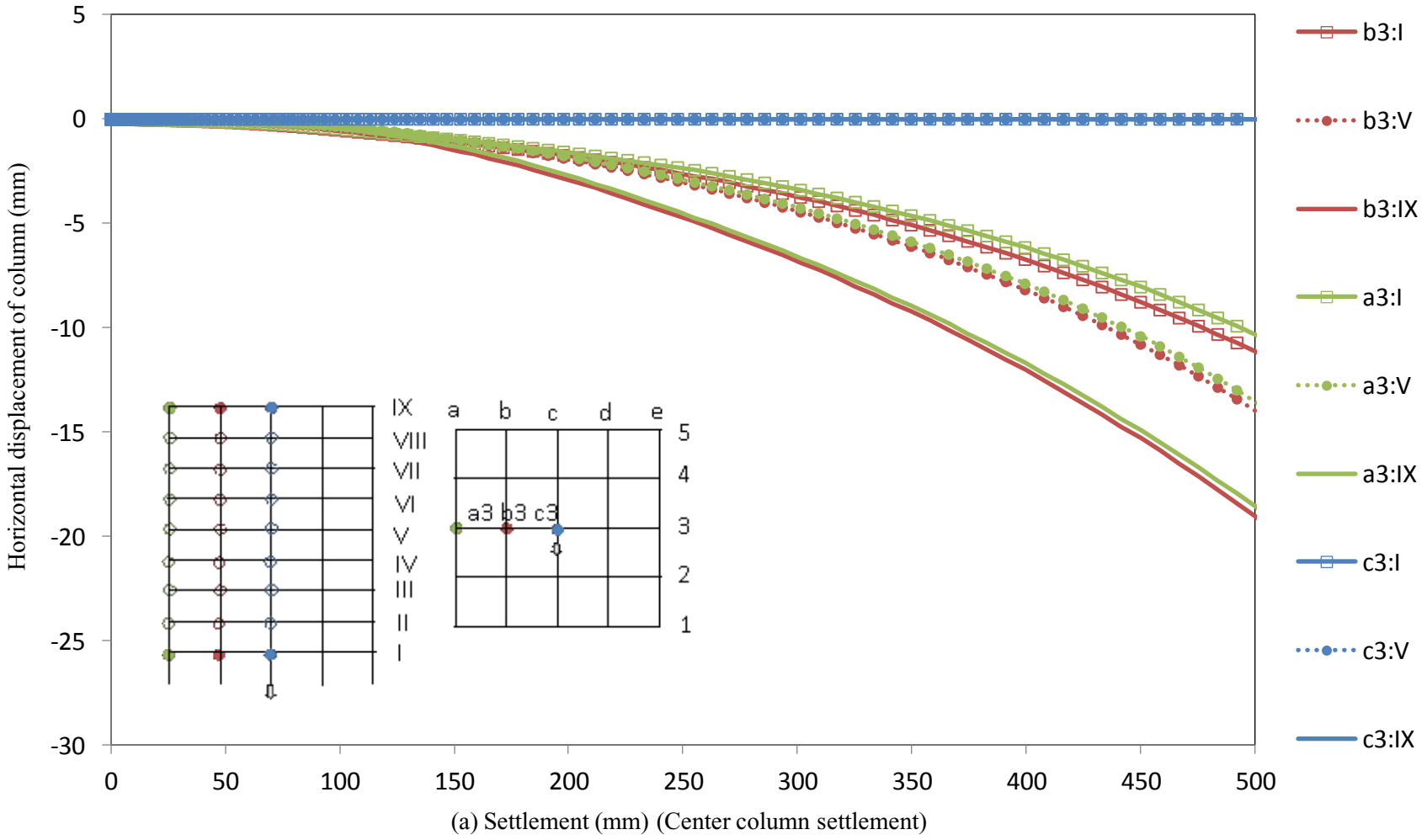
Horizontal displacement of column (mm)
5
0
-5
-10
-15
-20
-25
-30
0
50
100
150
200
250
300
350
400
450
500
(a) Settlement (mm) (Center column settlement)
b3:I
b3:V
b3:IX
a3:I
a3:V
a3:IX
c3:I
c3:V
c3:IX
IX
VIII
VII
VI
V
IV
III
II
I
a
b
c
d
e
5
4
3
2
1
a3 b3 c3

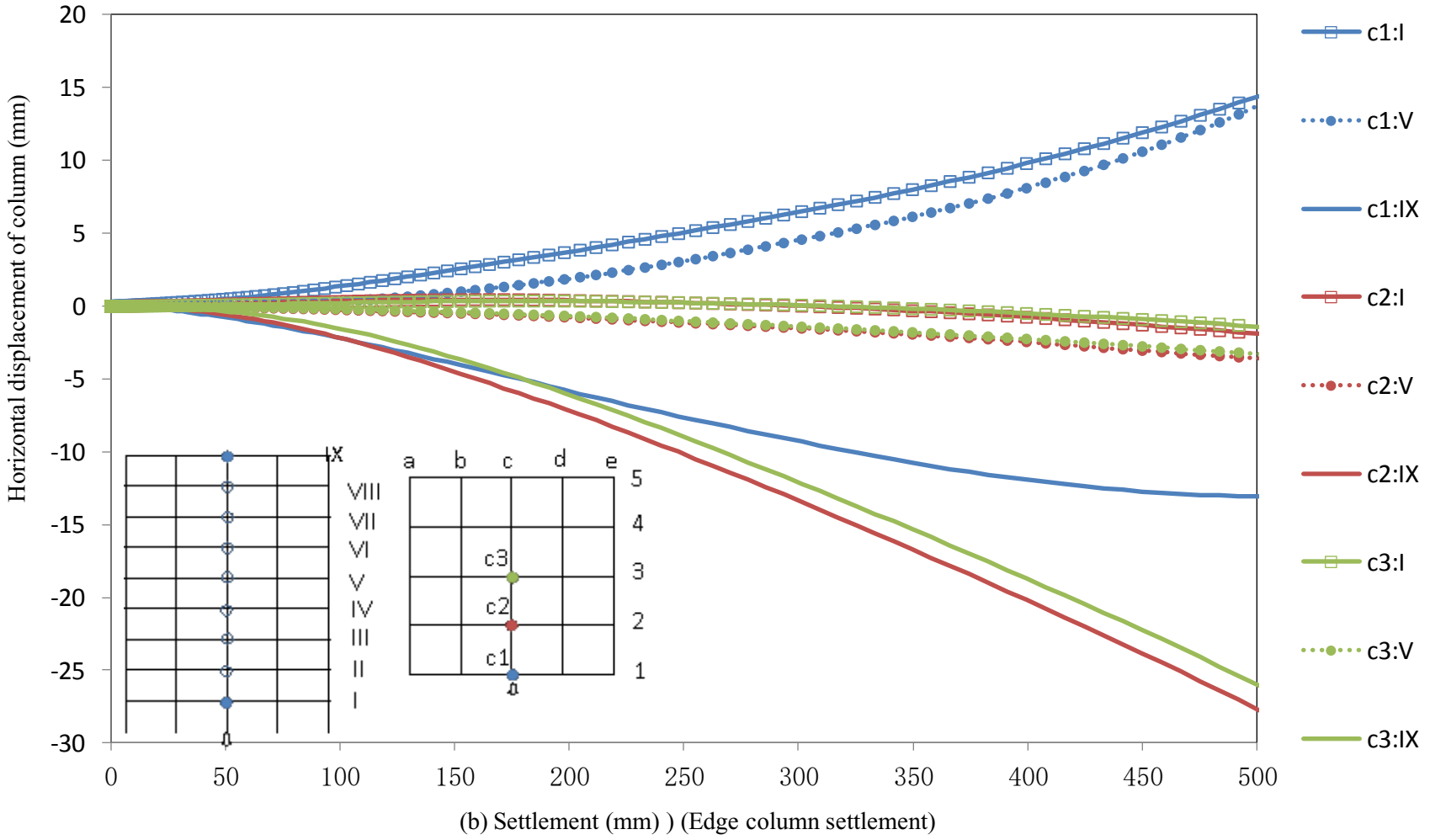

(b) Settlement (mm)) (Edge column settlement)

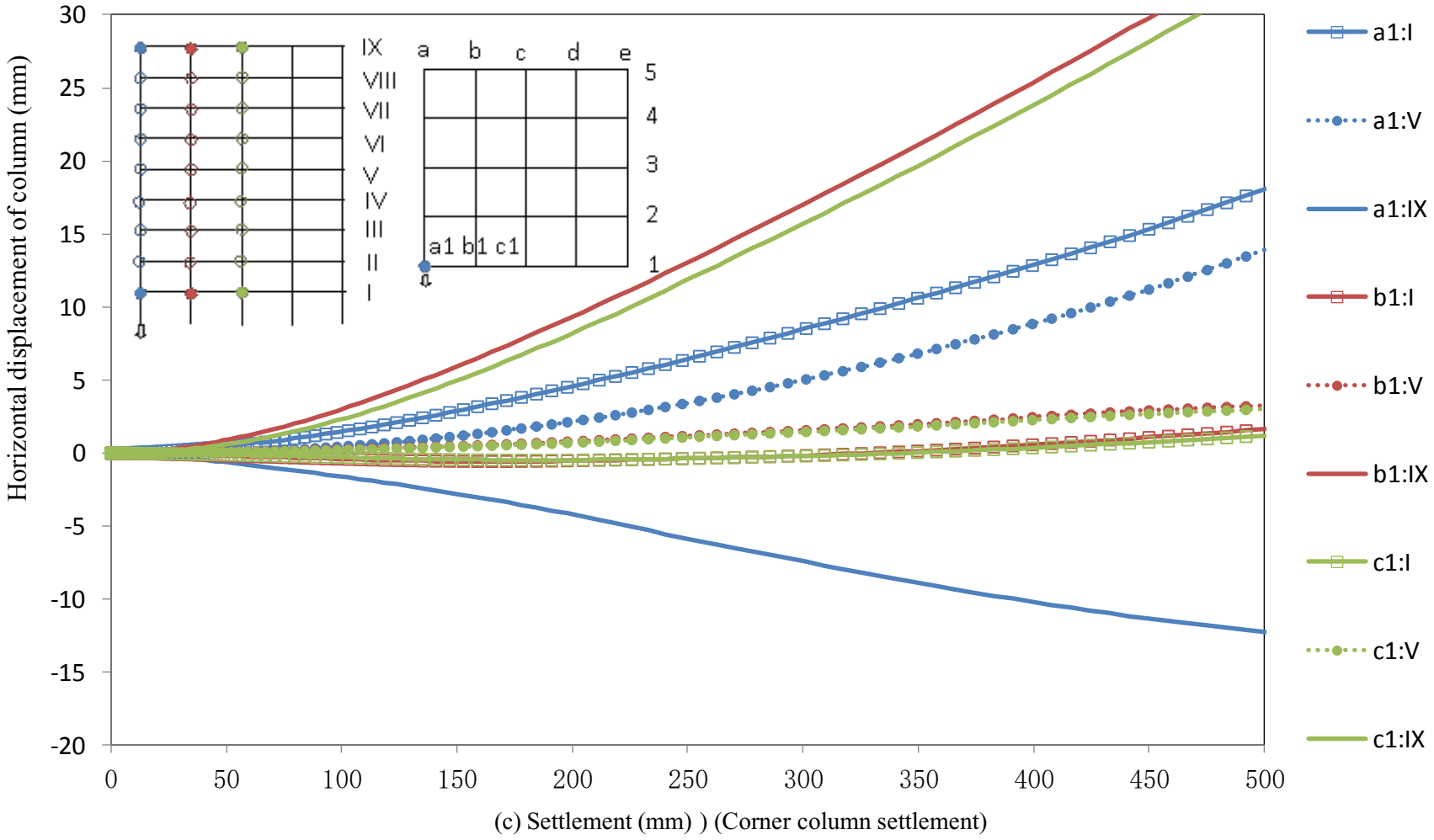

Figure 5.14 horizontal displacements versus settlement during the settlement of the center, edge and corner columns.

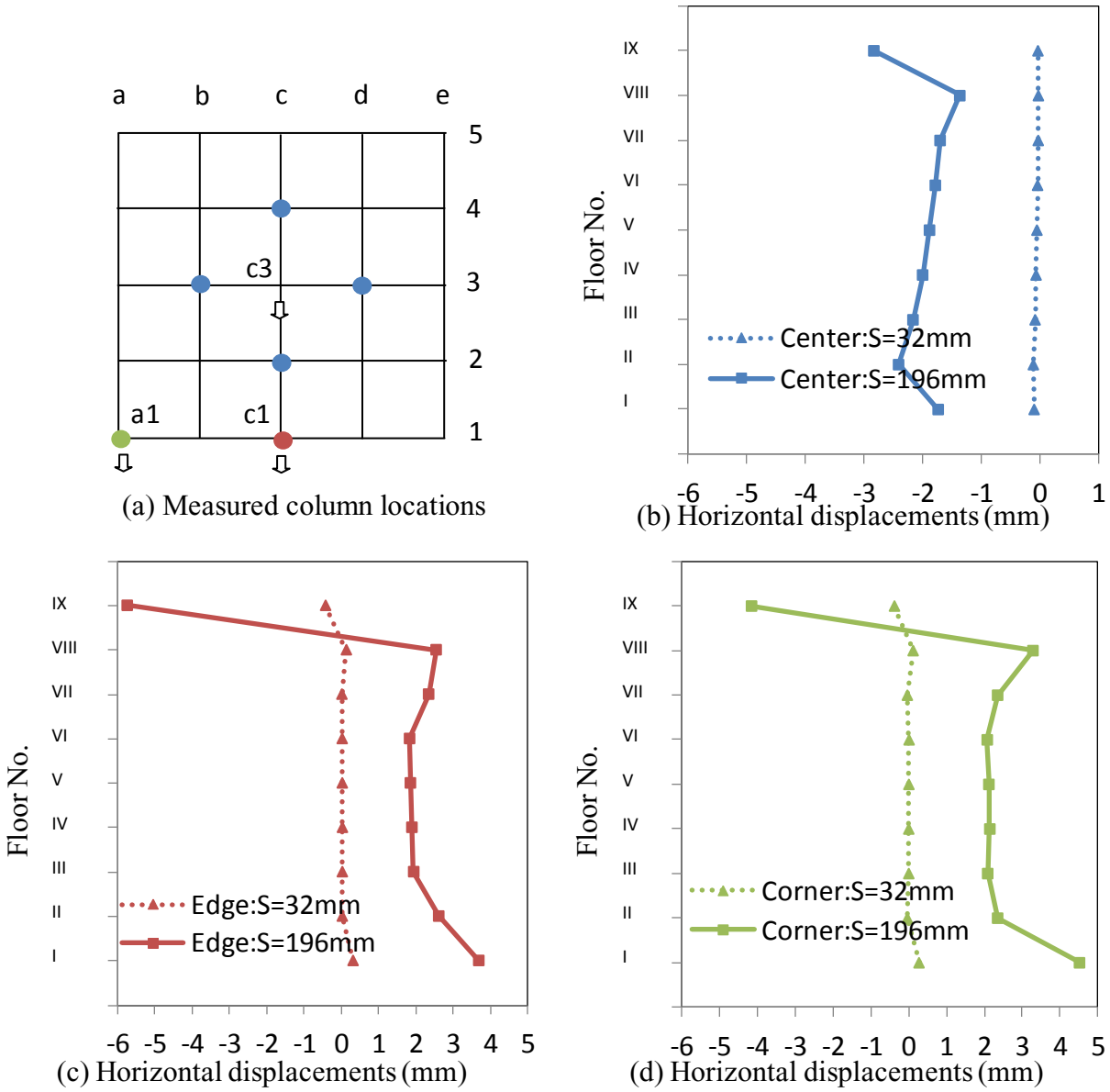

Figure 5.15 Maximum horizontal displacement vs Floor level on columns during settlement

5.4.2.4 Axial Forces of Column versus Settlement

Figure 5.16 presents the axial forces developed in columns due to the settlement of the center, edge and corner columns, c3, c1 and a1 respectively. It can be noted that for the center column, the settlement develops tensile force in all floors. However, for the edge and corner columns, the top floor experiences the compression forces. These forces in columns decrease with

the increase of the floor level. Furthermore, the axial force increases with the column settlement, until it reaches the maximum value of 8931 kN at settlement of 80 mm for center column settlement, 6040 kN at the settlement of 93 mm for edge column and 4310 kN at the settlement of 98 mm for corner column, respectively.

Figure 5.17 to Figure 5.19 present the axial forces of columns versus floor level at the settlement of 32 mm (elastic phase), 80 mm (elastic plastic phase) and 196 mm (plastic phase) in three scenarios of settlement in center column, edge column and corner column. It can be concluded that axial forces of settling columns are obviously higher than adjacent columns for all three settlement scenarios. And the axial forces of columns in center column settlement are higher than in edge column settlement and following in corner column settlement.

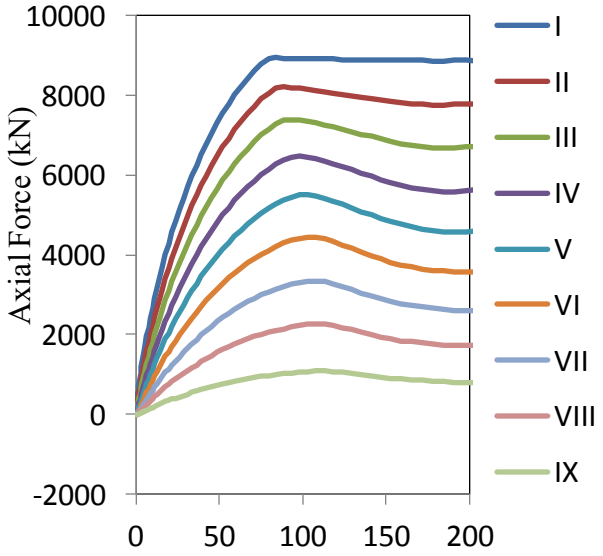

(a) Settlement (mm) at the center column

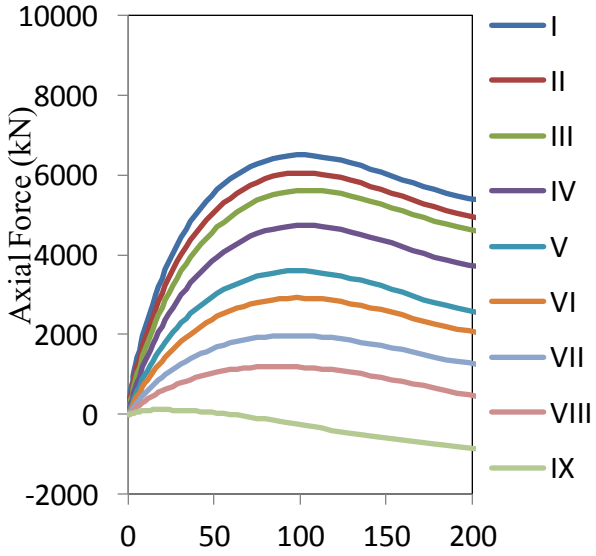

(b) Settlement (mm) at the edge column

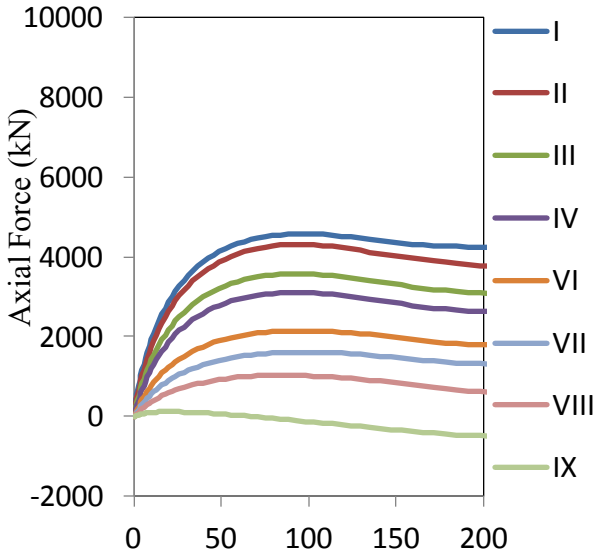

(c) Settlement (mm) at the corner column

Figure 5.16 Axial force developed in columns during the settlements of center, edge and corner columns

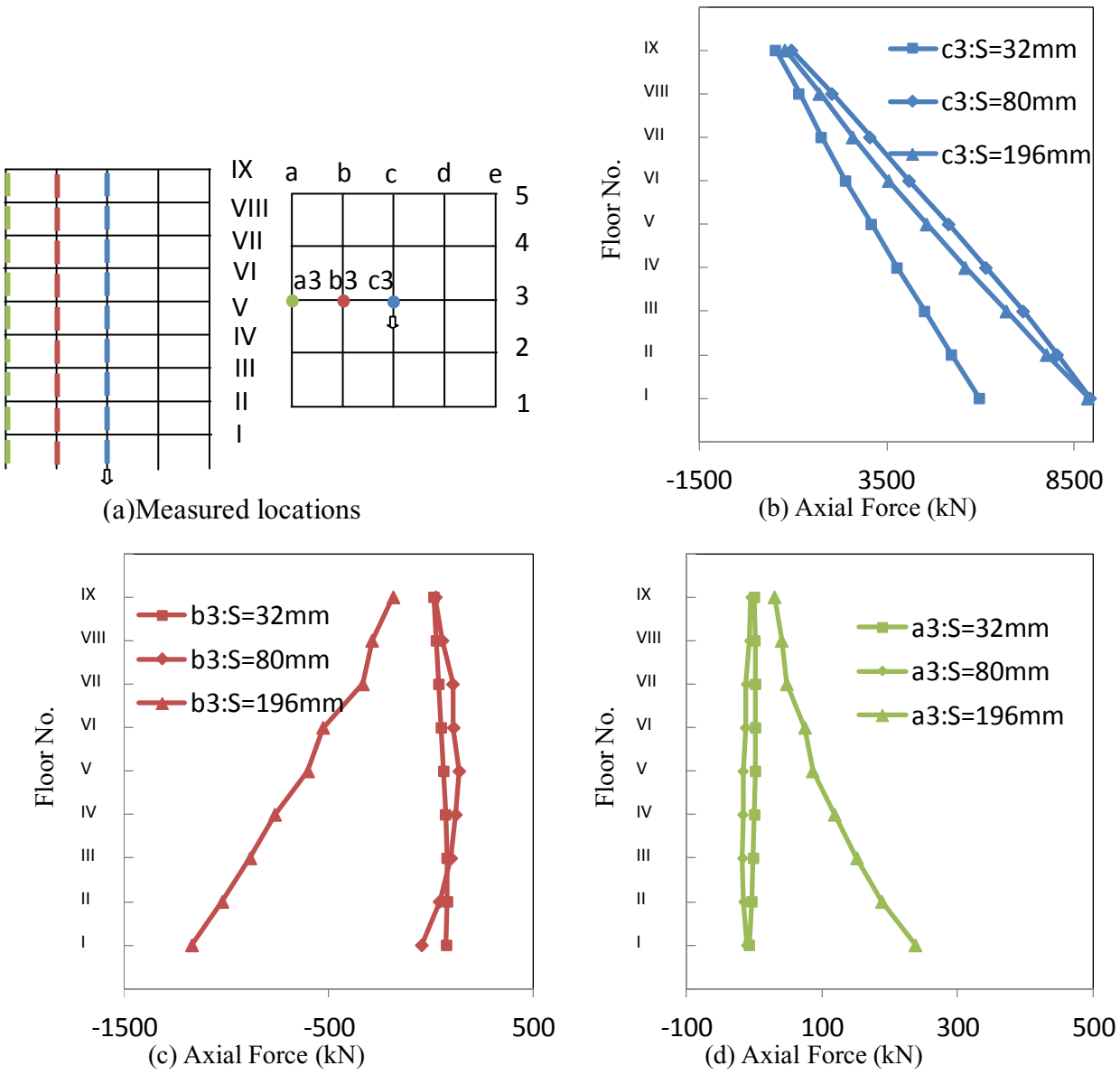

Figure 5.17 Axial forces in columns due to settling the center column c3

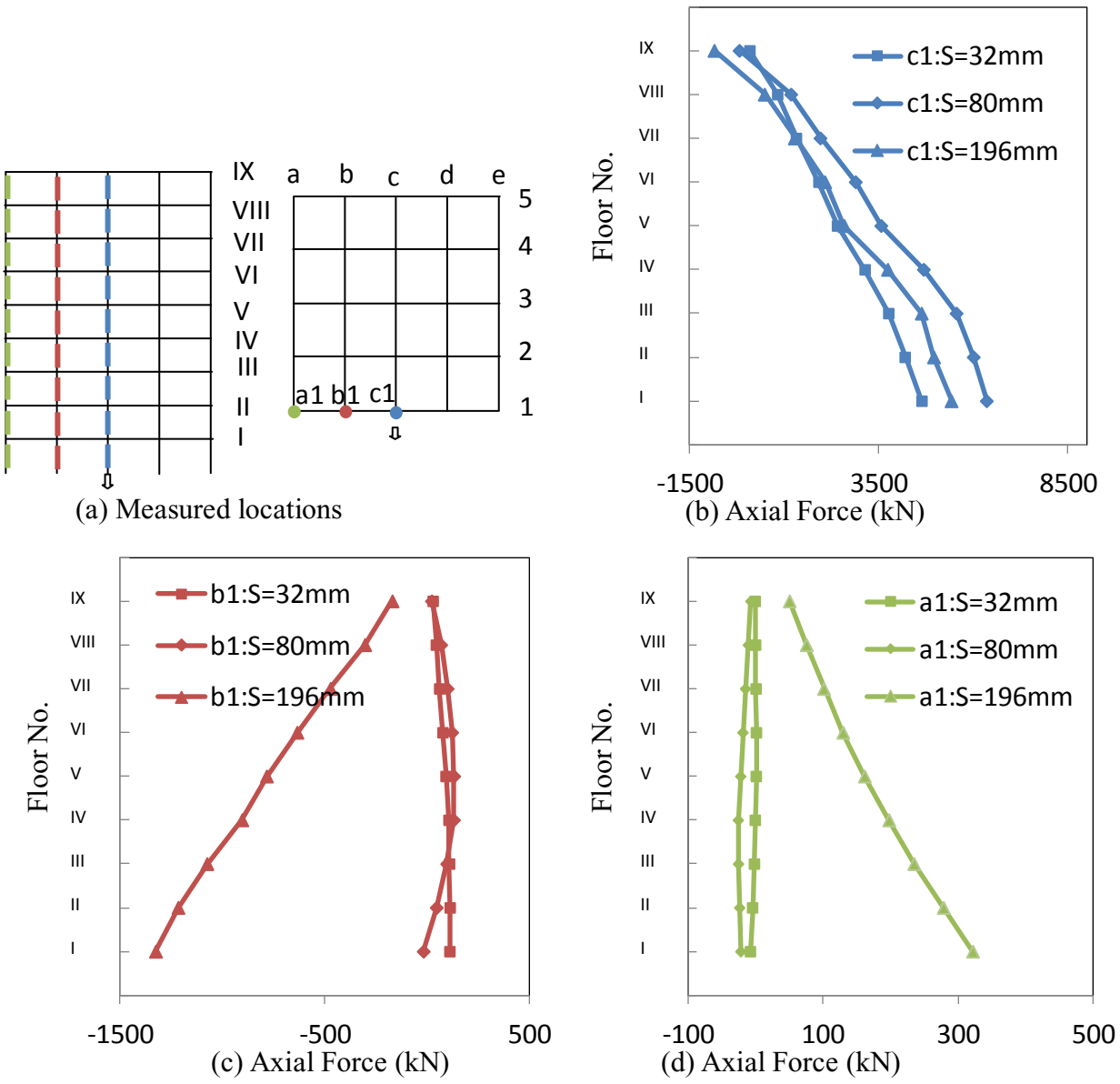

Figure 5.18 Axial forces in columns due to settling the edge column c1

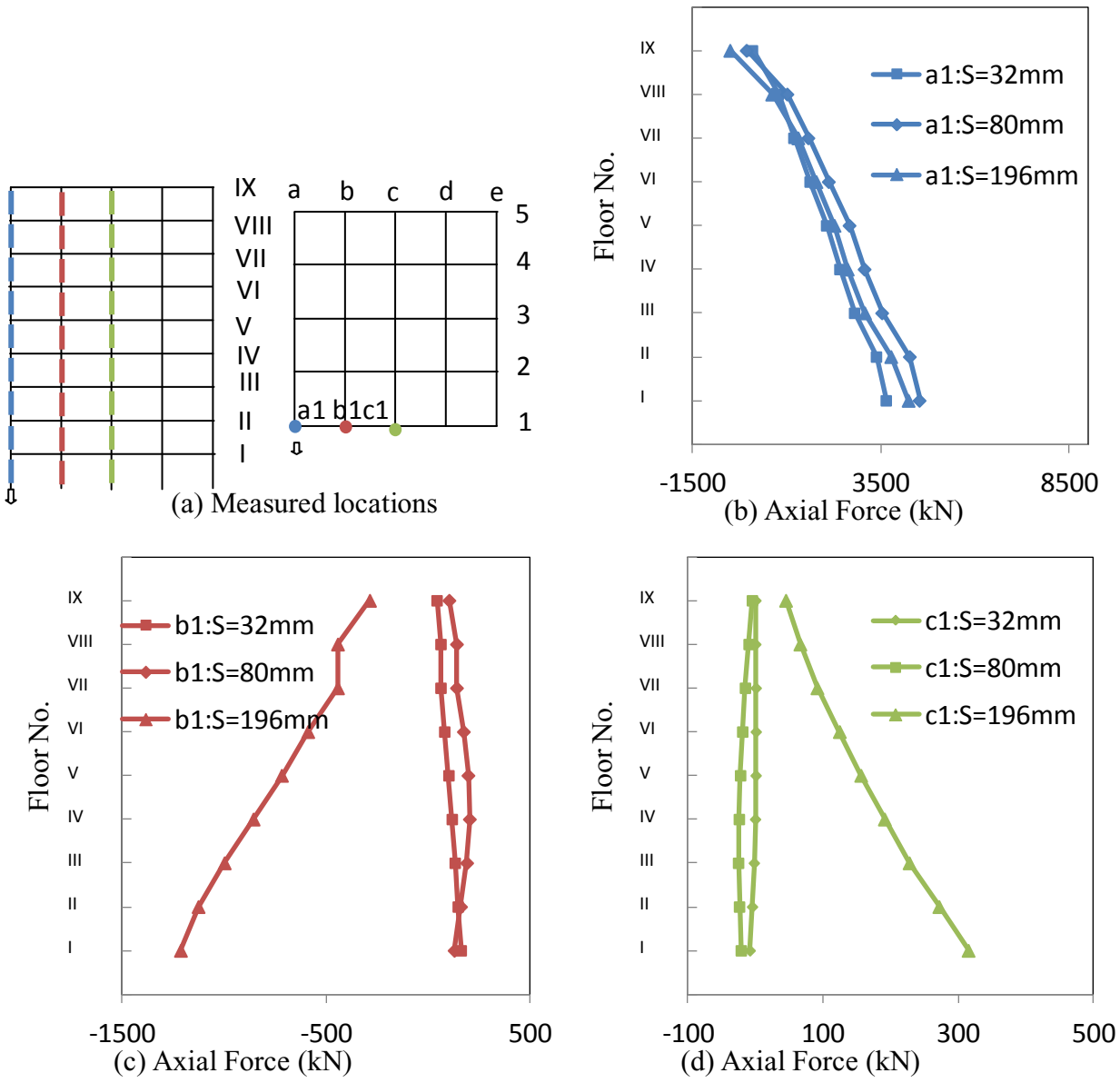

Figure 5.19 Axial forces in columns due to settling the corner column a1

5.4.2.5 Bending Moment Development in Beams vs Settlement

Figure 5.20 presents the bending moments developed at the end of the beam connected to the column during the settlement of the center, edge and corner columns. It can be noted that negative moments and positive moments were generated in the two ends of the beams connected to the settling column. The largest positive bending moment occurred at the end of the beam, which is connected to the settling column, which decreases with the increase of floor level at the settlement of 32 mm and no big changes at the settlement of 196 mm.

Figure 5.21 presents the maximum bending moments of beams for c3 settlement, c1 settlement and a1 settlement (Rigid). The maximum moment took place in edge column settlement case comparing with other two cases. Corner column settlement generates least moment due to the settlement.

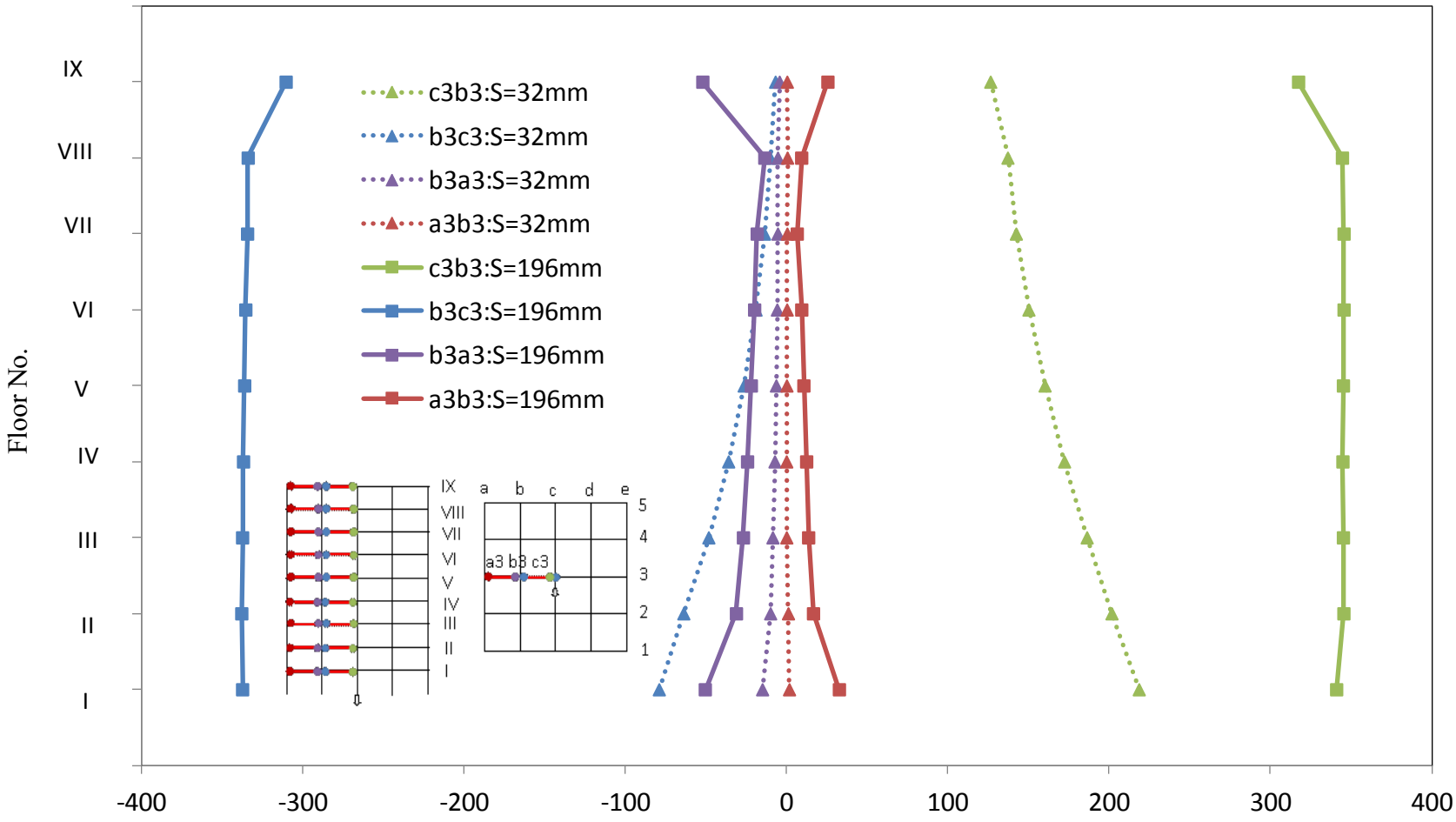

(a) center column c3

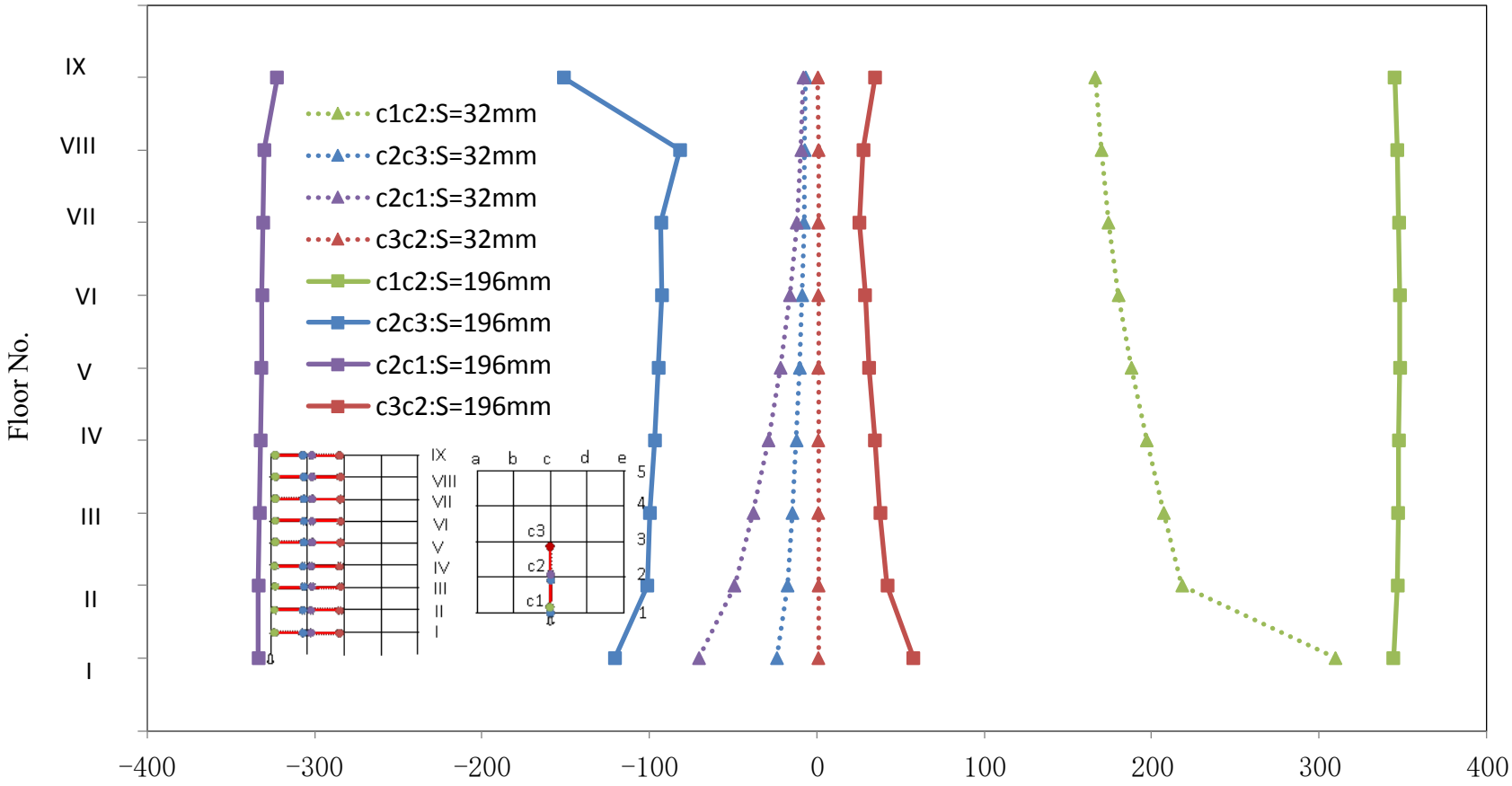

(b) edge column c1

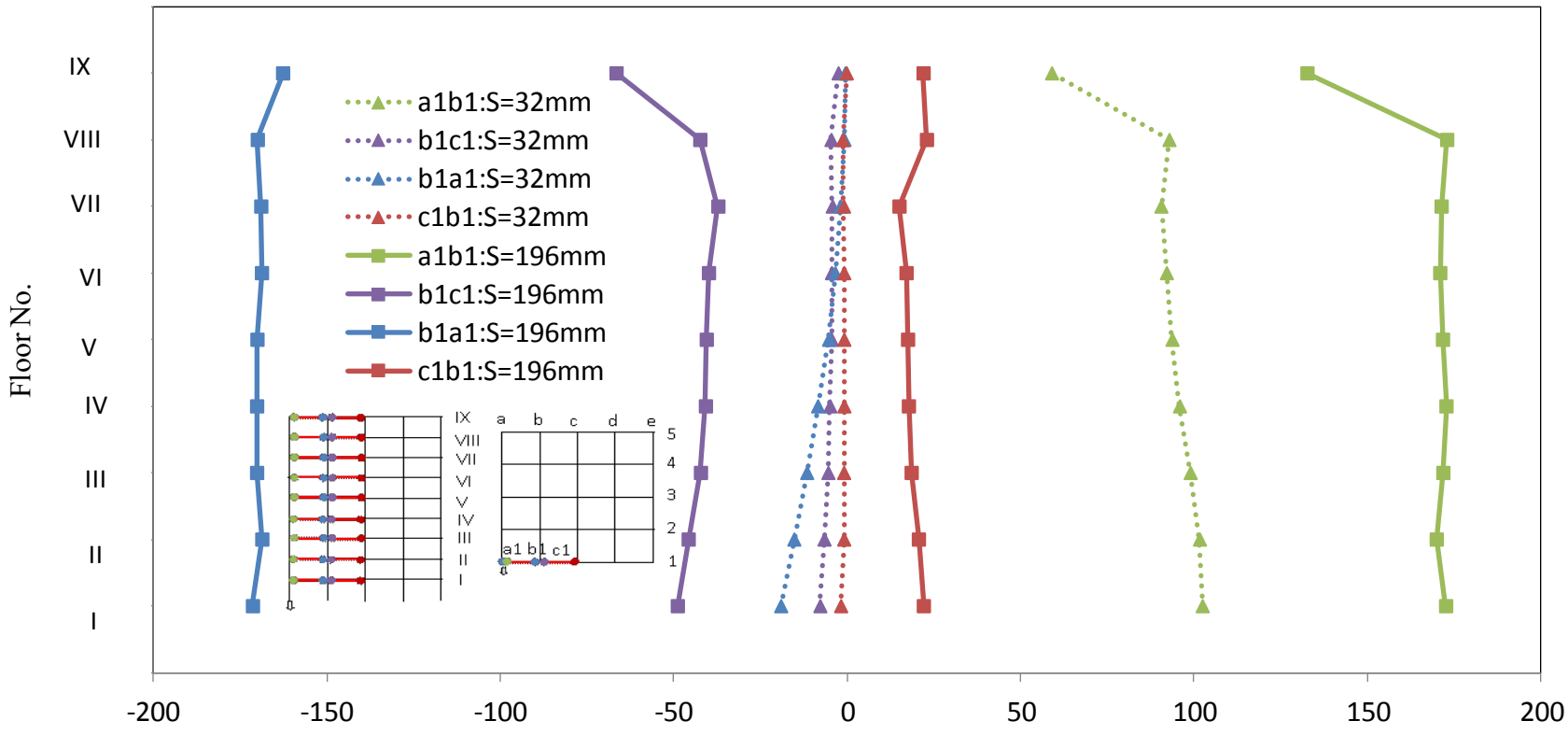

Figure 5.20 Moments at beam ends vs floor no. due to settlement

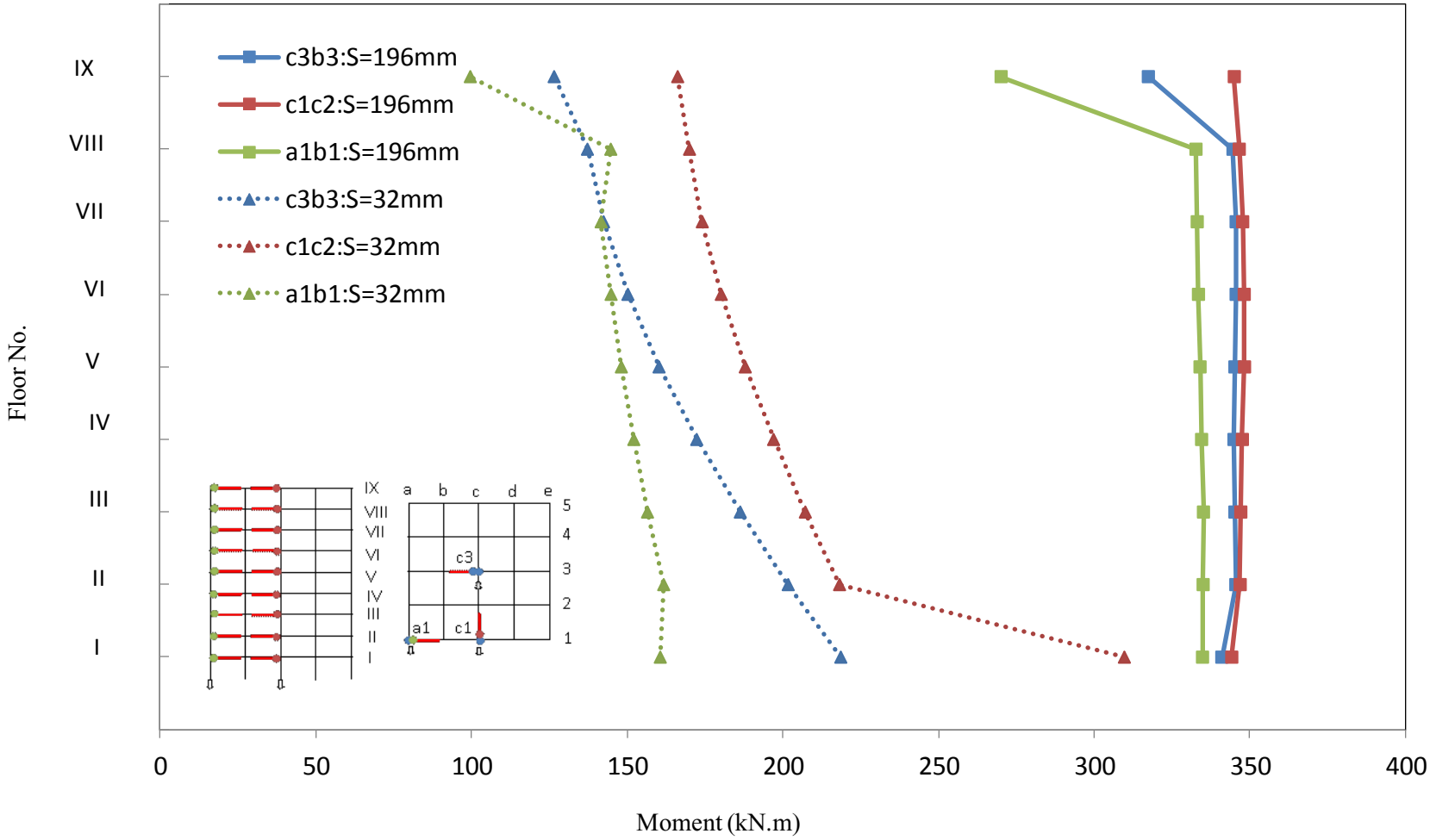

Figure 5.21 Maximum bending moments of beams for c3 settlement, c1 settlement and a1 settlement (Rigid)

5.4.3 Comparison Analysis for Rigid and Semi-rigid Structures

In order to get the structural responses due to settlement of foundation to semi-rigid connection structure, the same investigation was conducted for the semi-rigid structure. The following sections only present the differential results for semi-rigid connection structure comparing with rigid connection structure. The semi-rigid connection structure was designed with web angle connection, which stiffness of connection Ks only is 1/20 of stiffness of rigid connection.

5.4.3.1 Plastic Strain versus Settlement

Theoretically, a rigid connection can be considered to be the beam or column at the position where the elastic-plastic deformation first occurs, rather than the connection itself. For semi-rigid connections, it can be considered that the first elastoplastic deformation occurs in the connection itself. Numerical simulation results comparing rigid connection and semi-rigid connection structures also show this point. The plastic strain happened mainly on the beam ends connecting to settling columns for the rigid connection structure, but there is almost no plastic strain on the beams of the semi-rigid connection structure. The plastic strain mainly happened on the angles and webs of connection for the semi-rigid connection structure. Whether it is beam deformation or angle deformation, the deformation always expands from the bottom floor to the upper floor as the settlement increases. The effect of settlement on the deformation of the bottom and top floors is greatest in the case of corner settlement, followed by edge settlement, and finally central settlement. In the design of corner columns and edge columns, not only should attention be paid to the impact of settlement on the bottom floor, but also the impact of settlement on the top floor should be paid attention to.

5.4.3.2 Vertical Displacement of Column versus Settlement

Figure 5.22 presents the vertical displacements of the settling column versus the floor level at settlement of 196 mm for rigid and Semi rigid structures. It can be noted that the vertical displacements of rigid connection structure are relatively higher than for the semi rigid for the same floor. The deference gets wider for higher floors. For the settlement column of the semi-rigid connection structure, the settlement effect of adjacent columns is the same as that of the rigid connection structure. The difference is that the overall impact has become smaller. This is mainly because the connection stiffness decreases, and the reaction force given to the connected columns becomes smaller.

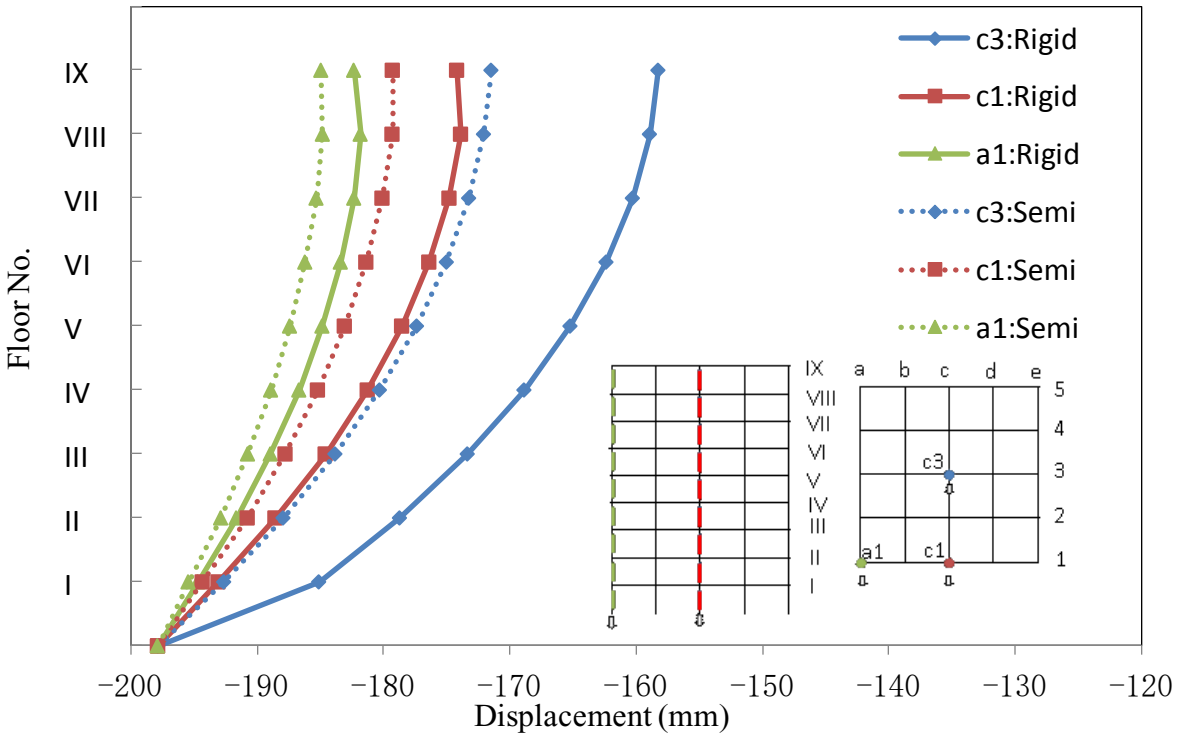

Figure 5.22 Vertical displacements of settling columns versus floor level at settlement of 196 mm for rigid and Semi rigid structures

5.4.3.3 Horizontal Displacement of Column versus Settlement

Figure 5.23 presents the horizontal displacement versus floor level at settlement of 196 mm for rigid and Semi rigid structures. It can be noted that the rigid connection structure provides more resistance to horizontal displacement as compared to the semi rigid structure. Furthermore, for the case of edge or corner settlement, the horizontal displacement in each floor for the rigid connection structure and the semi-rigid connection structure is basically the same. However, the horizontal displacement directions of the rigid connection structure and the semi-rigid connection structure are opposite. The same rules apply to the settlement of the central column, mainly because the beam and the column are closely connected in the rigid connection structure, and the main deformation occurs in the beam. The beam is displaced during the settlement process, which causes the beam to elongate in horizontal direction.

In addition, to the two connection structures, the largest relative displacement occurs on the top floor, followed by the bottom floor. The relative horizontal displacement of rigid structures is greater than that of semi-rigid structures. For both structures, the relative horizontal displacement of the middle floor is relatively small and it can be ignored. As the stiffness increases, the influence on the horizontal displacement of the top floor seems to increase. The total relative horizontal displacement from the bottom to the top floor also has the same trend, that is, the greater the stiffness, the greater the horizontal displacement. Designers need to pay attention to the horizontal displacement of the top floor.

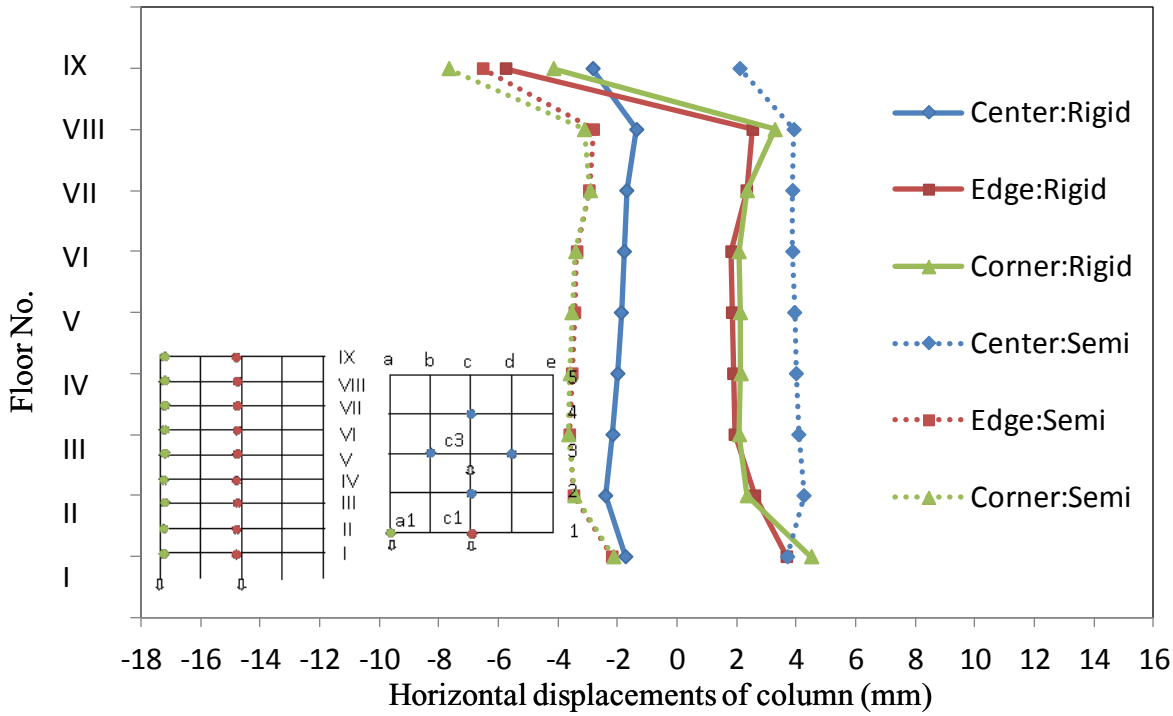

Figure 5.23 Horizontal displacement versus floor level at settlement of 196 mm for rigid and Semi rigid structures

5.4.3.4 Axial Forces

Figure 5.24 presents the axial force versus floor level at settlements of 32 mm and 196 mm for rigid and Semi rigid structures. It can be noted that the highest value is at the ground floor, and that value reduces with the increase of the floor level for both types of connections. Under the same settlement, the axial force generated by the rigid connection structure is greater than that of the semi-rigid connection structure. Moreover, the central column settlement produces the largest axial force, followed by the edge columns, and finally the corner columns. However, the axial force generated by the edge and corner columns settlement is relatively similar above the 7 floors for rigid connection structure.

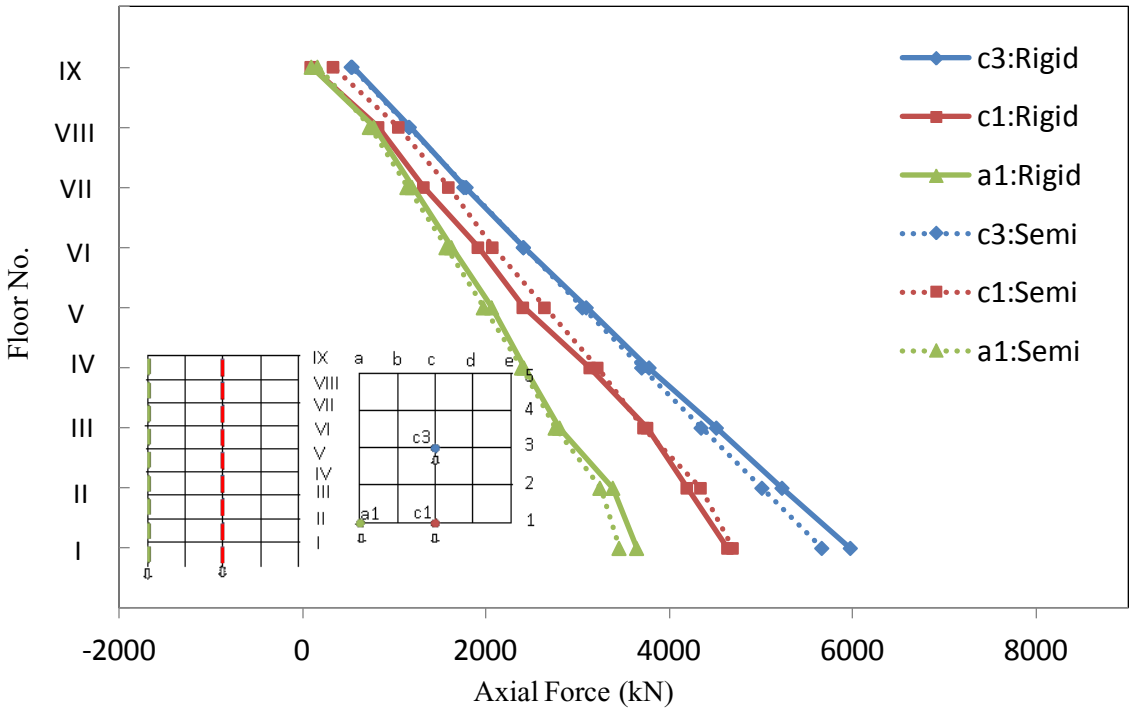

(a) Settlement of 32 mm

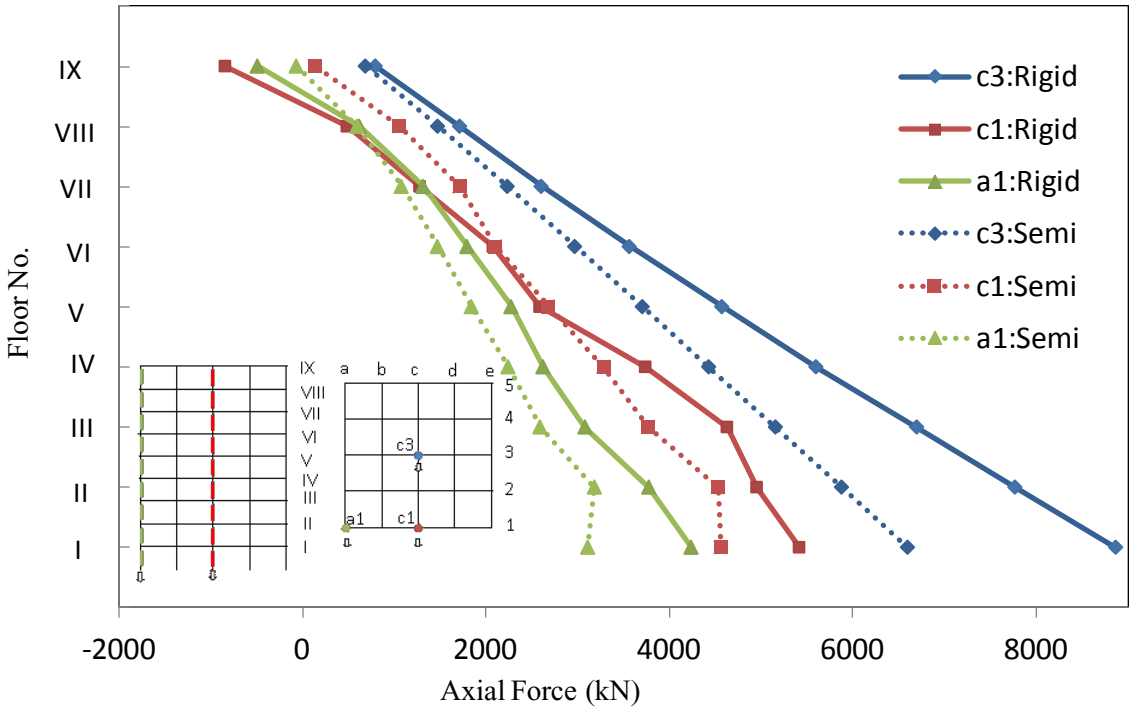

(b) Settlement of 196 mm

Figure 5.24 Axial force versus floor level at settlement of 32 mm (a) and 196 mm (b) for rigid and Semi rigid structures

5.4.3.5 Moment of Beam versus Settlement

Figure 5.25 presents moment versus floor level at settlement of 32 mm and 196 mm for rigid and Semi rigid connection structures. It can be noted that the moment decreases with the increase of the floor level for the three cases and for the two types of connections. Yet, the settlement at the three columns displays almost same moment at all floors, except for the top floor, when the settlement is at 196 mm. Furthermore, the moment for the rigid structures is relatively higher than those for semi-rigid structures. Furthermore, for rigid connection structure the maximum moment takes place for the edge column settlement, followed by the center column and the corner column. The same observation was reported for the semi rigid structure in the elastic stage of structure.

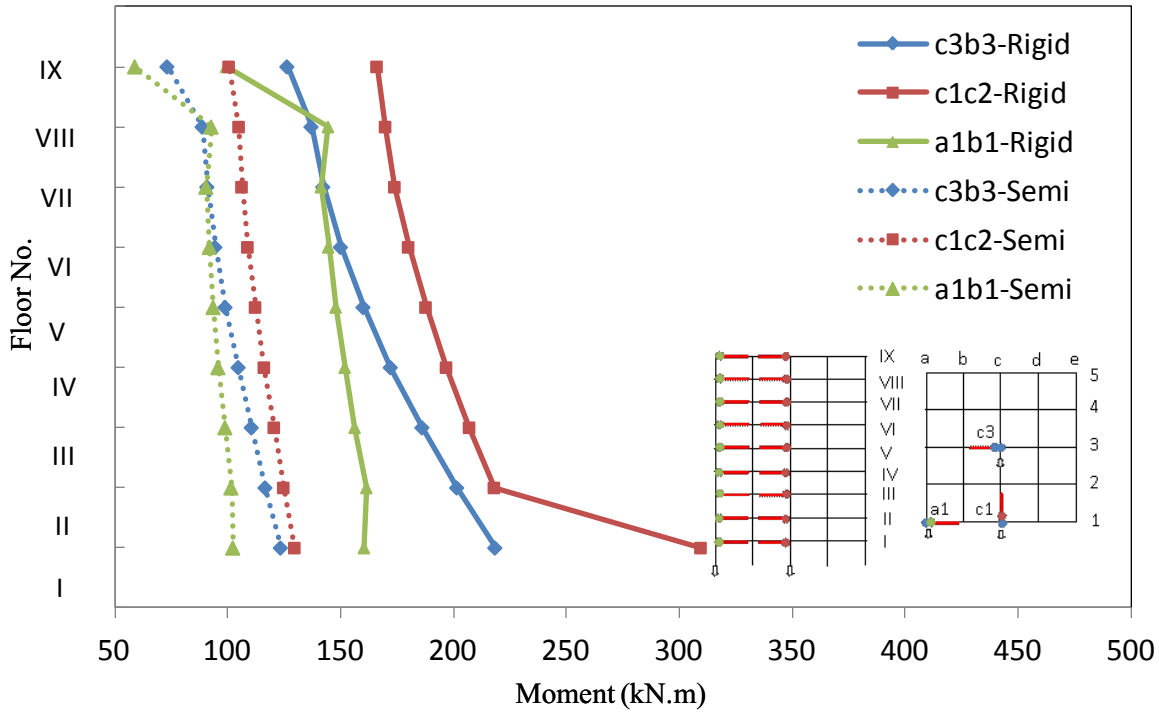

(a) Settlement of 32 mm

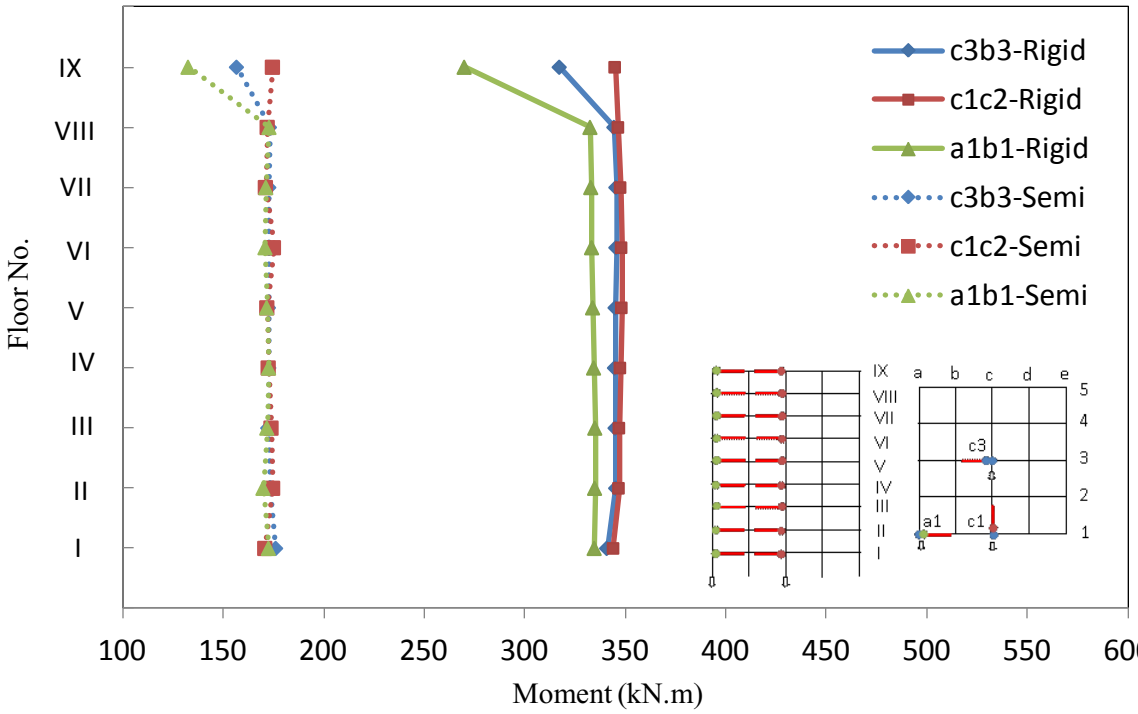

(b) Settlement of 196 mm

Figure 5.25 Moment versus floor level at settlement of 32 mm and 196 mm for rigid and Semi rigid structure

5.5 Parametric Study

The stiffness of the structure members affects directly the response of the structure to foundation settlement. This section examines the parameters governing the rigidity of the structure, namely, the number of spans and span length, the number of floors and floor height of the structure

5.5.1 Effect of Number of Spans and number of Floors on Connection Stiffness

In theory, the number of spans and number of floors in a structure should not have an effect on the design of beam-column connection. In order to validate this statement, a numerical model

of a structure having 2-span 2-floor (2S2F) and another having 4-span and 9-floor (4S9F) were developed. Both structures have the same level of rigidity and boundary conditions, and are subjected to the settlement of the center, edge and corner column.

Figure 5.26 presents the moment-rotation and rotation-settlement curves, which relate to the settlement and connection rotation. It can be noted that the settlement-rotation curve is almost linear for the three cases tested for structures with different number spans and floors. Accordingly, the number of spans and the number of floors have no effect on the bending moment-rotation relationship during settlement, that is, the stiffness of the connections are not affected by the number of spans and floors.

5.5.2 Effects of Span Length and Floor Height on Connection Stiffness

The model developed above with 2-span and 2-floor having semi-rigid connections was tested for a span of 5000mm and a floor height of 4000mm, a span of 6000mm and a floor height of 4000mm and a span of 6000 mm and a floor height of 3000 mm were analyzed on the effect to the settlement.

Figure 5.27 presents the moment-rotation and settlement-rotation curves from the same length of floor in different of span structure. It can be noted that the moment-rotation curves are almost the same for the two different span length, however, the settlement-rotation curves are different. This confirms that the longer the span, the higher moment resistance, i.e. the larger the span, the smaller the torque. In fact, during the settlement process, the span has no influence on the connection stiffness. However, it has a great influence on the rotation-settlement.

Figure 5.28 presents the moment-rotation and settlement-rotation curves from the same span with different floor height. It can be noted that the height of the floor has almost no effect on the

connection stiffness during the settlement process, and has no effect on the rotation-settlement relationship as well.

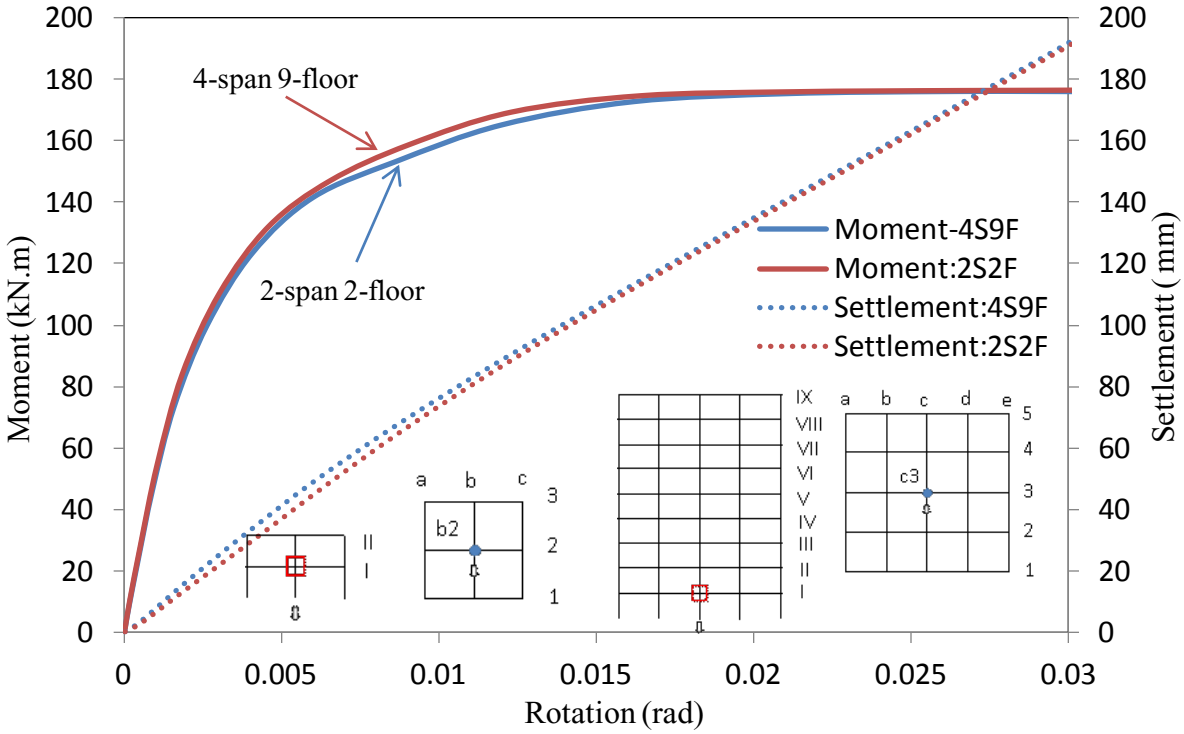

(a) Center column settlement

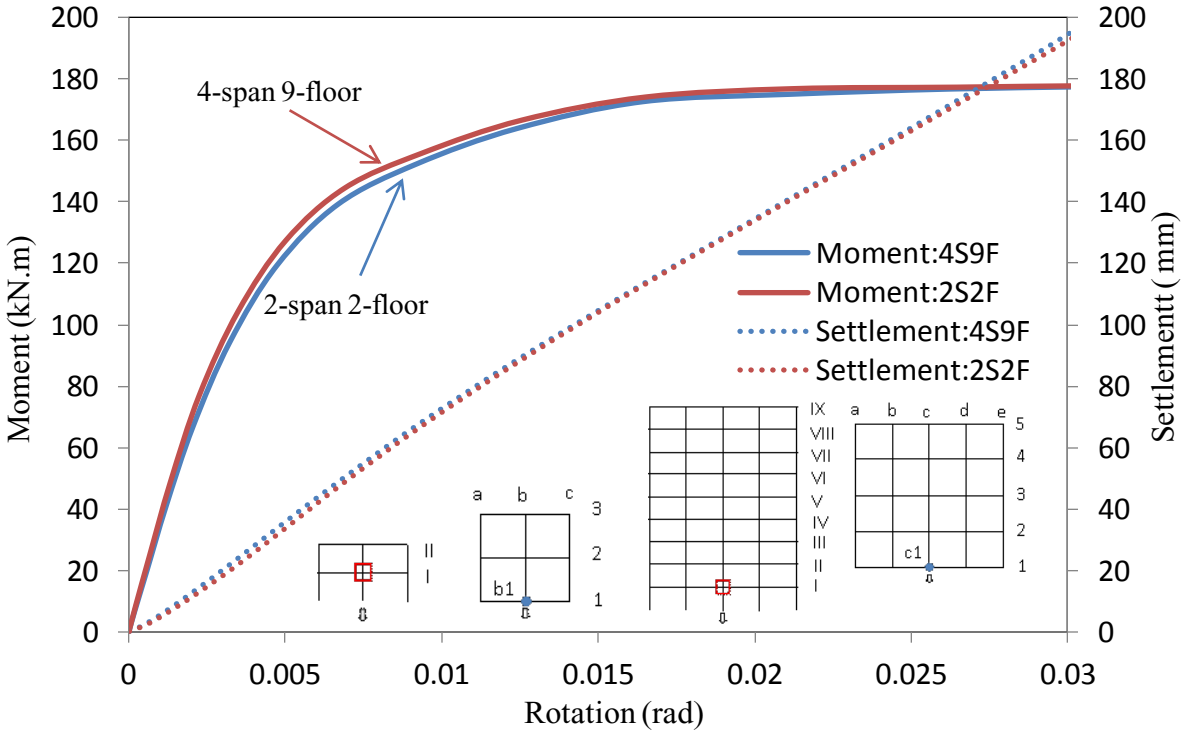

(b) Edge column settlement

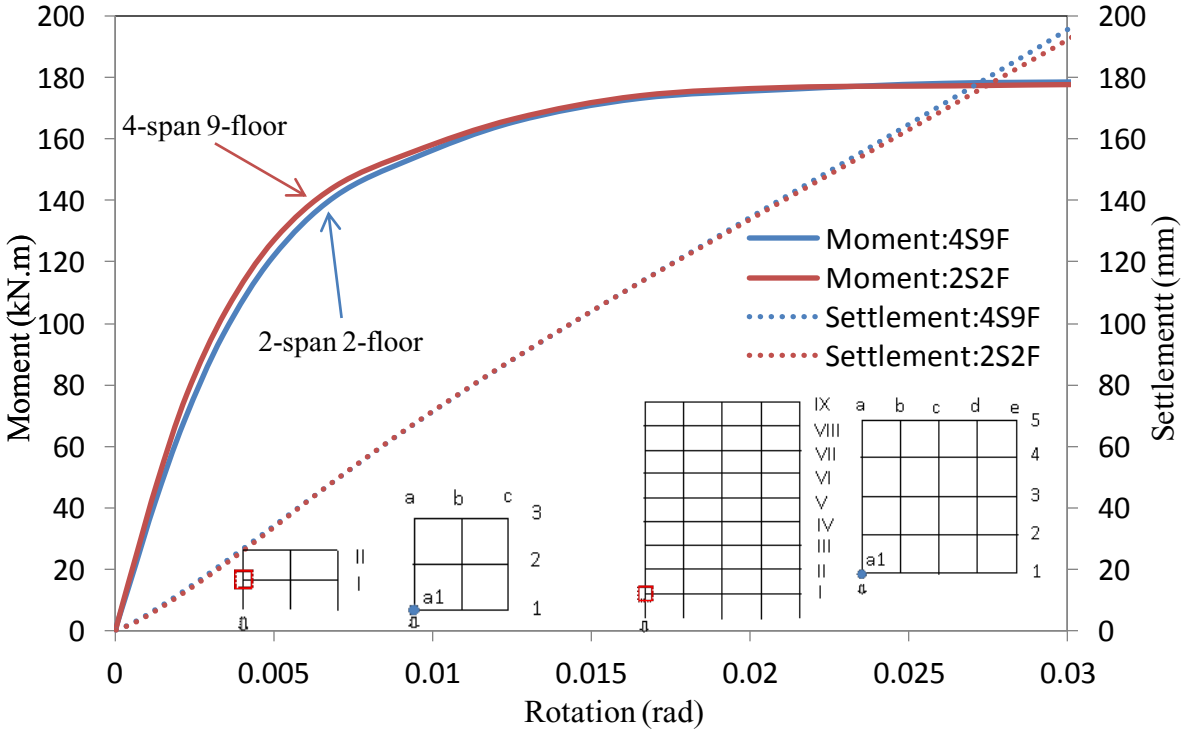

(c) Corner column settlement

Figure 5.26 Moment-rotation curves and rotation-settlement curves for different span number and floor level (2-span 2-floor vs 4-span 9-floor)

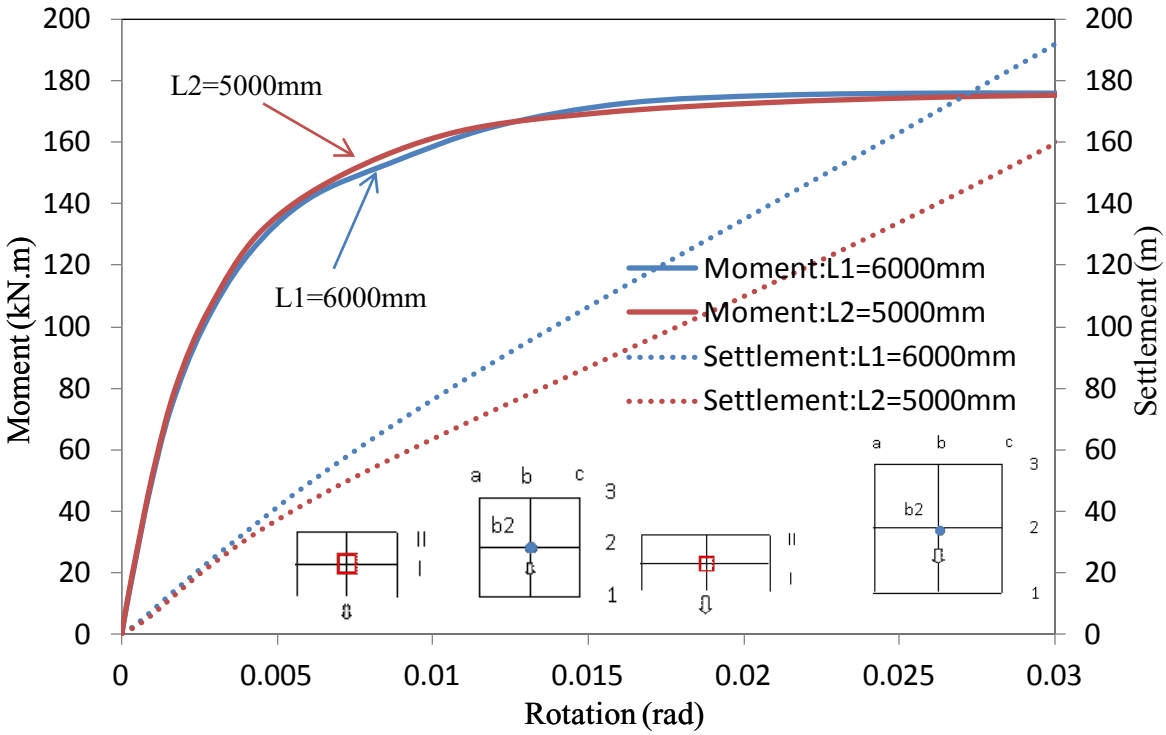

Figure 5.27 Moment-rotation curves for different span length (5000mm vs 6000mm)

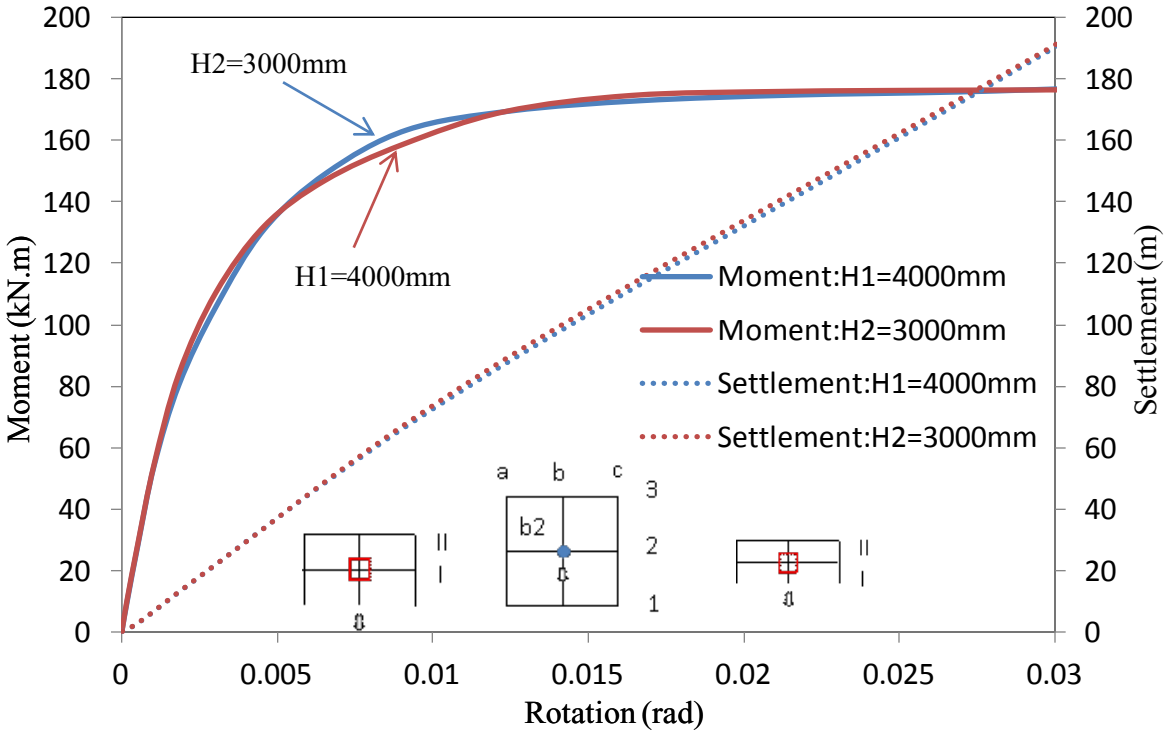

Figure 5.28 Moment rotation curves for different floor height (3000mm vs 4000mm)

5.6 Summary

The elastic-plastic deformation of the rigid connection structure first occurs in the beam or column during the settlement process and the semi-rigid connection structure first occurs in the connection itself.

According to the comparison of the distribution of plastic strain and beam bending moment between rigid connection and semi-rigid connection, it can be seen that the critical element is mainly connected to the bottom beam of the settlement column and its connection, followed by the top beam of the settlement column and its connection.

The bending moment-settlement curve can quickly and intuitively obtain the relationship between settlement and bending moment. By pre-setting the maximum bending moment to get the generated settlement; or setting the maximum settlement to get the maximum bending moment.

Parameter studies show that the simplest 2-span 2-floor structure's bending moment-settlement curve can represent complex structures, such as 4-span 9-floor structures. Therefore, the maximum bending moment generated by the settlement of a complex structure can be obtained by simple numerical simulation of the 2-span 2-floor structure, which can greatly reduce the simulation time and improve the design efficiency.

Chapter 6

Summary and Conclusion

General

Differential settlement between foundation units of a structure has been responsible for serious damage to buildings, and often catastrophic failure and loss of life. The dynamic changes in the superstructure due to loading and environmental conditions, and variability of the underlying soil condition are causing the unavoidable differential settlement, which is manifested in the form of additional stresses and distortion of structure elements, local and catastrophic failure of the structure.

In the literature, little to none address this problem, accordingly, in practice allowable differential settlement was determined based on some empirical formula, recommendation available in the literature, and the use of the structure factor of safety. This can be explained by the fact that communication between the structure engineer and the geotechnical engineer is poor at best, accordingly, research in this field is lagging behind.

This study presents an experimental investigation and a 3-D numerical modelling on the problem stated. Experimentally, a prototype of an instrumented experimental model of a four floor aluminum structure was developed in the laboratory to measure the stresses induced in the structure elements due to the settlement of a center, edge and corner column respectively. After validating the numerical model, the model was used to analyze a 9-floors steel structure and to perform sensitivity analysis.

The following was concluded:

Conclusion

1. Based on the present experimental investigation, during the settlement of the center, edge or corner columns the beams and columns did not undergo obvious plastic deformation, nevertheless, they showed downward rotational displacement. In fact, the damage was concentrated at the connecting angle and bolts.
2. Based on the present experimental investigation, the angle at the top of the beam bears the vertical load, while the angle at the bottom of the beam bears the lateral load, accordingly, the top angle experienced less deformation than the angle at the bottom. Furthermore, the deformation caused by the settlement of the central column is the largest, followed by the edge columns, then the corner columns.
3. Based on the present experimental investigation, the load-settlement curves for the three cases tested, all elements begin at the linear elastic state, then moves to the elastic-plastic then plastic deformation. Due to the increase of the settlement, the beam will then provide the lateral resistance to maintain the rigidity of the beam-column connection, resulting in a quadratic linear state.
4. Based on the present experimental investigation, the plastic-strain starts at the first floor for all the three cases tested, then propagates to the higher floors until it reaches the top floor. The plastic-strains for the top floor is the lowest for the center column, and slightly increase for the edge column, and they reach a relatively higher value for the corner column.
5. Based on the present experimental investigation, the elastic-plastic deformation for structure with rigid connection starts first in the beam and the column, which are connected to the settling column, while for semi-rigid connection structures the elastic-plastic occurs starts at the connection itself.

6. Comparing the results between the present numerical and experimental models in the form of load-settlement relationship, strain-settlement in beams and strain-settlement in columns for three scenarios settlement show that the maximum differences are 15%, 19% and 13%, which is acceptable for validation of numerical modeling.
7. Based on the present numerical investigation, a linear relationship was observed for the three cases tested. Furthermore, for the center column at the linear relationship, the strain generated by the beams at different floors does not change much, while for the edge and corner columns, the strain produced by beams on different floors varies greatly. In fact, the change from linear to nonlinear is due to failure of bolts, which start first, then propagate to the angles at higher settlement first at the top angles, then at the bottom angles.
8. The center column represents the most critical case for the structure, followed by the edge column then the corner column. Furthermore, the maximum vertical displacement takes place in the first floor for all three columns.
9. The angle at the top of the beam bears the vertical load, while the angle at the bottom of the beam bears the lateral load, accordingly, the top angle experienced less deformation than the one at the bottom. Furthermore, the deformation caused by the settlement of the central column is the largest, followed by the edge columns, then the corner columns.
10. The vertical load-settlement curve takes place in three stages, all elements begin at the linear elastic state, then moves to the elastic-plastic then plastic deform, where the vertical load changes from a linear relationship to a nonlinear stage. Due to the continuous increase of the settlement, the beam will provide the lateral resistance, in order to maintain the rigidity of the beam-column connection, resulting in a quadratic linear state.
11. In semi-rigid connections, the first-floor experiences the highest moment due to its location to the settling columns, the rest of the floors experience less. The top floor experiences slightly

higher moment as compared to the other floors. This can be explained by the fact that the top floor has only five degrees of freedom, while other floors have six. Furthermore, the moment increases with the increase of the rotation up to a given point, beyond which any increase of the rotation, does increase the moment.

12. The vertical displacement of the center column decreases with the increase of the floor level. This behavior is similar for the neighboring columns at low settlement values, and reversed to tension for higher settlements.
13. Deferential settlement between foundation elements in a structure generates horizontal displacement of the settling column (drift), which is materialized in the form of horizontal forces acting on the structure. These horizontal forces are often ignored during the design of the structure, especially for steel structure for the design of the bracing.
14. The largest relevant horizontal displacement (drift of column) first happens on the top floor for three settlement cases and then the second floor. The horizontal displacement direction is opposite for the top floor comparing with other floors as the horizontal force distribution on columns from the settlement of the column. The drift and the horizontal forced imposed on the structure due to deferential settlements should be considered for the design of the bracing. Especially, the top floor column drifts value needs to be considered as a limitation parameter in design work.
15. The center column represents the most critical case for the structure, followed by the edge column then the corner column. Furthermore, the maximum vertical displacement takes place in the first floor for all three columns.
16. Charts are proposed to predict the bending moment-settlement curve and rotation-settlement curve, which can be used to establish the relationship between settlement and bending moment. This can be used to trade-off between settlement and stresses in the structure.

17. As the settlement increases, the structure moves to the nonlinear stage, where the bending moment decreases due to the increase of the number of floors then, increases only for the top floor. However, the maximum bending moment for the structure remained at the bottom floor.
18. In steel structures, rigid connections, the moment-rotation relationship, showed no rotation, while the moment is increasing. The maximum bending moment occurs at the connection, which is transferred to the columns. While for Semi-rigid connections, the moment-rotation relationships vary with the degree of its rigidity. However, in practice, it is impossible to achieve fully rigid steel connections.
19. For Rigid connection structure, the moment continues to increase with the increase of the rotation up to a maximum value, beyond which the rotation continues to increase without any increase in the moment. Furthermore, this relationship is almost similar for all floors except for the top floor, which showed slightly lower moment. This is due to the fact that the top floor has only five degrees of freedom; while other floors have six. Similar observation was reported for semi-rigid connection.
20. Design charts are presented to predict moment and settlement for semi-rigid connection, for a given level of rigidity.

Future work

Based on the findings of the current study, additional research is recommended as following:

1. More experimental investigations are needed to obtain data to model the response of the structure to foundation settlement.

2. Model concrete structure for studying the relationship between structural response and

differential settlement of foundation.

3. Experiments and numerical simulations corresponding to different combinations of settlement of columns.

4. Collect field data.

References

ACI Committee 318. (2014). Building code requirement for structural concrete (ACI 318M-14) and commentary (ACI 318RM-14). Building Code Requirements for Structural Concrete.

Ameri, M. R., Asce, S. M., Massumi, A., Masoomi, H., and Asce, S. M. (2019). "Effect of Structural Redundancy on Progressive Collapse Resistance Enhancement in RC Frame Structures." Journal of Performance of Constructed Facilities, 33(1).

ASCE/SEI 7-16. (2016). Minimum Design Loads and Associated Criteria for Buildings and Other Structures.

NBCC. 2010. National Building Code of Canada 2010. Institute for Research in Construction, National Research Council of Canada, Ottawa, Ontario, Canada.

AASHTO. 2010. Standard Specifications for Highway Bridges, American Association of State Highway and Transportation Officials, Washington, D.C., USA.

Boone, S. J. (1996). "GROUND-MoVEMENT-RELATED BUILDING DAMAGE By Storer." JOURNAL OF GEOTECHNICAL ENGINEERING, 122(11), 886–896.

Boscardin, B. M. D., and Cording, E. J. (1989). "Building Response to Excavation - Induced Settlement." 115(1), 1 – 21.

Brown, P. T. (1975). "The Significance of Structure-Foundation Interaction." Second Australia-New Zealand Conference on Geomechanics, 79–82.

Burland, J. B., and Worth, C. P. (1974). "Settlement of Buildings and Associated Damage." British Geotechnical Society's Conference, 611–654.

Canadian Geiotechnical Society. (2006). Foundation engineering manual.

Anastasopulos, I. 2013. "Building damage during nearby construction: forensic analysis", Engineering Failure Analysis, 34: 252-267.

Camos, C., Molins, C., and Arnau, O. 2014. "Case study of damage on masonry buildings produced by tunneling induced settlement", International Journal of Architectural Heritage: Conservation, Analysis, and Restoration, 8(4), 602-625.

Boone, S. J.,Westland, J., and Nusink, R. 1999. "Comparative evaluation of building responses to an adjacent braced excavation." Can. Geotech. J., 36, 210–223

Brown P. T. 1975. "The significance of Structural-Foundation Interaction" 2ed Aust. – N. Z. Conf. Geomechs., Brisbane.

Jieren Song. 2010. Analysis on reasons for integral collapse of Shanghai Lotus River Garden No.7 Building, Architecture Technology, 41(9), 843-847.

Terzaghi, K. & Peck, R.B. 1948. Soil Mechanics in Engineering Practice, 1st Edition, John Wiley and Sons, New York.

Myerhof G.G. 1974. "The settlement Analysis of Building Frames", Structural Engineer, Vol. 25(9), pp. 369-409.

Laefer, D., Ceribasi, S., Long. J., and Cording, E. 2009. "Predicting RC frame response to excavation-induced settlement", Journal of Geotechnical and Geoenvironmental Engineering, 135(11): 1605-1609.

Lefebvre D. and Theroux S. 2000. "Soil-structure Interaction for the Design of Buildings Shallow Foundation", 53ed Canadian Geotechnical Conference. Montreal. pp. 1099.

Son, M., and Cording, E. 2011. "Response of buildings with differential structural types to excavation-induced ground settlement", Journal of Geotechnical and Geoenvironmental Engineering, 137 (4): 323-333.

Skempton A. W. and MacDonald D. H. 1956. "Allowable Settlement of Buildings". Proc. Insyn. Civ. Engrs., Pt III, Vol. 5, pp. 727-768.

Burland, J. B., and C.P. Worth. 1970. Allowable and differential settlement of structures,

including damage and soil-structure interaction, in Proc., Conf. on Settlement of structures, Cambridge University, U.K.:11.

Bray, J., and Dashti, S. 2014. "Liquefaction-induced building movement", Bull., Eq., Eng. 12(3): 1129-1156.

Holtz, R.D. 1991. "Stress distribution and settlement of shallow foundation" Chapter 5, Foundation Engineering handbook, H.S. Fang, editor, Van Nostrand Reinhold, New York, pp. 166-222.

DoD. (2016). DESIGN OF BUILDINGS TO RESIST PROGRESSIVE COLLAPSE.

FEMA 356. (2000). Prestandard and commentary for the seismic rehabilitation of buildings.

Hanna, A. (2003). "Interactions between superstructure and substructure of buildings for achieving economical building design." International Journal for Housing Science, 27(3), 167–175.

Hou, J., Song, L., and Liu, H. (2016). "Progressive collapse of RC frame structures after a centre column loss." Magazine of Concrete Research, 68(8), 423–432.

Hun, K., and James, R. (2014). "Response of framed buildings to excavation-induced movements." Soils and Foundations, Elsevier, 54(3), 250–268.

Kishi N, Chen WF. (1990) Moment- rotation relations of semi-rigid connections with angles. J Struct Eng ASCE 116(7):1813–1834

Kim, Y. J., Gajan, S., and Saafi, M. (2011). "Settlement Rehabilitation of a 35-Year-Old Building : Case Study Integrated with Analysis and Implementation." PRACTICE PERIODICAL ON STRUCTURAL DESIGN AND CONSTRUCTION, 16(4), 215–222.

Laefer, D. F., Ceribasi, S., Long, J. H., and Cording, E. J. (2009). "Predicting RC Frame Response to Excavation-Induced Settlement." JOURNAL OF GEOTECHNICAL AND GEOENVIRONMENTAL ENGINEERING, 135(11), 1605–1619.

Lahri, A., and Garg, V. (2015). "EFFECT OF DIFFERENTIAL SETTLEMENT ON FRAME FORCES - A PARAMETRIC STUDY." International Journam of Research in Engineering and Technology, 4(9), 453–464.

Lin, L., Sinha, A., Tirca, L., and Hanna, A. 2014. "Stresses induced in concrete frame structure due to differential settelement of its foundation", Proceedings of the annual conference of the Canadian society for civil engineering, Halifax, May.

Lin, L., Hanna, A., Sinha, A., and Tirca, L. (2015). "Structural Response to Differential Settlement of Its Foundations." Journal of civil engineering research, 5(3), 59–66.

Liu, Z., and Zhu, Y. (2018). "Progressive collapse of steel frame-brace structure under a column-removal scenario Progressive collapse of steel frame-brace structure under a column-removal scenario." International Conference on Civil, Architecture and Disaster Prevention.

Meyerhof, G. G. (1947). "The settlement analysis of building frames." The Structural Engineer, September, 370–409.

Pearson, C., Delatte, N., and Asce, M. (2005). "Ronan Point Apartment Tower Collapse and its Effect on Building Codes." journal of performance of constructed facilities, 19(May), 172–177.

Polshin, D. E., and Tokar, R. A. (1957). "Maximum Allowable Non-uniform Settlement of Structures." Fourth International Conference on Soil Mechanic and Foundation Engineering, 402–405.

Qian, K., Asce, A. M., and Li, B. (2013). "Performance of Three-Dimensional Reinforced Concrete Beam-Column Substructures under Loss of a Corner Column Scenario." JOURNAL OF STRUCTURAL ENGINEERING, 139(4), 584–594.

Roy, R., and Dutta, S. C. (2001). "Differential settlement among isolated footings of building

frames : The problem , its estimation and possible measures." International Journal of Applied Mechanics and Engineering, 6(1), 165–186.

Russo, G., Pauletta, M., and Scibilia, N. (2013). "Long-Term Structural De fi ciencies in a Mat Foundation on Clay Soil." journal of performance of constructed facilities, 27(3), 295–302.

Sasani, M., and Kropelnicki, J. (2007). "PROGRESSIVE COLLAPSE ANALYSIS OF AN RC STRUCTURE." The Structural Design of Tall and Special Buildings, 17, 757–771.

Sheidaii, M. R., Bayrami, S., and Babaei, M. (2013). "Collapse Behavior of Single-Layer Space Barrel Vaults under Non-Uniform Support Settlements." International Journal of STEEL STRUCTURES, 13(4), 723–730.

Skempton A. W., and MacDonald, D. H. (1956). "The allowable settlement of buildings." Surveyor and municiul and country engineer, 155(3344), 355.

Yi, W., He, Q., Xiao, Y., and Kunnath, S. K. (2008). "Experimental Study on Progressive Collapse-Resistant Behavior of Reinforced Concrete Frame Structures." ACI Structural Journal, (July-August), 433–440.